Journal Pre-proofs

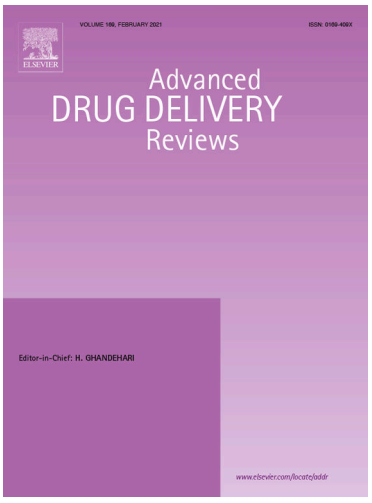

Non-viral nanoparticles for RNA interference: Principles of design and practical guidelines

Zehua Liu, Shiqi Wang, Christos Tapeinos, Giulia Torrieri, Voitto Känkänen, Nesma El-Sayed, Andre Python, Jouni T. Hirvonen, Hélder A. Santos

PII: S0169-409X(21)00182-4
DOI: https://doi.org/10.1016/j.addr.2021.05.018
Reference: ADR 13808

To appear in: *Advanced Drug Delivery Reviews*

Received Date: 5 April 2021
Revised Date: 4 May 2021
Accepted Date: 15 May 2021

Please cite this article as: Z. Liu, S. Wang, C. Tapeinos, G. Torrieri, V. Känkänen, N. El-Sayed, A. Python, J.T. Hirvonen, H.A. Santos, Non-viral nanoparticles for RNA interference: Principles of design and practical guidelines, *Advanced Drug Delivery Reviews* (2021), doi: https://doi.org/10.1016/j.addr.2021.05.018

Non-viral nanoparticles for RNA interference: Principles of design and practical guidelines

Zehua Liu[a], Shiqi Wang[a], Christos Tapeinos[a], Giulia Torrieri[a], Voitto Känkänen[a], Nesma El-Sayed[a], Andre Python[b], Jouni T. Hirvonen[a], Hélder A. Santos[a,c,*]

[a] Drug Research Program, Division of Pharmaceutical Chemistry and Technology, Faculty of Pharmacy, University of Helsinki, Helsinki FI-00014, Finland

[b] Center of Data Science, Zhejiang University, Hangzhou 310058, China

[c] Helsinki Institute of Life Science (HiLIFE), University of Helsinki Helsinki FI-00014, Finland

Corresponding author: helder.santos@helsinki.fi

Keywords: RNA interference; non-viral nanoparticles; RNA encapsulation; leukocytes targeting; endosome escape; clinical translation.

Abstract

Ribonucleic acid interference (RNAi) is an innovative treatment strategy for a myriad of indications. Non-viral synthetic nanoparticles (NPs) have drawn extensive attention as vectors for RNAi due to their potential advantages, including improved safety, high delivery efficiency and economic feasibility. However, the complex natural process of RNAi and the susceptible nature of oligonucleotides render the NPs subject to particular design principles and requirements for practical fabrication. Here, we summarize the requirements and obstacles for fabricating non-viral nano-vectors for efficient RNAi. To address the delivery challenges, we discuss practical guidelines for materials selection and NP synthesis in order to maximize RNA encapsulation efficiency and protection against degradation, and to facilitate the cytosolic release of oligonucleotides. The current status of clinical translation of RNAi-based therapies and further perspectives for reducing the potential side effects are also reviewed.

1. Introduction

At the forefront of medicine, gene therapy is one of the most exciting therapeutic armamentarium developed during the past decade. U.S. Food & Drug Administration (FDA) defines gene therapy as a process of replacing a disease-causing gene with a healthy copy of the gene, inactivating a disease-causing gene that is not functioning properly or by introducing a new or modified gene into the body to help treat a particular disease [1]. The categories potentially leading to three general modalities for gene therapy are: (1) gene addition, where the nontoxic functional gene is transferred into human somatic or germline cells, and the process is usually achieved via vectors, such as, retroviruses and adeno-associated viruses capable of undergoing reverse transcription and deoxyribocucleic acid (DNA) integration but lacking replication potential; (2) gene edition, where a nuclease-induced double-stranded break is occurred on target DNA, followed by efficient creation of variable length insertion or deletion mutations at the break site – tools including early stages zinc finger nucleases, meganucleases and the sequentially discovered clustered regularly interspaced short palindromic repeat (CRISPR)–CRISPR associated 9 (Cas9) nucleases can be efficiently programmed to cleave DNA at sites of interest; and (3) gene intervention, where the target gene expression or translation is inhibited or sequestered by cognate genes. Gene intervention is a post-transcriptional gene silencing process, which is usually achieved by ribonucleic acid (RNA) interference (RNAi).

RNAi in mammalian cells is firstly demonstrated by Elbashir *et al.* in 2001 [2], in which they showed the RNAi in mammalian cells is initiated by double-stranded RNA

(dsRNA) with homologous sequence to the silenced gene. This finding suggested that comparing to other two modalities, RNAi is more straightforward as the targeted silencing is governed via the specificity of Watson-Crick base pairing interactions. The ensuing advantage is a more broad application scenario, as the translation repression strategy is theoretically suitable for all types of gene-related diseases. Thus, efforts are sequentially made to develop corresponding delivery vehicles for RNAi, and comparing to viral-based vectors, non-viral vehicles have drawn increasing attention due to some favorable characters, including retained immunostimulatory effects, lack of risk for mutagenic events, feasible for extra modification, and potentially increased targeting capability and relatively low costs [3]. Thus, exploring non-viral materials as RNAi vectors has been extensively investigated in the pharmaceutical field.

However, different from fabricating delivery systems for other drugs (*e.g.*, small molecules, peptides, and proteins), the vulnerability of RNA and meticulous RNAi process in cells render particular requirements for vehicles design and fabrication [4]. Therefore, in this review, we summarize the general principles for the design of RNAi vectors, discuss the practical issues that should be considered during these vectors fabrication, the critical aspects of the vehicle that affects the RNA encapsulation, targeting yield and successful cytosolic release of RNA, and finally reviewing recent advances in RNAi vectors and their further perspectives for resolving the therapeutic obstacles and promoting the clinical translations.

2. General requirements for the delivery systems

In this section, we will briefly discuss the major modalities of RNAi and the detailed biological process for RNAi. Here, we aim to illustrate the RNAi's subcellular sites of function, time of function, dosage of function and form of function, which are indispensable for understanding the basic requirements and potential challenges for RNAi vector fabrication.

2.1. Natural process and the gene silencing mechanism of RNAi

The dsRNA is thought to be the initiator for RNAi, as firstly purposed by Fire *et al.* in 1998 [5]. In eukaryotic cells, dsRNAs exert the RNAi function by being sequentially processed into: (1) short interfering RNAs (siRNAs), which may recognize the targeting messenger RNA (mRNA) through complementary sequence and further guide cleavage of targeting mRNA; or (2) microRNAs (miRNAs), which mediate translational repression or cleavage of mRNA targets [2, 6]. Despite the initiator function of dsRNAs, delivering dsRNAs for RNAi may not be applicable for mammalian systems, as dsRNAs are strong interferon pathway agonists, promoting the activation of the nuclear factor κB, and both synthetic and viral dsRNAs were shown to potentially lead to cell death [7].

The dsRNA is produced by two main routines: (1) RNA-templated RNA polymerization process with the assistant from RNA-dependent RNA polymerase (RdRP); or (2) by through the overlapping transcripts to achieve RNA hybridization [6], whereas primary miRNA (pri-miRNA), also a type of dsRNA, is processed in

nucleus and transported to cytoplasm by nuclear export receptor, exportin-5 [6]. Once the dsRNA is formed or transported in the cytoplasm, it will be processed by dsRNA-specific RNase-III-type endonucleases, or Dicer, which contain catalytic RNase III and dsRNA-binding domains (dsRBDs) [8]. dsRNA or miRNA precursor (pre-miRNA) is further cleaved into short segments miRNA/siRNA (typically about 21–25 nucleotides in length) by Dicer monomer [9]. Two complementary single-strand RNA segments are produced from Dicer cleavage, but only one (termed as guide strand) is integrated with Argonaute (Ago) protein [10]. Afterwards, the rearrangement of miRNA/siRNA-duplex-containing ribonucleoprotein particles (RNP) is initiated to form into RNA induced silencing complex (RISC) [11]. After forming into RISC, the single-stranded siRNA in RISC binds to the complementary target mRNA in these complexes, and cleaves the target mRNA with the assistance from Ago-protein family to accomplish the RNAi, whereas miRNA, usually featured with imperfect complementarity, will inhibit the mRNA translation or induce a mRNA degradation (**Figure 1**) [11, 12].

An alternative method for generating siRNA is through short hairpin RNA (shRNA) [13]. Similar to pre-miRNA hairpin structure, the double-strand like structure from single-stranded shRNA is generated from the intramolecular base-pairing due to its inverted repeats [14]. Rather than a natural process, shRNA is most often produced through the use of transcription vectors [15]. After transfected by plasmid DNA or virus-derived constructs, the primary transcript shRNA (pri-shRNA) will be processed and transported to the cytoplasm, followed by integrating into RISC as delineated above **(Figure 1)** [13, 15].

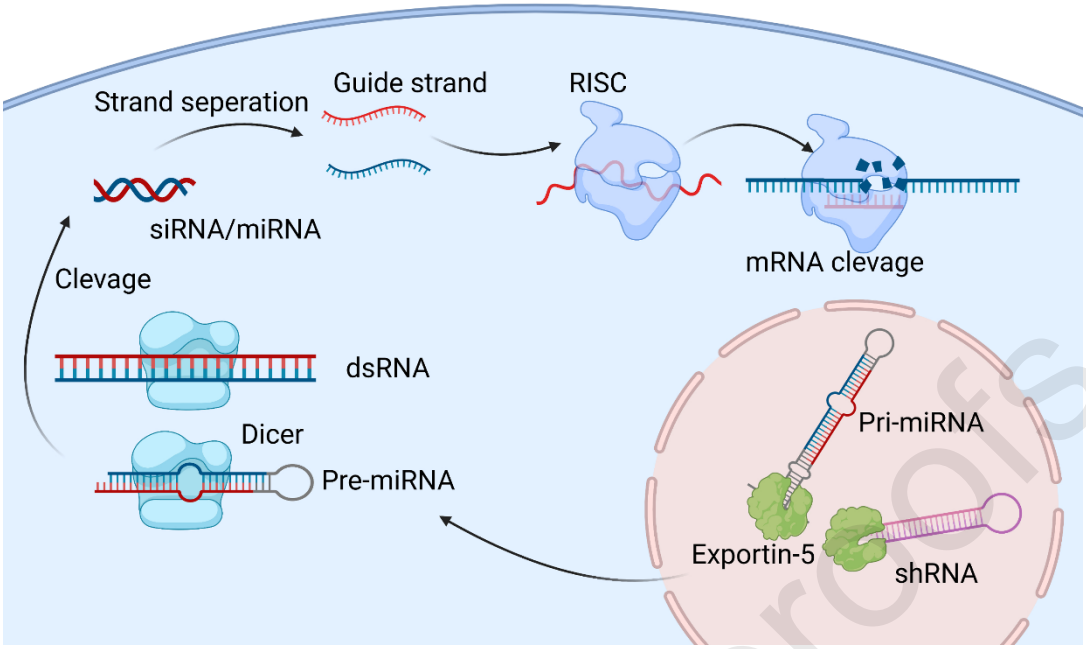

Figure 1. Graphic scheme of RNA interference. Primary micro-RNA (pri-miRNA) and short hairpin RNA (shRNA) is exported to cytoplasm via exportin-5. The enzyme, Dicer, will cleave the miRNA precursor (pre-miRNA), shRNA, or long double-stranded RNA (dsRNA), into microRNA (miRNA) or small interfering RNA (siRNA), separately. Followed by strand separation and forming into the RNA-induced silencing complex (RISC), the guide strand will bind to complementary mRNA sequences to perform the RNAi process. Figure is generated using Biorender.com.

2.2. Nanoparticles based RNAi

Apart from the natural process and the gene silencing mechanism of RNAi, for non-viral nanoparticles (NPs) based RNA delivery, three fundamental questions are concomitantly proposed: (1) considering the subcellular location for RNA interference machinery, when and how the RNA is released from the NPs and transferred to the cytosol? (2) how many RNA can successfully reach to the cytosol, and what is the RNA

concentration threshold for accomplishing their corresponding functions? and (3) whether the RNA should be in a fully free form to fulfill the RNAi?

Understanding the nanoparticles (NPs) transport across the cell membrane is the pre-requisite for answering these questions. Cellular uptake pathways of NPs can be roughly divided into three categories: macropinocytosis, phagocytosis, receptor assisted endocytosis (*e.g.* clathrin-mediated, clathrin-caveolin independent, caveolae-mediated or other receptors-mediated endocytosis) [12, 16, 17]. Despite various internalization processes described in the literature, once taken-up, the NPs are entrapped by several endocytic compartments, which are sequentially named as early endosomes, late endosomes and lysosomes [18]. A more detailed discussion regarding to the physiochemical properties of each compartments will be discussed in Section 6.1. Generally, each compartment has a specific time window and physiochemical properties [19], and it is important to understand from which compartments are RNA released and how efficient this process can be achieved.

So far, the machinery of siRNA delivery through NPs has been the most widely investigated. One of the first systematic work was conducted by Zerial *et al.*, who adopted siRNA containing lipid NPs (LNPs) with the size ~60 nm for analyzing the intracellular trafficking of siRNA [19]. To visualize the siRNA transport process, they labelled the siRNAs (which knockdown the expression of destabilized green fluorescent protein, d1-eGFP) with fluorescein Alexa Fluor 647 (siRNA-AF647) or gold nanocrystals (6 nm, siRNA-gold). Three types of biomarkers, Rabankyrin-5 for cell membrane, early endosome antigen 1 (EEA1) for early endosomes and lysosomal-

associated membrane protein 1 (LAMP1) for lysosomes, were separately applied for identifying endocytic compartments from different stages of transport. Transmission electron microscopy (TEM) images first suggested the LNP-siRNA-gold NPs were mainly accumulated in the early and late endosomes but not in the lysosomes within 6 h. Furthermore, time-lapse confocal fluorescent microscopy was applied to observe the release of siRNA-AF647 into the cytosol, and the results showed the number of LNPs containing endosomes were stable for over 12 min after they were uptake by different cells, suggesting the majority of siRNAs were still entrapped in the endosomes. Further quantitative evaluation of siRNA release efficacy was achieved by visualizing cytosolic siRNA-gold NPs. In line with the confocal results, an endosome release efficiency of 1.3%, with only 250 siRNA-gold per HeLa cells was observed after 6 h NPs incubation, and for *in vivo* experiments (hepatocytes), the number was further reduced to 186 siRNA-gold per cell (accounts for 1.7% of the overall siRNA-gold). To explore the siRNA intracellular escape time-window, and further understand from which endosomal compartment do the siRNAs escape from, the authors proposed two mathematical models: (1) a liner siRNA release kinetics, suggesting the release of siRNAs occurred at all endosomal stages under a zero-order manner; and (2) a sigmoidal siRNA release kinetics, suggesting siRNA is mainly released from a specific endosomal compartment. Quantifying the ratio of cytosolic siRNA were achieved by TEM through visualizing the siRNA-gold NPs, and the results showed the endosome escape of siRNA-gold was in a sigmoidal manner both *in vitro* (GFP-expressing HeLa cells) and *in vivo* (hepatocytes). Moreover, the data semi-quantitatively showed that

siRNA release occurred in a particular yet narrow time-window (< 30 min).

However, the major quantitative observation of the aforementioned work was achieved by siRNA-gold NPs, which may have distinct physiochemical properties comparing to pristine siRNA. Thus, a more detailed information regarding to the siRNA release amount and time-point is also elusive. To solve these problems, Lieberman *et al.* developed a high-dynamic-range (HDR) like confocal microscopy, which can maximally promote the bright/dark contrast to distinguish the cytosolic siRNA from the densely packed un-released siRNA in endosomes [20]. siRNA (labelled with Alexa Fluor 647, siRNA-AF647) was encapsulated by LNPs and the precise quantification of cytosolic siRNA was achieved by monitoring the fluctuation of fluorescent intensity, where an intra-endosome fluorescent signal increase suggests the partial LNP disintegration, yet an intra-endosome fluorescent signal decrease and cytosol fluorescent signal increase indicates the cytosolic siRNA release [20]. In this way, the authors found that the endosome siRNA escape was initiated at 5 min after maximal EEA1 expression on endosomes (early endosomes). Moreover, the endosome became $EEA1^-$ when the siRNA release occurred. As a biomarker for immature early endosome, the maximal appearance of Rab5 was 3 min earlier than cytosolic siRNA release, whereas $Rab7^+$ endosome, a biomarker representing the maturation to late endosome, was almost coinciding with the cytosolic siRNA release. In contrast, Rab9 (late endosome) markers were observed simultaneously or shortly after the siRNA release, and LAMP1 (lysosome) markers became evident only after ~40 min post siRNA release. The overall duration of siRNA release only lasted for ~10 min with a burst release

duration for 10–20 seconds. These results demonstrated a narrow yet particular time-window for siRNAs endosome escape, and the siRNAs released from $EEA1^{-}Rab5^{+}Rab7^{+}Rab9^{\pm}LAMP1^{-}$ early endosomes within 5–15 min upon cell uptake (**Figure 2**).

Besides of the thoroughly delineated siRNA endosome escape time-point, the authors also suggested only few cytosolic copies of the siRNA (< 2000, ~ 2.5 $\times 10^{-9}$ pmol) are needed to achieve a maximal gene knockdown efficiency, which is in good line with previous results [19, 21]. Moreover, despite by increasing the siRNA concentration within the LNPs, one can linearly increase the cytosolic siRNA concentration, yet no significant difference was observed in terms of gene knockdown yield [20]. This may be mainly caused by the RISC components saturation [22, 23], and the excess siRNA that cannot form into RISC could potentially be degraded or excreted from the cell. Ultrahigh concentration of siRNA or miRNA may even conversely upregulate the gene expression as a result of competitive RISC binding [22, 24, 25], suggesting the concentration thresholds for efficient RNAi is low.

Regarding to whether siRNAs should be completely released from the NPs to fulfill the RNAi, Lieberman *et al.* suggested that free siRNA, rather than intact siRNA-LNPs, will perform the gene knockdown effects. It is plausible that free RNA will maximally perform the RNAi tasks as the steric hindrance may inhibit RNA to interact with the targeted genes or RISC. However, it also should be noted that siRNA conjugated or entangled with small molecules [26], peptides [27], proteins [28], polymers [29] or even NPs [30] may also exhibit gene knockdown potency. For example, Gilleron *et al.*

demonstrated that at the same siRNA concentration (20 nM), LNPs loaded with pristine siRNA or LNPs loaded with siRNA conjugated on gold NPs exhibited the same gene knockdown efficiency [19]. This is in good line with other reports, suggesting proper chemical conjugation, even with macromolecules or particles, may not interfere the RNAi efficiency [31-33]. However, chemical modification exhibits a positional effect on RNAi activity [34, 35], and readers may refer to more comprehensive reviews regarding to the chemical modification of oligonucleotides [36-38].

Overall, the previous machinery explorations of non-viral NPs based RNAi revealed the major challenges for the carrier design. These are: (1) NPs should provide robust encapsulation and protection towards pristine oligonucleotide for avoiding pre-mature degradation; (2) NPs with endosome escape capability are necessary as endosomal release is a discrete limiting step of gene knockdown; (3) NPs with responsive burst release manner is preferred for maximizing the cytosolic RNA delivery; however, this responsive release is not indispensable as only minimal oligonucleotide copied may achieve efficient RNAi; and (4) considering the ultrahigh sensitivity for RNAi, proper and precise targeting of the nanocarrier may reduce the off-target RNAi induced side effects. Therefore, in the following sections, we will sequentially highlight these four aspects by illustrating the principle of design of the NPs' fabrication process for RNAi intracellular delivery.

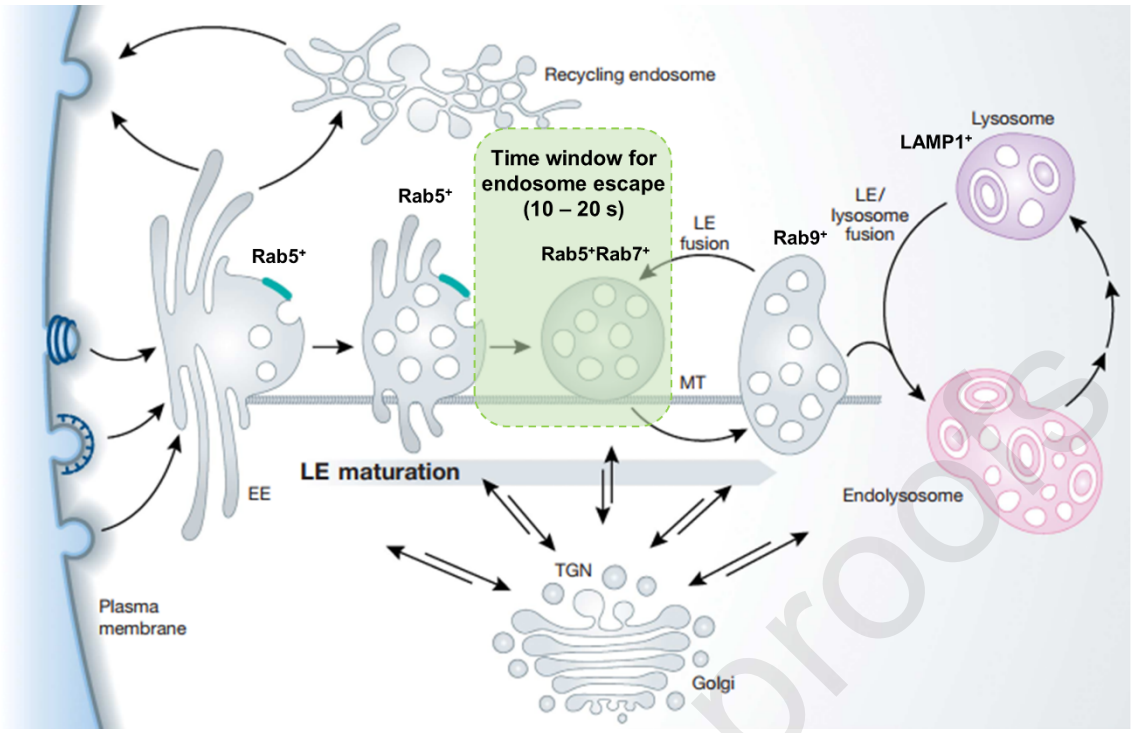

Figure 2. Endosome maturation process and the corresponding time window for siRNA endosome escape. After the primary endocytic vesicles formation, the NPs containing vesicles sequentially form into early endosomes (EE) featured with $Rab5^+$. EEs are moving in perinuclear space along microtubules (MT), where the conversion of $Rab5^+$ EE to $Rab7^+$ EE take places. The endosome escape of siRNA will be initiated just before nascent late endosome (LE, $Rab9^+$) undergo homotypic fusion reaction with $Rab5^+Rab7^+$ EE, where the majority of siRNA will be released within 10-20 seconds. The unreleased siRNA will accumulate in LE and lysosome ($LAMP1^+$) for degradation. Reproduced and modified with permissions from ref. [39]; Copyright © 2011, John Wiley & Sons.

3. NPs synthesis conditions affecting the RNA stability

During the NPs' synthesis, factors liks pH values, organic solvents, salt/metal ions and most importantly, the potentially existed ribonuclease (RNase), may potently affect the stability of RNAs and the efficiency of RNAi. Therefore, prior to introducing the specific design principles of NPs, we will first discuss about the influence of the commonly applied NPs' synthesizing conditions on the stability of RNA.

3.1 RNase

RNase free environment is a particular requirement for synthesizing RNAi NPs. However, maintaining RNase-free condition is a vexing challenge not only because the universal existence of RNase, but also due to its ultra-stability. Common ways to remove enzymes, such as metal chelation, autoclaving, boiling or UV irradiation cannot fully deactivate RNase [40-43]. The commercialized RNase inhibitors are usually not broad-spectrum RNase inhibitor but rather inactivating certain RNases, and usually a reducing condition by adding at least 1 mM of dithiothreitol (DTT) is required [42]. Trivial steps during the NPs synthesis will make the situation more pernicious, therefore the best way to keep an RNase-free environment during NPs synthesis should be removing the RNase at the first step.

The de-RNase of containers (*e.g.*, beakers and vials) for NPs synthesis can be achieved by baking the glassware in 200 ℃ (or higher) for at least 4 h [42, 44]. Although some reports suggest treating the glassware with 0.01–0.1% of diethyl pyrocarbonate (DEPC) at room temperature or 37 ℃ for overnight, further autoclave the container to remove

the residue DEPC [45, 46], yet, other sources indicate an incomplete DEPC decomposing by autoclaving, and the remaining DEPC will react with adenosine residues in the RNA to interfere the RNA stability [42, 47]. Therefore, for thermal tolerant materials, such as glassware or metal spatula, high temperature baking is the most convenient method. For plastics, de-RNase can be achieved by immersing the items with 0.1% of DEPC for overnight at room temperature. After rinsing the items several times with RNase free H_2O, autoclaving them for 15 min at 15 psi (1.05 kg/cm^2) on liquid cycle [48]. For microfluidic chips, which are also commonly applied for RNAi NPs fabrication, no detailed description regarding to the de-RNase process for microfluidic chip has been reported, but it has been shown that washing the microfluidic channel and equipment with DEPC water [49], the sequential removal of DEPC may be achieved by constant RNase-free water, N-2-hydroxyethylpiperazine-N-2-ethane sulfonic acid (HEPES) buffer or tris-(hydroxymethyl) aminomethane (Tris) buffer rinsing due to the DEPC hydrolysis [48]. Amine or amine derivative based buffer (*e.g.*, HEPES and Tris buffer) will accelerate the DPEC hydrolysis, but it should be noted that the hydrolysis product, urethane, is a potent carcinogen, which needs further caution.

The solutions should be prepared with RNase-free water, and the organic solvent should be prepared via filtering through disposable ultrafiltration membrane [50, 51], as RNase may be more stable under neat organic solvent [52], and papers have suggested the effectiveness of ultrafiltration to avoid RNase contamination [51]. If possible, the solutions should be prepared as high concentrated stock solutions and be kept at –20 ℃

[44]. All the solutions cannot be used for long time, therefore it is suggested their storing in small aliquots, and discard each aliquot after use [42, 44].

3.2. pH-Values

The pH value is in specific importance for NPs synthesis, as the fabrication process of some NPs, *e.g.* chitosan (CS) or ionizable lipid [53-55], will involve pH-value changes. Comparing to DNA linkages, RNA linkages have shown to be on average ~100,000-fold less stable under physiological condition [56]. This is mainly because of the ribose sugar difference between DNA and RNA. Instead of the deoxyribose found in DNA (2'-hydride), ribonucleotides is composed by pentose sugar ribose (2'-hydroxyl group, **Figure 3**). The 2'-hydroxyl group is in favor of the nucleophilic attack, where a transesterification will take place upon the deprotonated 2'-oxygen attacking the adjacent 3'-phosphorus center [57, 58]. As a result, the 3'-5' phosphodiester bonds are cleaved to produce fragments containing 2',3'-cyclic phosphate and 5'-hydroxyl termini (**Figure 3**) [59, 60]. Thus, most of the RNA is not stable in alkaline pH-value due to the 2'-hydroxyl group deprotonation. However, experimental data suggested RNA hydrolysis can be both catalyzed by acidic and basic buffers [58, 59, 61]. For example, the 3'-5' phosphodiester bonds cleavage and/or isomerization in acetic acid buffers (acetate/acetic acid) showed a buffer concentration dependent manner in a second-order kinetics [61]. The major catalytic activity was contributed by buffered acid, whereas non-buffer H^+ species made minor contribution to the catalytic activity [61]. The mechanism for this reaction involves the hydrogen bond formation between acetic acid and phosphodiester, and the protonated phosphoryl oxygen is attacked by

the 2'-hydroxyl group with acetate functioning as catalyst (**Figure 3**) [61]. A detailed pH stability study was conducted by Lönnberg *et al.*, who investigated the hydrolysis profile of 2'- Uracil RNA (3'-5' UpU) under different pH-values at the temperature of 363 K, and the pH was adjusted by adding hydrogen chloride or sodium hydroxide in acetic acid (0.045 mM)/sodium acetate (0.015 mM) buffer [62]. Results demonstrated that the major RNA hydrolysis was observed at the pH < 3 or pH > 7, suggesting RNA is still overall more stable in acidic-neutral like conditions compared to alkaline solutions.

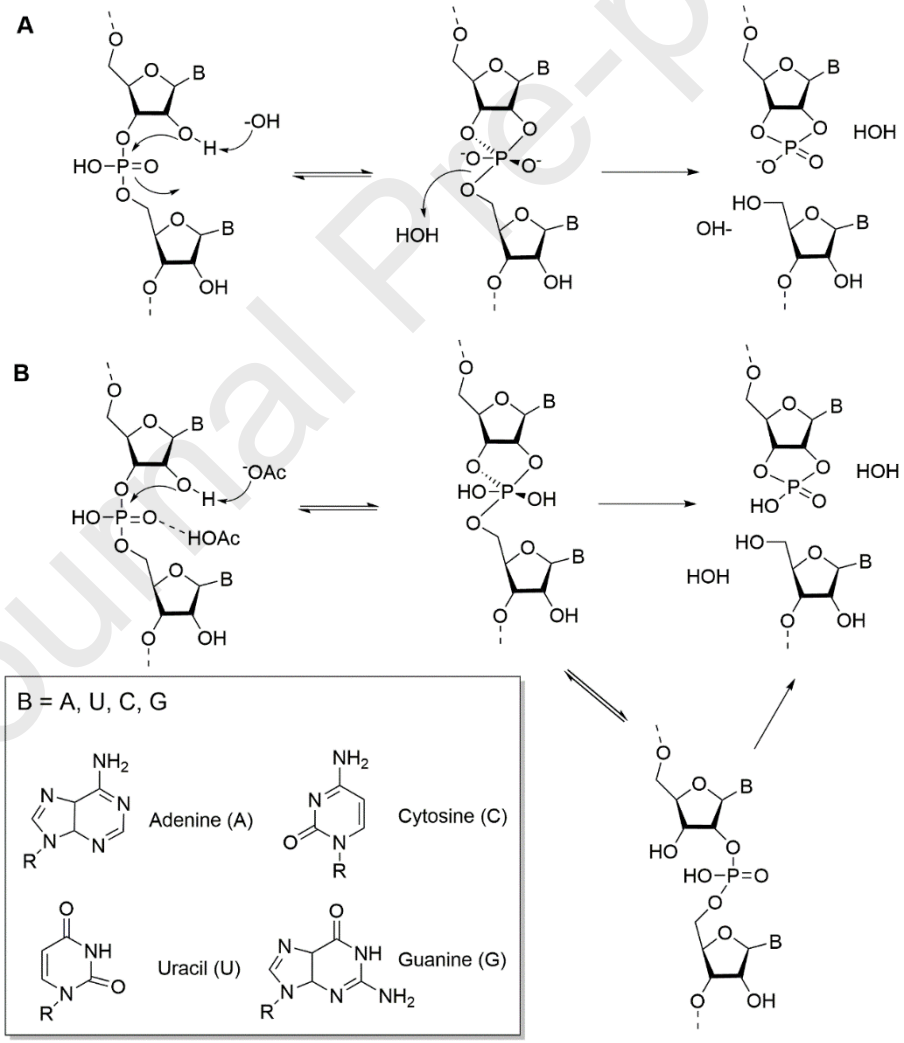

Figure 3. Chemical scheme of the RNA hydrolysis. RNA can be hydrolyzed under both

(A) alkaline and (B) acidic conditions. However, acid catalyzed RNA hydrolysis is mainly observed under acidic buffer instead of plain acid solution.

3.3. Organic solvents

A variety of NPs fabrication methods (*e.g.*, nanoprecipitation, single/double emulsion and micellization) will inevitably involve organic solvents, and the solvents choice has impact on the RNA stability as RNA secondary and tertiary structure are governed by the RNA sequence-dependent interaction, including base stacking, hydrophobic bonding and hydrogen bonding, whereas the strength of these interactions is solvent-dependent. RNA denaturation by organic solvents have long been observed [63, 64], however, there are also reports suggesting proper solvents choice may protect RNA from degradation [65-67]. **Table 1** briefly summarizes the effects of commonly used organic solvents on RNA's stability, which may provide guidance for readers to choose the solvent systems. **Table 1** is divided into two categories, separately delineating the effects of organic solvent on the stability/integrity of RNA and the effects of organic solvents on the function of RNAi.

Table I. Commonly used organic solvents for RNA-encapsulated NPs fabrication and the effects on RNA stability.[a]

Organic solvents	Solvent percentages [a]	RNA	Effects	Reference
Effects of the organic solvent on the stability/integrity of RNA				
MeOH	0%-25%	58-nucleotide ribosomal RNA (rRNA) fragment	Addition of MeOH stabilizes tertiary structure of the RNA linearly correlated with methanol percentages	[67]
EtOH	96%-100%	Total RNA, mRNA	Storage under −70 ℃ for several month showed no RNA degradation	[65, 66, 68]
EtOH	100%	Total RNA	Some RNA with small segments failed in producing RT-PCR products, of note, this phenomenon is dependent on the source of RNA	[69, 70]
FA	100%	Total RNA	Formamide protect RNA against RNase catalyzed degradation	[71]
DMSO	0%-99.6%	Synthetic polynucleotide rG:rC, double-stranded bacteriophage RNA	Major denaturation of RNA was observed in DMSO solution with volume ratio higher than 40%	[63]
MeOH, EtOH, DMSO, DMF, ACN, THF, acetone, FA	20%	Synthetic 11-nucleotides RNA duplex which is the substrate of hammerhead ribozyme	The doublehelical structure of the RNA duplex remained stable as confirmed by the maintained circular dichroism spectrum of the RNA	[72]
Effects of organic solvents on functions of RNAi				
Acetone	83%	siRNA	Preserved RNAi efficiency from siRNA in co-solvent	[73]
ACN	9%	siRNA	Preserved RNAi efficiency from siRNA in co-solvent	[74]
Chloroform	90%	siRNA	Preserved RNAi efficiency from siRNA in single emulsion	[75]
EtOH	22.5%-25%	siRNA, sgRNA, mRNA	Preserved RNAi efficiency from siRNA in co-solvent	[1, 76-79]
MeOH	5%-34%	siRNA	Preserved RNAi efficiency from siRNA in co-solvent	[80, 81]
DCM	4%	siRNA	Preserved RNAi efficiency from siRNA in single emulsion	[82]

EA	83%	siRNA	Preserved RNAi efficiency from siRNA in single emulsion	[83, 84]
THF	95%	siRNA	Preserved RNAi efficiency from siRNA in co-solvent	[85]
THF/MeOH/chloroform co-solvent	83% THF, 16%; MeOH, 45%; chloroform, 22%	siRNA	Preserved RNAi efficiency from siRNA in co-solvent	[86]

[a]Percentages indicate the volumetric percentage of organic solvent in the organic solvent/water co-solvent. ACN, acetonitrile; DCM, dichloromethane; DMSO, dimethyl sulfoxide; DMF, dimethylformamide; EA, ethyl acetate; EtOH, ethanol; THF, tetrahydrofuran; FA, formamide; MeOH, methanol.

3.3. Salt and metal ions

Various aqueous buffers are usually involved in the NPs' production. However, the choice of the buffer may also hinder the stability and integrity of RNAs. Metal ions can induce the degradation of RNA under certain conditions, and RNAs are much more vulnerable than DNAs. At the zinc concentration of two Zn^{2+}/nucleotide, about 5000 breaks occur in adenine-containing polyribonucleotides (Poly(rA)) strand for one break in a DNA strand [87]. It should be noted that not all metal-binding events trigger RNA hydrolysis, and for long RNA strand, metal ion binding is even indispensable for preserving the function of RNA by inducing the RNA folding into stable tertiary structures [88, 89]. However, this is not the case for oligonucleotides that typically contain ~30 nucleotides. The accelerated RNA cleavage is mainly observed in divalent metal ions and some lanthanide ions, and the mechanism is similar to alkaline induced RNA hydrolysis, as described above (**Figure 3**) [42, 90], where the metal hydrate will interact with the phosphate oxygen, sequentially abstracting the proton from 2'-

hydroxyl group to induce the phosphate rearrangement [91]. Therefore, the metal hydrates with low pK_a value exhibit higher RNA cleavage efficiency [91, 92]. This is consistent with the results from investigating metal ions induced scission of oligonucleotides bearing an acridine [92], where RNA scission efficiency from different metal ions is: $La^{3+} \geqslant Eu^{3+} \geqslant Lu^{3+} > Zn^{2+} \geqslant Mg^{2+} \geqslant Ca^{2+} > Mn^{2+} > Co^{2+} > Cu^{2+} > Ni^{2+}$; Na^{+} and K^{+} showed no obvious effect on RNA hydrolysis. Therefore, it is preferred to apply de-ionized water for preparing RNA solution, and to avoid metal ion catalyzed RNA scission, 0.1–1 mM of ethylenediaminetetraacetic acid (EDTA) can be applied for chelating potential metal contamination [42]. Other specific chelators, such as trinitriloacetate (TNA, for Zn^{2+}) or ethylenebis(oxyethylenenitrilo)tetraacetic acid (EGTA, for Ca^{2+}), can also be applied based on the NPs synthesizing condition [42].

4. RNA encapsulation

The choice of proper materials to formulate and effectively encapsulate RNAs, and protect them from degradation is the foremost step for RNAi nanosystem fabrication. In this section, we discuss the general methodologies to formulate nanosystems for RNA encapsulation, a potential mechanism for effective RNA protection and encapsulation, and identify and describe parameters which play a key role in encapsulation efficiency and vehicle stability.

To identify recent changes in the materials used for RNAi nanosystem fabrication, we implemented a query on the retrievals “nano” + “RNA interfering”, using Scopus

Search application programming interface (API) in R software (https://github.com/christopherBelter/scopusAPI) [93]. After extracting the keywords from the 200 most relevant scientific articles (sorted by their number of citations), we manually cleaned the data and selected all relevant words associated with biomaterials that appeared in the database. The results suggest changes over time of most commonly applied biomaterials for RNA encapsulation. **Figure 4** (*left*: bar plot, *right*: word cloud) provides an illustrative comparison of the frequency of the most relevant words associated with materials for two investigated periods (2016–2018 and 2019–2021).

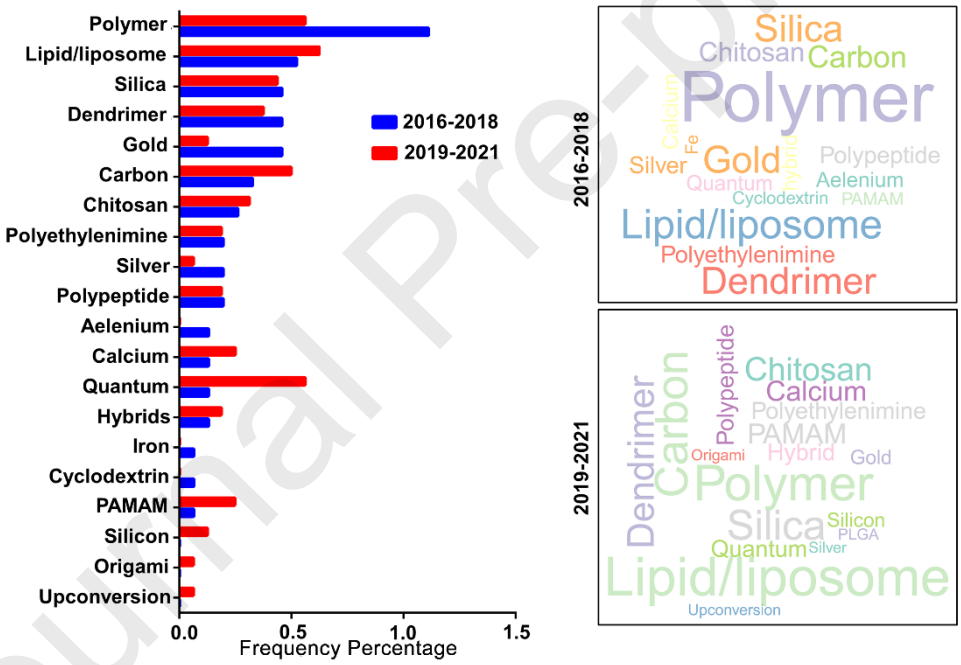

Figure 4. Visualization of the most frequent words related to the materials from keywords of scientific papers using Scopus Search "Nano" + "RNA interference" over two the periods 2015–2018 and 2019–2021.

4.1. Lipid-based NPs

Lipid-based NPs (LNPs) have been used to deliver various drug substances, including therapeutic RNAs [53, 54, 94, 95]. The majority of the fabricated LNPs consist of four main components that include an ionizable lipid, a phospholipid (*e.g.,* 1,2-distearoyl-sn-glycero-3-phosphocholine, DSPC), cholesterol, and a poly(ethylene glycol)-conjugated lipid (PEG-lipid) [53]. The ionizable lipid, which is positively charged at low pH-values, allows the binding with the negatively charged RNA through electrostatic interactions. This ionization is also responsible for the RNA release inside endosomal compartments due to the low pH-derived protonation (pH ~ 5) [96], and a more detailed discussion regarding to the design of lipid for facilitating endosome escape will be presented in Section 6.4, whereas in this section we will mainly focus on delineating the mechanism and methodologies of RNA encapsulation by LNPs. One major advantages for LNPs is the simplicity of manufacturing – LNPs are usually prepared in a rather straightforward method. They can be both produced through the most basic bulk method, such as static mixing or pipet mixing [97-99], that is the lipid compositions are dissolved in water miscible organic solvents like ethanol or acetone, whereas the RNAs are dissolved in aqueous solution. Rapid mixing is then used for spontaneous formation of the RNAs containing LNPs. LNPs can be dialyzed in aqueous buffer (such as PBS) to remove the organic solvent and free RNAs, and the yielded product are diluted in aqueous buffer to achieve the desired final RNA concentration. Microfluidic methods have also been widely applied in RNAs containing LNPs fabrication due to its advantages in reducing the mixing time and batch-to-batch variation [76, 100, 101]. A proper control over the flow rate, flow ratio with the

microfluidic technology can also avoid post-treatment like in bulk methods, such as dialysis or direct dilution [76].

The effective protection from LNPs towards the encapsulated RNAs is generated from the structure of LNPs. The phospholipid and cholesterol are essential for the lipid structure, which may provide preliminary protection towards the encapsulated RNAs [102], where the PEG-lipid shields the RNA from degradation, while providing in tandem colloidal stability and stealth properties [102]. Leung *et al.* elaborated the potential mechanism of the RNAs encapsulation process by LNPs [103]. The cryo-TEM images of a typical siRNA containing LNPs (constituted by 1-palmitoyl-2-oleoyl-sn-glycero-3-phosphocholine (POPC), cholesterol and an ionizable cationic lipid DLinKC2-DMA) showed that, in contrast with bilayer vesicle nanosystems, LNPs showed an electron-condensed core, which is further confirmed to be the encapsulated siRNA complexed composed by siRNA, cationic lipid and the cholesterol. Along with the increasing siRNA concentration, more cationic lipid will be transferred from external lipid monolayer to the cavity to form into complex with siRNA, and this lipid/siRNA complex renders effective protection towards siRNA. Sequential molecular modelling demonstrated that an aqueous compartment inside of the LNPs cavity, this periodic structure is composed by nucleic acids and the polar moiety of the lipid, which is further surrounded by cholesterol (**Figure 5A**), whereas the PEG layer was consistently presented in the outer layer to provide further shielding and protection. However, a different RNAs packing model was recently proposed by Kulkarni *et al.*, who investigated the LNPs morphology changes during the siRNAs encapsulation

process with pH changes [104]. An improved cryo-TEM instrument with higher acceleration voltages (300 kV) and better detection was adopted for improving sample penetration to better image the LNPs core. The authors suggested a more detailed description regarding to the siRNA encapsulation process, which is initiated by the formation of small vesicles that contain siRNA between closely apposed lipid monolayers at lower pH value, under which the ionizable lipids are protonized to be cationic. With increased pH-value, the deprotonation of ionizable lipids will facilitate fusion of these small vesicles due to the reduced inter-vesicle electrostatic repulsion. Along with this process, siRNA is packed into a closely apposed lipid bilayer, which will further sandwiching the siRNA and segregate it from the outer layer of LNPs, and this process eventually halted by the phase separation of PEG-lipid (**Figure 5B**). This observation is consistent with a more recent study by the same group [98], where they showed the gradual absence of the amorphous solid lipid core with increasing siRNA loading concentration (Nitrogen/phosphorous ratio, N/P, decreasing from 3 to 1), indicated the encapsulation of siRNA converts associated ionizable lipid into a form of siRNA/lipid/cholesterol complex. It should be noted that, different from previous molecular-modelling results [103], these findings suggested the encapsulated siRNA will not disperse in a "currant bun" pattern inside of the LNPs (**Figure 5A**), but rather densely packed by the lipid bilayer, and at high N/P ratio, the redundant lipids will be enriched in the cavity center in amorphous oil-phase like state.

Overall, these studies suggest that the potential mechanism for the RNAs encapsulation and protection by LNPs is due to the RNAs/ionizable cationic lipid/cholesterol complex

formation inside of the LNPs, where the surface lipid are transferred into the LNPs core along with RNAs loading.

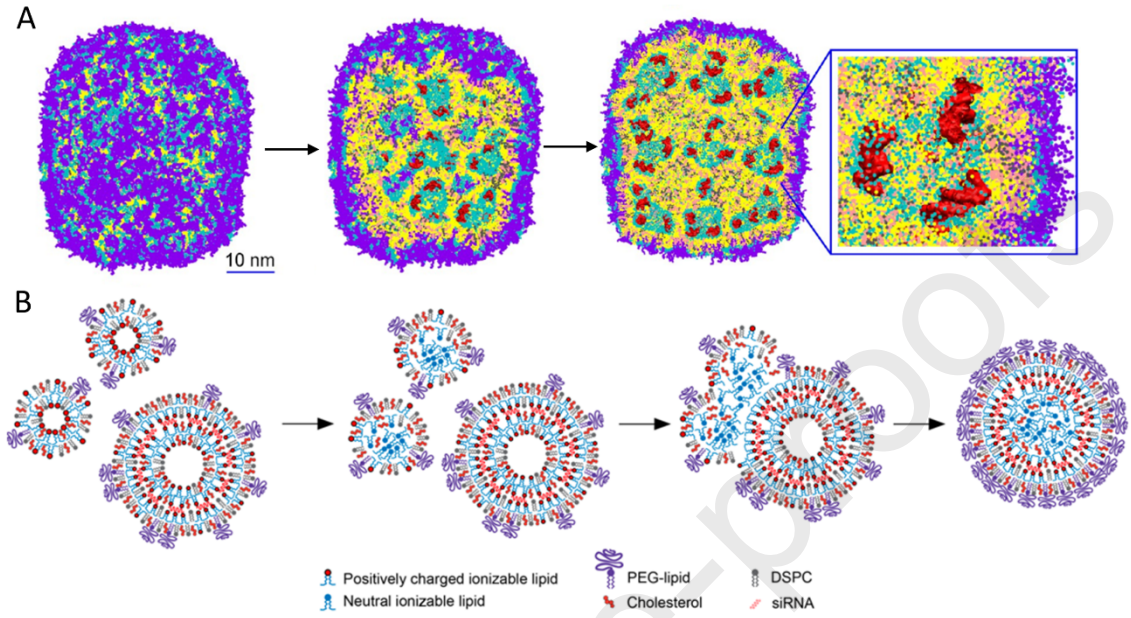

Figure 5. (A) Molecular-modelling approach for illustrating the RNAs encapsulation process by LNPs. Ionizable cationic lipid is shown in yellow, cholesterol in pink, DSPC in gray, lipid polar moiety in cyan, PEG-lipid in violet, and nucleic acids (duplex DNA) in red; water not shown for clarity. **(B)** Different from the "currant bun" model as shown in **(A)**, new model is purposed for describing the RNAs encapsulation process, where siRNA containing small vesicles are first formed under low pH value (pH =4). Along with the pH value increase, neutralized ionizable lipid start to fuse with each other and in the end, a "siRNA sandwich" structure is formed where siRNAs are tightly packed by closely apposed lipid monolayers, and the redundant lipid will accumulate in the cavity center in an oil-phase. Modified and reproduced with permission from (A) ref. [105]; Copyright © 2012, American Chemical Society; and (B) ref. [104]; Copyright © 2018, American Chemical Society.

Considering the mechanism and process of RNA encapsulation by LNPs, corresponding parameters can be tailored to optimize the size, stability of LNPs and the encapsulation efficiency of RNAs. Formulation optimization majorly accounts for the satisfied physiochemical characterization of LNPs. However, conventional formulation optimization process is vastly dependent on phenomenological or empirical approaches, and further understanding of the RNAs encapsulation mechanism and process may provide an alternative practical guideline for promoting the LNPs performance. For example, considering the theoretical LNPs model established by previous studies [103-106], under higher N/P ratio (such as 3 or 6, which is the typical formulation applied clinically [107, 108]), the redundant bulk of the lipids will accumulate into a central oil phase [104], therefore the stability of corresponding LNPs may be affected by the solubility of the lipid components with one each other. Another example, in a typical LNPs formulation composed by ionizable cationic lipid/DSPC/cholesterol/PEG-lipid, the stability of the corresponding LNPs is dominated by the proportions of each components, especially the proportions of ionizable cationic lipid and cholesterol. As considering the solubility of cholesterol in ionizable lipid oil phase is only 8 mol-%, and an equimolar level of cholesterol is presented in the DSPC surface monolayer [109], with the formulation of ionizable lipid/DSPC/cholesterol/PEG-lipid = 50/10/38.5/1.5 (mol-%), only 14% of the total cholesterol can be dissolved and well dispersed in LNPs, whereas the surplus

cholesterol may be potentially precipitated into crystalline form and affect the stability of the LNPs.

Understanding the RNAs loading process may also provide guideline for maximizing the encapsulation efficiency. As RNAs are densely packed by the ionizable lipid bilayer, which is stabilized by cholesterol, thus it is intuitively speculated that the ratio and contents of lipid and cholesterol may govern the RNA loading capacity of LNPs. Cullis *et al.* [98] demonstrated that with a fixed component of LNPs containing 2,2-dilinoleyl-4-(2-dimethylaminoethyl)-[1,3]-dioxolane (KC2, ionizable lipid), DSPC (helper lipid), cholesterol and PEG-lipid, when the cholesterol proportion is lower than 2.5 mol-%, the siRNA encapsulation efficiency is negligible (< 10%), whereas this number is increased to ~40% when cholesterol reaches to 10 mol-%, and the siRNA encapsulation efficiency is further progressively enhanced to over 80% at 20 mol-% of cholesterol. Simply enhancing the cationic lipid concentration (94 mol-%) showed reverse effects on siRNA encapsulation efficiency, confirming the stable formation of siRNA/ionizable lipid complex need the stabilization effects from cholesterol. Despite the addition of helper lipids (in the current case, DSPC) will not directly participate in the formation of siRNA/lipid complex [104-106, 110]; however, as we discussed above, due to the limited solubility of cholesterol in ionizable lipid oil-phase [104, 111], the addition of DSPC amplify the siRNA encapsulation efficiency by preventing crystalline cholesterol formation and stabilize the siRNA/lipid complex.

The strategy by tailoring cholesterol to optimize the RNA encapsulation efficiency was also recently investigated by Patel *et al.* [112], who demonstrated the cholesterol

replacement with other analogs like betuline, lupeol, ursolic acid, and oleanolic acid significantly affects the RNAs encapsulation efficiency of LNPs. Results suggested that for those cholesterol analogs wherein the C-20 to C-27 tail is modified into a 5th ring structure (**Figure 6**), the RNAs encapsulation efficiency is dramatically reduced to < 50%. This phenomenon can also be explained by the aforementioned mechanism that the existence of extra ring structure in the cholesterol analogs yields additional steric hindrance, which disturbs the regular organization of lipid component [113], and leads to poor encapsulation of RNAs.

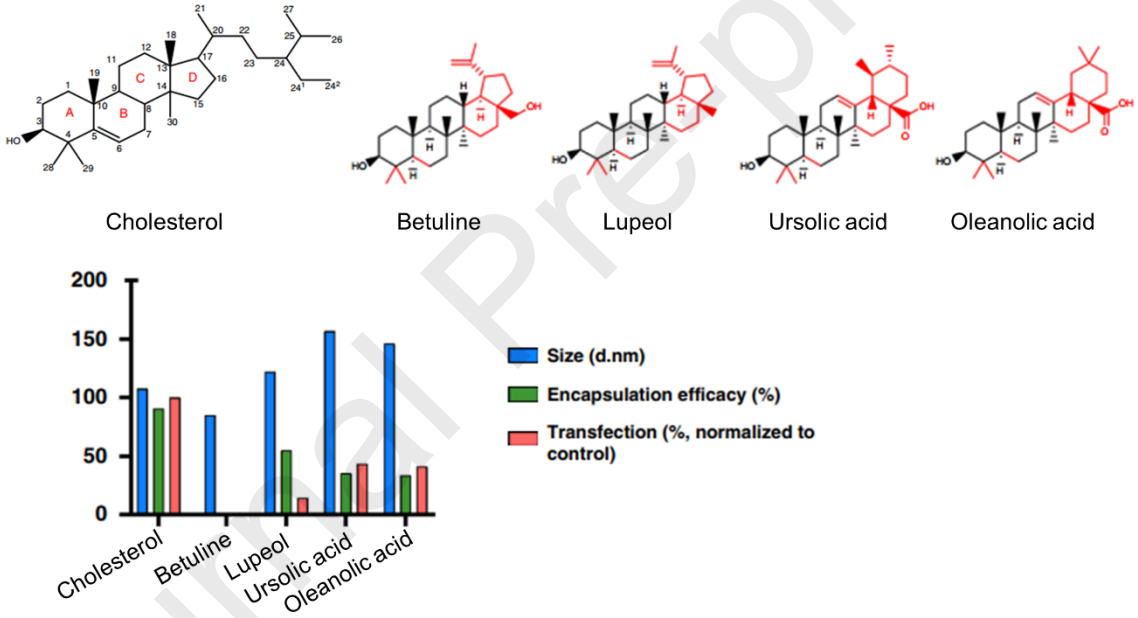

Figure 6. Chemical structure of cholesterol and its corresponding analogues. The addition of 5th ring in cholesterol tail dramatically reduces the encapsulation efficiency of siRNAs. Modified and reproduced with permissions from ref. [96]; Copyright © 2020, Springer Nature.

The mechanism of RNAs encapsulation by LNPs can also be adapted in guiding and interpreting cationic lipid choice. Lou *et al.* [114] investigated the impact of the cationic

lipid selection on RNAs encapsulation and delivery. The authors used a variety of ionizable lipids, including 1,2-dioleoyl-3-trimethyl ammonium-propane (DOTAP), 1,2-dimyristoyl-3-trimethyl ammonium-propane (DMTAP), dimethyl dioctadecyl ammonium (DDA) and 1,2-stearoyl-3-trimethyl ammonium-propane (DSTAP). The most obvious difference was observed between DOTAP and DSTAP. The only structural difference is that DSTAP contains two saturated aliphatic tails, while DOTAP contains a cis-double bond in each of its two aliphatic tails. Whereas the RNAs encapsulation efficiency from DSTAP based LNPs was dramatically reduced from 97% to 70%. Although the authors did not further elaborated the potential mechanism behind this phenomenon, previous studies demonstrated that the existence of double bond in the hydrophobic tail potentially increases the lipid fluidity, and contributed to the stabilization of lamellar phases of the lipid [115, 116]. This feature may further contribute to the maintenance the opposed bilayer structure of RNA/lipid complex, as such promote the encapsulation efficiency. Similar phenomenon was also observed by Ball *et al.* [97], who have noticed the increasing proportion of DOPE (contain cis-double bond) along with decreasing the proportion of DSPC (saturated tails) progressively increased the encapsulation efficiency of both siRNAs and mRNAs.

4.2. Polymeric NPs

Polymer NPs constitute an alternative approach for the delivery of various oligonucleotides [117-119]. The precise control over their physicochemical properties and architecture, using bottom-up chemical approaches, provides a significant advantage over the lipid-based systems described above [120]. In fact, the various

chemistries allow for the fabrication of nanoparticles with tailor-made properties like control over the loading and release profiles, degradability, and stimuli-responsiveness [119, 121, 122]. The practical issues regarding to the particular cautions related to synthesizing conditions (organic solvents, pH, aqueous solutions etc.) are discussed in Section 3. Here, we will mainly focus on parameters which may affect the RNAs encapsulation by synthetic polymeric materials and the corresponding manipulating methods. Similarly, prior to introducing the detailed discussion regarding to the RNAs encapsulation and release from polymeric NPs, we first introduce the general RNAs encapsulation process in different polymeric materials.

As we discussed previously, in LNPs, oligonucleotide binding is governed by two main contributing interactions, electrostatic and hydrophobic. The former are responsible for the RNA binding and indirectly control the loading efficiency, where the latter are responsible for nanoparticle stabilization and RNAs' degradation protection. Evidently, the RNAs' encapsulation efficiency and release profile, the degradation protection efficiency and the nanoparticle's location where RNA resides in, are depending on the used polymer and the approach used for the nanoparticle synthesis. Hydrophobic ionic polymer, such as PLGA, can only encapsulate the RNA through double-emulsion method to load the siRNA in its interior for protecting it from exogenous factors [123], where a positively charged polymer will result in a more 'exposed' RNA binding [124]. In the case of a hydrophilic/hydrophobic co-polymer (**Figure 7**), the RNA's residency and subsequently the protection efficiency will be determined by which interacting force prevails during nanoparticle synthesis. Finally, and as it is discussed later [125,

126], RNAs can also reside in the interspace of polymer brushes resulting in core-independent oligonucleotide-delivery nanocarriers. Notably, another driving force for RNA binding that is not commonly used, but should be considered, is intercalation [127]. As Zhou *et al.* reported [127], the use of intercalating groups in siRNA-loaded nanocarriers enhances siRNA protection at physiological pH, over nanocarriers that present only hydrophobic groups.

Besides the non-covalent approaches that are mainly used due to their simplicity in the fabrication of RNA-loaded nanoparticles, covalent binding has also been reported [128, 129]. Although covalent binding improves stability and pharmacokinetic profiles, the higher complexity during nanoparticles' formulation makes this approach less attractive compared to the 'easy' non-covalent binding.

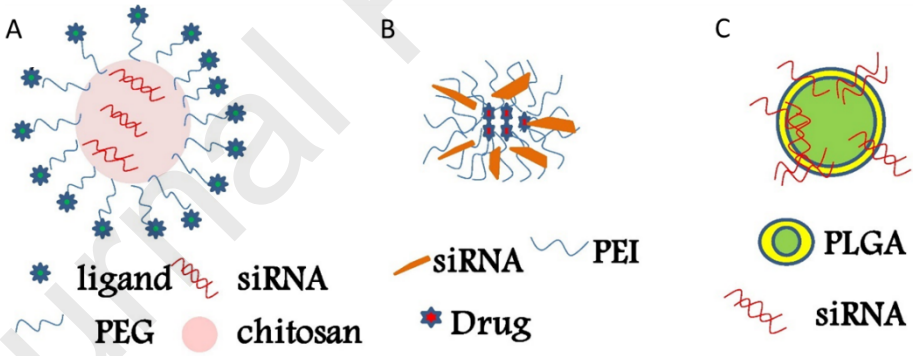

Figure 7. RNAs encapsulation model by different materials including: **(A)** chitosan; **(B)** PEI; and **(C)** PLGA. Modified and reproduced with permissions from ref. [130]; Copyright © 2017, Elsevier B.V.

As described above, the binding of the chosen RNA-therapeutics is mainly achieved through electrostatic interactions between the positively charged groups of specific

polymers (*e.g.,* poly ethylene imine-PEI and poly amidoamine-PAMAM) and the negative charge of the oligonucleotides. Notably, the positively charged polymer amine groups (N = nitrogen) to the negatively charged nucleic acid phosphate groups (P) are among the most important physicochemical parameters determining properties like stability, surface charge, and size. As a result of the low charge of siRNA, high N/P ratios result in higher RNA complexation. However, the higher this ratio is, the higher the positive surface charge and the higher the toxicity.

Therefore the optimization of N/P ratio is the preliminary step for efficient RNAs encapsulation, and a proper N/P ratio can improve complexation without increasing the cationic polymer. For example, Yu *et al.* [131] presented a strategy that involved the use of polymerized siRNA (multi-siRNA). This strategy resulted in increased charged density and chain flexibility in the multi-siRNA, leading to a higher complexation degree and improved biological stability even at a low N/P ratio. The multi-siRNA was complexed with PEI through a hybrid rolling circle amplification (RCA) co-carrier. As it was demonstrated, it could not be replaced by other high molecular weight polymers. Degradation studies of the PEI_y-RCA_{18}-siRNA (N/P = 2) showed no siRNA degradation, where the free RCA_{18}-siRNA degraded in just thirty minutes. Different N/P ratios were tested, resulting in low cytotoxicity when N/P $\leq$ 6. However, a higher N/P ratio was necessary (N/P=10) for effective transfection, ranging from 24% to 58%, depending on the used formulation (**Figure 8**).

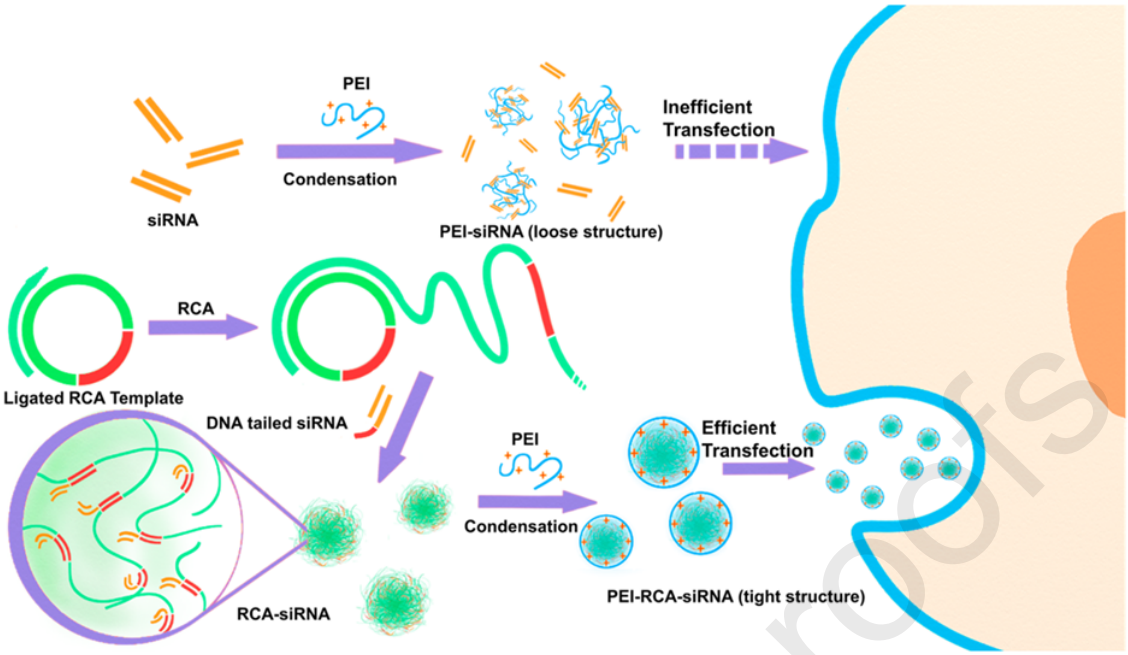

Figure 8. Illustration of the direct complexation of naked siRNA by PEI and the complexation utilizing RCA product as a co-carrier for siRNA transfection. Reproduced with permission form ref [131]; Copyright ©2019, American Chemical Society.

The optimized N/P ratio can also be affected by the length of RNAs. In a different study performed by Zhang *et al*. [132], PEI was conjugated with β-cyclodextrin to deliver single guide RNA (sgRNA). For N/P ≥ 20, all plasmids ranging from 3487 to 8506 base pairs formed large but loose complexes with cyclodextrin. When N/P reached 60, all plasmids was fully condensed into nanocomplexes with the size ~200 nm. When higher N/P ratios were used (≥ 60), induced apoptosis was observed.

Besides of the amine density, other factors like the backbone structure of the polymer also affects the encapsulation and release for RNAs. Blersch *et al*. [133] created a library of light-responsive nanoparticles (160 formulations) exhibiting

physicochemical diversity, aiming at studying their ability to act as nucleotide-delivery systems for siRNAs or miRNAs. Polymers with structural diversities were produced by Michael-type addition chemistry, which was based on the reaction between a photo-cleavable moiety [(2-nitro-1,3-phenylene)bis(methylene) diacrylate] with a set of bisacrylamide and amine monomers. Among which, only 14 types of the polymer exhibited siRNA encapsulation efficiency higher than 80%, and the authors suggested that the encapsulation efficiency of siRNA was rather not solely dependent on positive zeta-potential of the polymer, but also correlated to existence and type of aliphatic moieties in the polymer backbone. As the polymers prepared by bisacrylamide and amine monomers containing linear hydrophobic chains showed better chances for higher siRNA binding efficiency, whereas the polymers containing aromatic rings may interfere the siRNA encapsulation process.

It should be noted that RNAi vectors are usually composed as "hybrid materials", where different type of materials are adapted simultaneously for achieving different purposes. For example, the biocompatible anionic polymer PLGA has been applied in encapsulating siRNA/cationic lipid complex to reduce the toxicity of the cationic lipids and further protect the siRNA from degradation with robust polymeric matrix [73]. The potential mechanism of LNPs encapsulation by hydrophobic PLGA was investigated previously by Jiang *et al.* [134]. Dissipative particle dynamics (DPD) simulations were carried out to simulate the dynamical behavior between PLGA and lipids on the molecular scale. As a result of the surface tension, the lipids will form into a reverse micelles on the surface of water. Upon the addition of PLGA, PLGA molecules will

shrink under the interfacial tension between PLGA and water, along with the encapsulated small reverse micelles fusing to one bigger micelle (**Figure 9A**).

Polymers can also be conjugated with other materials for efficient RNA encapsulation. For example, Zhang *et al.* conjugated PAMAM with PEG_{2k}-DOPE and $mPEG_{2k}$-DOPE, creating mixed dendrimer micelles (MDMs) [135]. Subsequently, the MDMs were coated with HA-conjugated DOPE aiming at 'hiding' the positive charge and provide targeting towards $CD44^+$ cancer cells. When HA-DOPE to MDMs ratio was higher than 0.5, then a negative surface charge, followed by a complete complexation, was observed. The HA-DOPE/MDMs prevented siMDR-1 degradation *in vitro*, improved serum stability, and demonstrated decreased cytotoxicity compared to PAMAM alone.

Besides of that, several studies also focus on core-independent approaches by using polymer brushes. Polymer brushes constitute macromolecular structures with polymer chains densely tethered to another polymer chain or the surface of various structures (*e.g.,* NPs) through covalent or non-covalent binding [136-139]. These brushes cover the NPs' core or the surface they are applied to and allow the complexation of various therapeutics, including RNAs in the interspace, and the size and stability can be feasibly tailored by manipulating the characters of NPs core [125]. Polymer brushes reduce protein adsorption while in parallel enhance the oligonucleotide complexation due to an entropic stabilization, leading to stable oligonucleotide retention.

An example of the use of polymer brushes for RNA delivery was reported by Li *et al*. [125], where poly (dimethyl amino ethyl methacrylate) (PDMAEMA) was used for the

delivery of oligonucleotides with 22 base pairs. The PDMAEMA polymerization process is initiated on the silica NPs surface, and copolymer, poly (dimethyl amino ethyl methacrylate-*b*-oligo ethylene glycol methacrylate (PDMAEMA-*b*-OEGMA) brushes can further conjugated on the NPs surface. The existence of robust silica NPs core could yield a better control over size and NPs stability, whereas the existence of dense polymer brush (0.5 polymer chain/nm^2) will facilitate the RNAs encapsulation. The authors noticed that the polymer density increase can only enhance the encapsulation efficiency for the nucleic acids smaller than 100 base pairs. To further understand the encapsulation mechanism by such method, the authors applied surface plasmon resonance (SPR) chips whose surface is covered by PDMAEMA-*b*-OEGMA, then 0.5 μg oligonucleotides was injected in the chip for evaluating the interactions between polymer brushes and nucleic acids. The results suggested the nucleic acid encapsulation process is kinetically limited by molecular crowding, and the entropic drive for the adsorption of nucleic acids is related to the molecular size, where oligonucleotides (RNAs with the size of 22 base pairs) could penetrate into the core of the polymer brushes to show the best entropic stabilization, whereas large DNA plasmid are mainly anchored on the surface of polymer brush (**Figure 9B-C**). The main reason for the oligonucleotides penetration may be due to the frustrated conformation of polymer chains upon binding with RNAs [140], as when some hydrophobic groups of polymers are inserted in water molecules, the entropic effect leads to a rearrangement of water molecules around the non-polar groups of polymers to stabilize the structure [141].

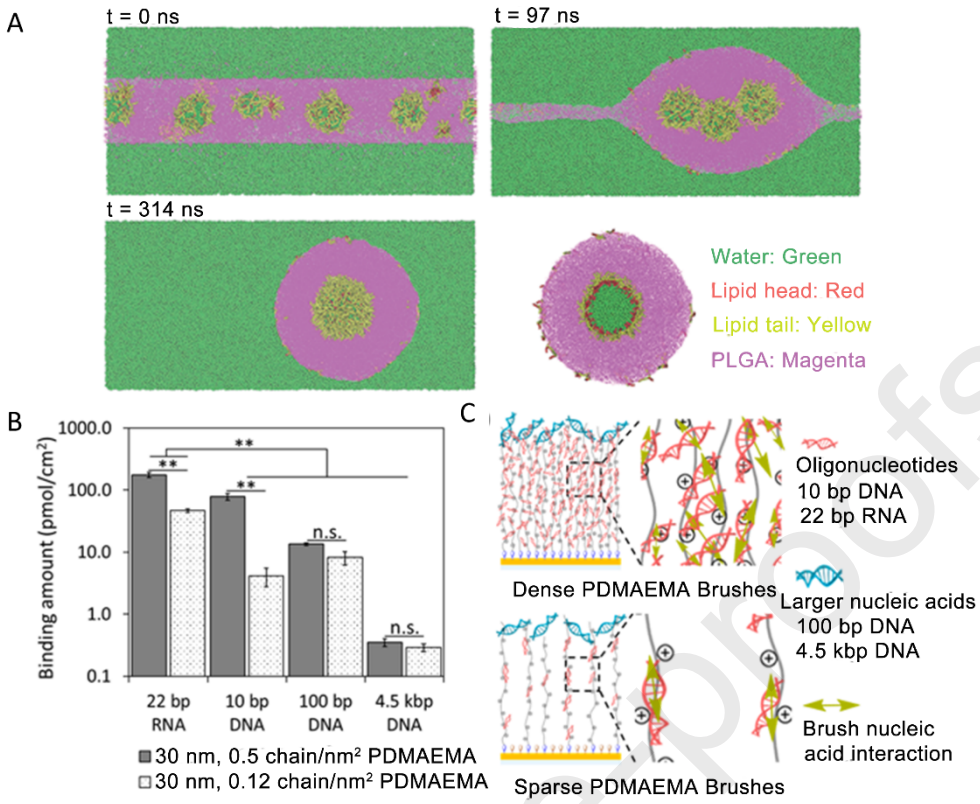

Figure 9. (A) Snapshots of DPD simulation to understand the lipids encapsulation process by PLGA. Water is shown in green, lipid head in red, lipid tail in yellow, and PLGA in magenta. **(B)** Quantitatively evaluation of nucleic acid encapsulation efficiency by brushes polymers with different polymer density. **(C)** Schematic illustration of the interaction between nucleic acid molecules with different base pair with PDMAEMA brushes. Reproduced with permission form (A) ref. [134]; Copyright © 2015, Wiley-VCH; and (B-C), ref. [125]; Copyright ©2018, American Chemical Society.

4.3. Biomacromolecules

Biomacromolecules constitute another class of material used for oligonucleotide delivery [142-145]. Although the term includes various sub-classes like carbohydrates,

proteins, and nucleic acids, due to the brevity concern, we will only focus on carbohydrates in this section. Among these, polysaccharides (*e.g.*, chitosan and dextran) and glycosaminoglycans (*e.g.*, hyaluronic acid) are the most studied carbohydrates for RNA delivery. As in lipid and polymer NPs, the various RNAs are complexed with the biomacromolecules through electrostatic interactions. Therefore the general guideline for optimizing the RNAs encapsulation also fits the principles described above. For example, cationic polysaccharides chitosan has long been investigated for oligonucleotides encapsulation, and previous studies suggested the molecular weight, degree of deacetylation, the chitosan salt form used, and N/P ratio could affect the RNA encapsulation efficiency [146, 147], however the underlying mechanism can be potentially attributed to the altered electrostatic interactions. For example, the work conducted by Holzerny *et al.* measured the binding thermodynamics between siRNAs and chitosan with different molecular weight (44 kDa, 63 kDa, 93 kDa and 143 kDa) and deacetylation degree (ranging from 78% to 86%) [148]. The results suggested, albeit the different molecular weight and deacetylation degree, the chitosan siRNA binding enthalpies (ΔH_{bind}) showed no significant difference among the tested chitosans (**Figure 10**), suggesting the binding type is the same for all types of chitosans. However, experimental molar binding stoichiometry (N_{sat}) was significantly lower than theoretical value, and this phenomenon was more obvious for chitosan with larger molecular weight, as the relative differences between experimental and calculated theoretical values between 44 kDa chitosan was only 86%, whereas this number reduced to 69% for 143 kDa chitosan (**Figure 10**). The difference can also be

explained as previously [149], larger chitosan with higher viscosity will hinder the electrostatic interactions. This phenomenon was also consistent with the saturated N/P ratio (N/P_{sat}) and binding constant (k_D), whose values are progressively increased with higher Mw and lower deacetylation degree.

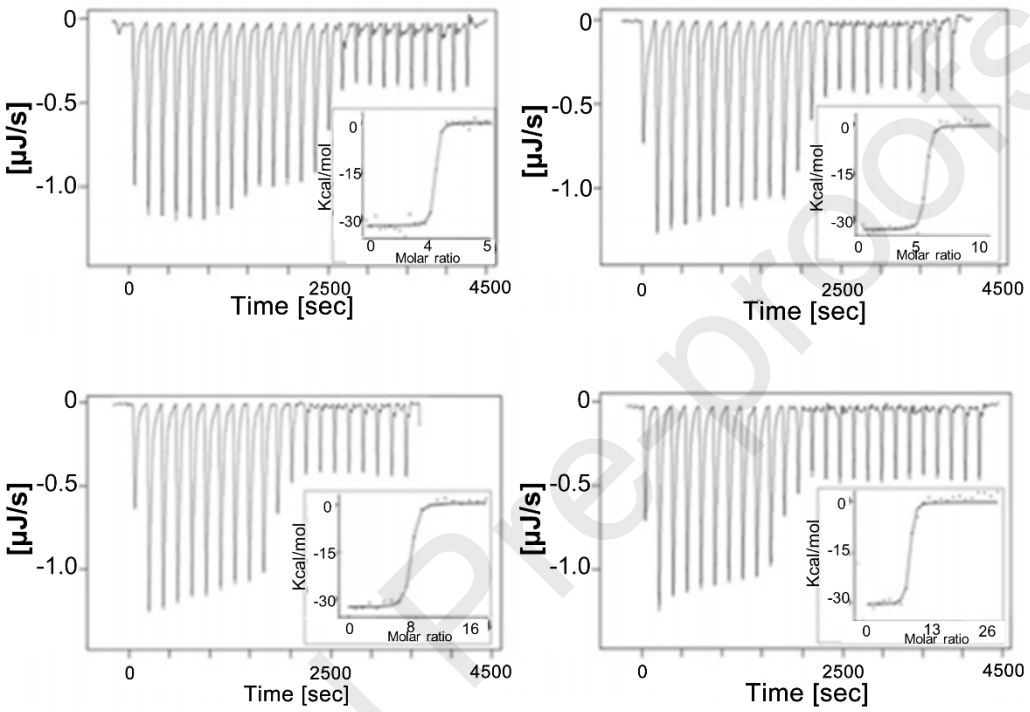

Chitosan Mw	K_d [nm]	ΔH_{bind} [kcal/mol]	N_{sat} (siRNA: chitosan) [mol]	N: P_{sat} [b]
44 kDa	1 ± 0.1	-102 ± 14	4.2 ± 0.5 (4.8)[a]	1.1
63 kDa	1.5 ± 0.6	-97 ± 5	5.2 ± 0.1 (6.7)	1.2
93 kDa	1.9 ± 0.6	-84 ± 5	8 ± 0.5 (9.6)	1.2
143 kDa	1.9 ± 0.7	-84 ± 5	9.6 ± 0.6 (14)	1.5

a Brackets: theoretical, calculated values for full saturation
b Experimentally determined values resulting fron N_{sat}

Figure 10. Representative examples of binding isotherms of interactions of chitosans with molecular weight (Mw) of 44 kDa (up-left), 63 kDa (up-right), 93 kDa (down-left) and 143 kDa (down-right) with siRNA, and the corresponding quantitative data. Reproduced with permission form ref [148]; Copyright © 2012, Elsevier B.V.

Practically, two parameters are mainly involved in optimizing the encapsulation efficiency of oligonucleotides by macromolecules. First one is the N/P ratio. Different from lipids based materials, where the N/P ratio is rather low. For polysaccharides, despite the theoretical saturated N/P ratio is around 1 [148], the actually applied N/P ratio usually ranges from 20 to 300 [147, 148]. As results suggested low N/P ratio will yield physically unstable complexes. Previous study showed that for chitosan/siRNA complex with the N/P ratio of 5, a severe aggregation can already be observed only after 15 min post complexation even under high ionic condition (150 mM NaCl) [150]. The RNA encapsulation efficiency and the colloidal stability will increase along with increased N/P ratio [147, 150]; however, this may result in a limitation in the release of the encapsulated RNA [151, 152].

The pH-value during RNAs encapsulation process also heavily impact the encapsulation efficiency, as their surface charge is closely dependent on the pK_a value [153]. For example, Alameh *et al.* showed the effect of chitosan's deacetylation degree, molecular weight, and N/P ratio on the siRNA encapsulation efficiency at two different pH levels. Under pH 6.5, the siRNA encapsulation efficiency was almost independent of any of these parameters, whereas a sharp contrast was observed under pH 8, that an efficient siRNA encapsulation can only be achieved with high N/P ratio, high chitosan molecular weight and high deacetylation degree (**Figure 11**) [150]. As under high pH-value, chitosan glucosamine units become deprotonated, and their interaction with siRNA phosphate groups decreases to promote payload release [153]. The general pK_a values for commonly used carbohydrates are, hyaluronic acid ~3.0 [154, 155], dextran

~ 6.0 to 7.1 [156, 157], and chitosan 6.4 to 6.6 [158, 159]. These values allow an optimal design for siRNA encapsulation/complexation since below a certain pH the elctrostatic interactions between the positively charged biomacromolecule and the RNA therapeutic are enhanced.

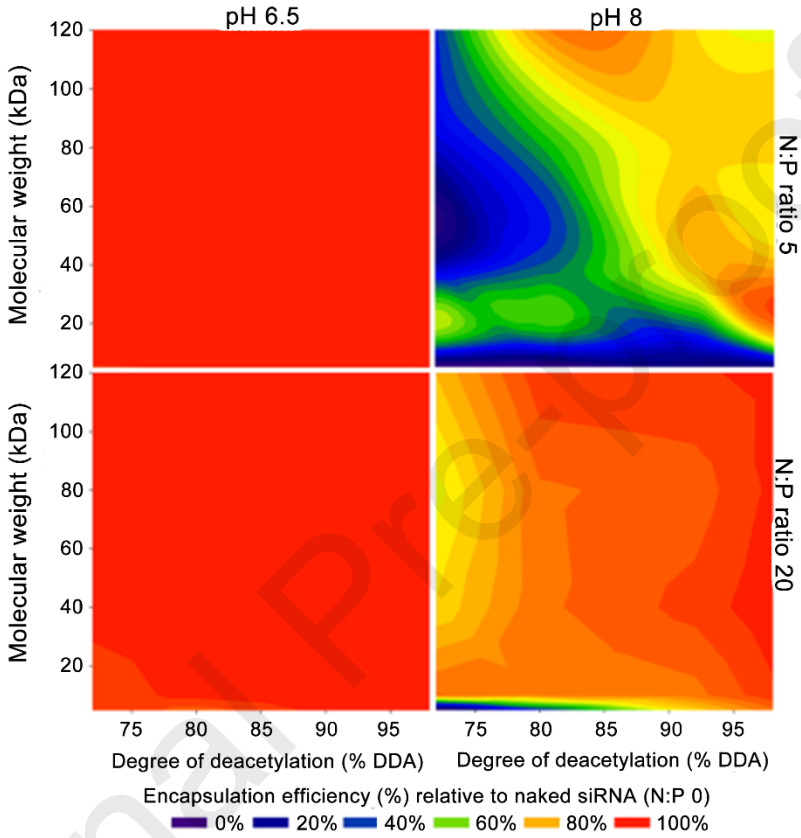

Figure 11. Synthesizing NPs under the pH value above the pK_a shows a significant impact on the encapsulation efficiency of siRNA. Figures are modified and reproduced with the permission from ref [150]; Copyright © 2018, American Chemical Society.

The complexation between anionic carbohydrates, such as dextran or hyaluronic acid, and oligonucleotides is challenging, and the common way to solve this issue is through chemical modification with cationic moieties [160, 161]. The chemical modification can simultaneously be achieved by on-demand linkages to further promote the release

behavior of loaded RNAs. As an example, Chen *et al*. [162] developed acid-degradable dextran NPs (conjugation of dextran with amine-containing molecules through acetal bonds) cleaved at low pH, allowing the encapsulated siRNA to be released intracellularly. Similar example by Qu *et al*. conjugated two different molecular weight dextran with two other peptides creating four independent systems that were tested for their knockdown efficiency on Proprotein convertase subtilisin/kexin type 9 (PCSK9) expression on HepG2 cells. The used peptides were composed of arginine (R) and lysine (K) that provided the nucleic acid binding domain, histidine (H) as the RNA binding moiety as well as facilitating endosome escape, and cysteine as a linker between dextran and short peptides [156]. These results showed that higher arginine content demonstrated better RNAs encapsulation as well as transfection efficiency.

4.4. Inorganic NPs

Major advantages from biocompatible inorganic NPs come from their ultrahigh stability and highly advanced physiochemical properties, such as electro, optical, thermal and magnetic capabilities, making them not only suitable for loading various type of cargos, but also highly efficient for imaging and diagnosis [163-165]. Different RNA encapsulation methods are adapted based on the morphology of inorganic NPs (dense, porous or hallow). For NPs with dense core, such as gold NPs or quantum dots, the efficient oligonucleotides loading can be achieved by simply covalent conjugation. Firstly proposed in 1996 [166], the most commonly applied covalent conjugation method is achieved by utilizing NPs with thiolated surface to stably form disulfide bonds with thiol-terminated synthetic RNAs, and the disulfide bonds can further be

cleaved by glutathione (GSH) to steadily release the RNAs [167, 168]. Besides of the disulfide bonds, other chemical groups such as maleimide, haloacetyl and pyridyl disulfide are also widely applied in NPs functionalization to form into RNAs-NPs conjugates [169, 170]. The RNAs loading or conjugation efficiency by this method is vastly dependent on the morphology of the NPs and the conjugation method. For example, Lei *et al.* demonstrated how the size of NPs affect the siRNA conjugation capacity [170]. Gold nanoclusters with the size of 2.6 nm exhibited near 100-fold higher siRNA conjugation efficiency (226 μmol siRNA per g of gold cluster) comparing to gold NPs with the size of 13 nm (2.62 μmol siRNA per g of gold NPs), and the authors attributed the difference to the smaller size induced larger specific surface area [170]. Besides of direct conjugation, the other commonly applied method is by modifying the NPs with cationic polymers, either by covalent conjugation or layer-by-layer deposition [167, 171], to facilitate the electrostatic binding of RNA, as we discussed in Section 4.2.

RNAs can also feasibly resides in inorganic NPs with porous or hollow cavity (porous silica/silicon NPs, carbon based NPs) [164, 172-174]. However, the issue of burst release has emerged as a major obstacle for directly loading the RNAs in porous or hollow nanostructures, and the engineering strategy by creating a core/shell structure has been extensively investigated to solve this issue [175]. The shell formation process can be further roughly divided into post-shell formation, where the RNAs are first loaded into the porous/hollow nanostructure, and the NPs are sequentially encapsulated by a shell structure [165, 176]; and *in-situ* shell formation, where the RNAs are

simultaneously co-encapsulated along with the shell deposition [177, 178]. For the post-shell formation protocol, the RNAs loading capacity is highly dependent on the porosity of the core inorganic materials. Based on the equation proposed by Sang *et al.* to describe absorption isotherm of biomolecules at their isoelectric point on nanoporous materials [179], using Equation (1):

$$\Gamma_{internal} = \left(\frac{N_{pore}M}{N_A\delta}\right)\left(\frac{V_t}{A_p}\right) \quad (1)$$

where, $\Gamma_{internal}$ indicates the totally absorbed materials in the pores per mass of porous NPs, M is the molar mass of the biomolecules, N_A stands for Avogadro's number, δ stands for the dimension of the biomolecules, V_t is the total pore volume, A_p is average cross-sectional pore area, and N_{pore} stands for the theoretical number of biomolecules that can reside in a single pore, which is correlated with the dimension of the biomolecules and pores.

Considering the typical hydrodynamic dimension of siRNA with 20 base pairs is 6 nm × 3 nm [180, 181], the degree of cationic groups functionalization may only exhibit low-to-no effect on increasing the siRNA loading capacity in mesoporous materials with the pore diameter lower than 3 nm. This hypothesis was confirmed by Steinbacher *et al.* [182], who demonstrated for mesoporous silica NPs with pore diameter of 4 nm, degree of surface functionalization by cationic diethylenetriamine (DETA) showed minimal effects on siRNA loading degree. As with the increasing amounts of amine functionalization (pristine silica NPs treated with 0.5%, 2.5%, 15% DETA), the maximum specific adsorption of siRNA only marginally increased from 14 μg

(siRNA)/mg (silica NPs) to 18 μg/mg. However, a sharp contrast was observed for mesoporous silica NPs with pore diameter of 8 nm and 15 nm, where a ~3-fold maximum siRNA adsorption was observed (13 μg/mg *vs.* 36 μg/mg) [182]. It should be noted that, large pore size will conversely result in a weaker siRNA interaction at higher siRNA loadings, as the dissociation constant, K_d, increased with increasing amounts of amine functionalization. As a result, in a typical amine-functionalized mesoporous silica NPs with pore diameter ranging from 4 nm to 15 nm, 20–40% of loaded siRNAs will be immediately released once upon re-dispersing into aqueous solution [182]. Thus, one potential issue for post-shell formation method is the potently reduced encapsulation efficiency due to the burst release of RNAs during shell formation process.

Typical *in-situ* shell formation process is usually achieved by adapting calcium ions. Calcium ions chelate and condense RNAs through the Ca^{2+}/P binding, and the Ca–RNA complexes can be reversely disintegrated by competitive Ca^{2+} chelating agent or acidic condition [183, 184]. Taking advantages of the RNAs capturing capability, an *in-situ* shell formation process was developed for sealing the porous silicon NPs. As a result of the fast silicon backbone degradation, a high local concentration orthosilicic acid will be generated at the pore site. Upon the addition of solutions containing high concentrations of Ca^{2+} and siRNA, the porous structure will be sealed by the *in-situ* formed Ca_2SiO_4 shell structure and siRNA will be simultaneously entrapped in the shell structure [177, 178]. Similarly, calcium can also anchor and mineralize lipid or polymer layer to stabilize the nanostructure or generate a responsive RNAs release manner [185-

187]. Comparing to directly adapting shell materials for loading RNAs, the core/shell formation is featured with self-limiting growth behavior, therefore can feasibly control the physiochemical characters of the nanocomplex by altering the core structure, and inorganic NPs core supported shell structure may also promote the stability of nanocomplex.

5. Targeting strategies

Efficient and precise targeting capability of NPs are of particular importance for NPs based RNAi due to the ultrahigh sensitivity of RNAi. However, in the field of NPs-based RNAi, targeting methods showed no major difference with other NPs based targeting modalities, and readers may refer to more specific reviews regarding to the NPs targeting [188, 189]. In this section, however, we will only discuss the tendency of the recent studies, and highlight their outcomes in detail.

We identified recent changes over time on the target of NPs based RNAi by investigating changes in keywords from the top 200 most relevant scientific papers that include “nano” and “RNA interfering” over the periods 2016–2018 and 2019–2021. We manually selected relevant words associated with organs, tissue, and cells to focus on the target of NPs based RNAi. Our results (**Figure 12**) suggest that cancer targeting remains the hottest topic for NPs based RNAi throughout the two investigated periods. However, while NPs based RNAi have been applied into broader diseases criteria, we observed an increasing tendency in research works focused on manipulating the immune responses or navigating the NPs interaction with immune cells, as reflected by

an increase over time of the frequency of keywords, including "Immunity", "Inflammation", "Vaccine", "Cytokine", "Macrophages", and "Lymphocytes". **Table 2** lists typical studies that conducted RNAi for immune cells during the recent years. Immune responses are pervasively involved in multiple diseases and can even be main pathogenesis regulator [190, 191]. Massive immune cells infiltration and accumulation is usually a key feature for lesional tissue [192, 193], therefore the targeting efficiency for organ or cells, such as heart and brain, which are conventionally thought to be difficult for targeting, can also be potentially increased by manipulating the NPs interactions with immune cells, and thus, are also drawing more attention for investigation (**Figure 12**).

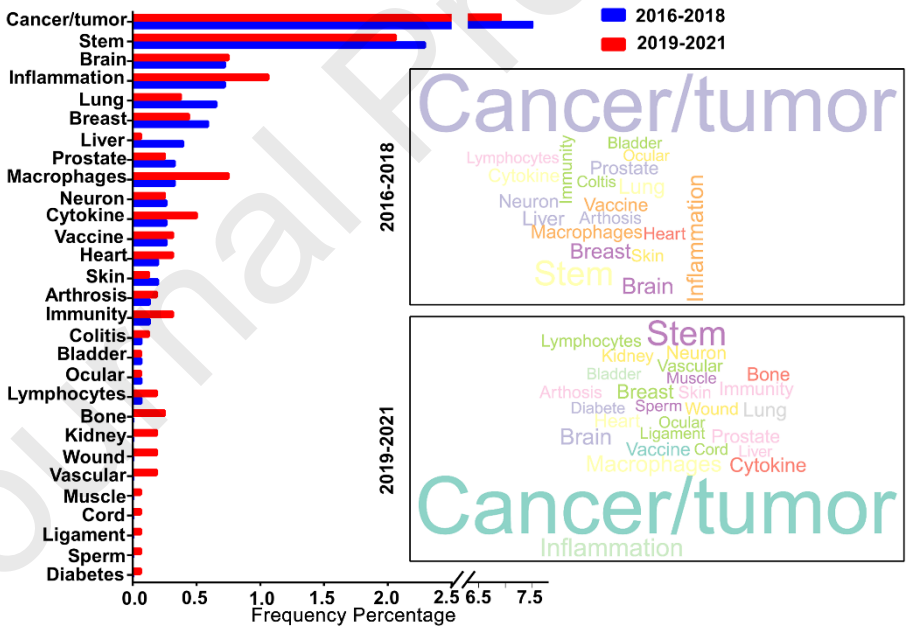

Figure 12. Visualization of the most frequent words related to the organ/tissue/cells from keywords of scientific papers using Scopus Search "Nano" + "RNA interference" over two time periods: 2016–2018 and 2019–2021.

Table 2. Recent examples of navigating NPs through targeting to immune cells.

Organ	Targeted immune cell subsets	Targeting method	Reference
Brain	Microglia	Radiation therapy facilitate macrophages recruitment + iRGD peptide modification for recognizing αvβ3 and αvβ5 integrins	[194]
	Microglia	Surface modification of mannose	[195]
Heart	Macrophages	Altering the size of NPs	[196]
	Macrophages	Surface modification of S2P peptide for targeting stabilin-2 receptor	[73]
	Macrophages	Surface modification of mannose	[197]
	Macrophages	Surface modification of CD36 antibody	[198]
	Macrophages	Passive targeting by chitosan based NPs	[158]
Solid tumor	Tumor associated macrophages	Passively uptake by tumor associated macrophages	[199]
	M2 macrophages	Surface modification of mannose	[200]
	Circulating monocytes	Changing the surface zeta potential from neutral to cationic	[201]
Spleen and lymph nodes	$CD4/8^+$ T cells	Surface modification of anti-integrin β7 monoclonal antibodies	[202]
Spleen	T cells	High throughput-screen to select the splenic tropism ionizable lipid	[203]
Liver and epididymal white adipose tissue	Neutrophils	Decreasing the PEG percentage on NPs surface and enhance the surface zeta-potential	[204]
Lung	Macrophages	Surface modification of fluorinated helical polypeptides	[205]
	Macrophages	Surface modification of cyclic peptide CRV (sequence CRVLRSGSC)	[206]
	T cells	Surface modification of cell-penetrating peptide dNP2	[207]
	Macrophages	Altering sizes of NPs	[208]
Colon	$Ly\text{-}6C^+$ leucocytes	Surface conjugation of Ly-6C antibodies	[209]
Bone marrow	Haematopoietic stem-cell niche to affect leukocytes behavior	Altering molecular weight and surface density of the PEG, altering the length of the lipid chain that anchors PEG, as a result, the formulation with lipid tail length C18, PEG Mw 5000 and PEG percentage of 10 mol-% showed the highest targeting capability	[210]
Not specified	Blood resident macrophages	In situ light irradiation to switch the surface charge of NPs from negative to positive	[211]

For example, Bejerano *et al.* [196] developed a system able to target the macrophages recruited to the heart after myocardial infraction (MI) by taking advantage of the leaky vasculature and their accumulation in the site of inflammation. It is known that in the

infarcted myocardium the vasculature is leakier and allows the accumulation of particles with size comprised between 20 and 200 nm [212, 213]. Based on that, the authors developed a siRNA loaded NPs composed by hyaluronan-sulfate, Ca^{2+} and miRNA. The spontaneously formed nanocomplex obtain the size of 130 nm with surface zeta-potential of −10 mV. The cardiac targeting capability of the NPs was evaluated on mice with MI, which is established by left anterior descending (LAD) coronary artery ligation. NPs were injected intravenously and the heart of mice was collected five hour post NPs injection, and the authors found the highest cardiac accumulation was observed at 3 days post MI. Comparing to health mice, the cardiac NPs accumulation in MI mice was increased for over 25% [196]. Similar work was recently conducted by Tao *et al.*, who specifically targeted lesional macrophages to improve atherosclerotic plaque stability [73]. siRNAs targeting Ca^{2+}/calmodulin-dependent protein kinase (CaMKIIγ) was loaded in cationic lipid–like material G0-C14, and the siRNA complex was further encapsulated by PLGA to better protect the siRNA core. Furthermore, a peptide called S2P, which recognizes the macrophage receptor stabilin-2, was conjugated to 1,2-distearoyl-sn-glycero-3-phosphoethanolamineN-[maleimide(polyethylene glycol)] (DSPE-PEG-Mal), and the yielded DSPE-PEG-S2P was applied for coating the siRNA encapsulated PLGA NPs. Murine atherosclerosis model was established by feeding low density lipoprotein receptor deficient ($Ldlr^{-/-}$) mice with adjusted calories diet (21.2% fat) for 12 weeks, followed with intravenous injection of NPs. *In vivo* results showed the specific macrophages targeting by S2P significantly increased the percentages of NPs containing macrophages in aortas

harvested from atherosclerotic mice 24 h after injection comparing to the non-targeted ones (14.4% *vs.* 5.7%), which resulted in lower plaque necrosis and increased lesional efferocytosis.

The immune cells targeting strategies are also adopted for targeting lungs. Kim *et al.* modified the siRNA containing fusogenic liposomes with a nine-amino peptide named CRV (sequence CRVLRSGSC) for targeting macrophages and further applied for *Staphylococcus aureus* lung infections [206]. CRV was selected in a phage library screen for cultured J774A.1 murine macrophages with selective macrophages targeting capability, and the CRV modification of fusogenic liposomes increased the lung accumulation of fusogenic liposomes to over 20% after 1 h of injection, which is mainly due to the specific NPs accumulation in macrophages after pulmonary *Staphylococcus aureus* infection (**Figure 13A**).

Besides of the direct targeting towards immune cells, other works by taking advantages of immune cells as RNAi vectors are also investigated. Wayne *et al.* cultured macrophages (C57BL/6 murine macrophages IC21) with siRNA loaded a commercially available lipoplex transfection reagent (geneSilencer, Genlantis) *in vitro*, and the adoptively transferred macrophages were further injected to mice for targeting breast cancer (xenograft model with MDA-MB-468 breast cancer cells) [214]. After injection, the macrophages infiltrated into solid tumor, with 2% of the total tumor cells were $siRNA^+$. And the siRNA can be further excreted to the tumor microenvironments through Rab27a recycling pathway, sequentially exerting the gene knockdown function to cancer cells (**Figure 13B**).

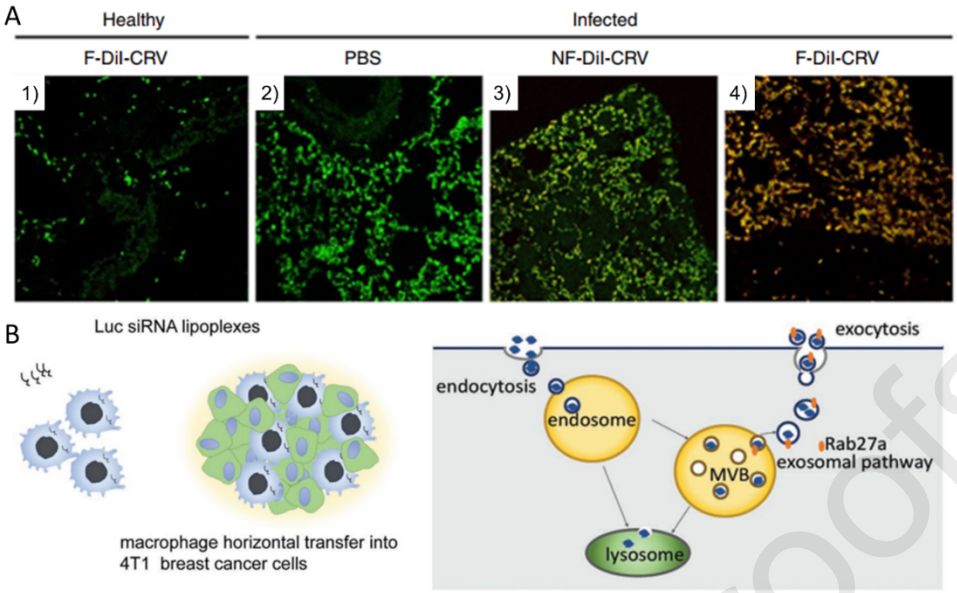

Figure 13. (A) Confocal microscope images of fluorescein (DiI) loaded fusogenic (F-DiI-CRV) and non-fusogenic nanoparticles (NF-DiI-CRV) homed to infected lung with macrophages targeting moiety CRV. Different NPs are injected intravenously under healthy (1) or *Staphylococcus aureus* infection (2-4) conditions. Green, macrophages; red, DiI from NPs. **(B)** Schematic of horizontal RNA transfer facilitated by macrophages and corresponding exosomal secretory pathway. Modified and reproduced with permissions from (A) ref. [206] © Copyright 2018, Springer Nature; and (B) ref. [214]; Copyright © 2019, Wiley-VCH.

From a technical point of view, for the targeting methods, the most commonly applied method is through the "targeting ligands functionalization" approach. However, chemical conjugation of targeting ligands may involve extra chemical reactions, which may be limited by complex procedures and high batch-to-batch variation. A recently developed biosynthetic method allow a customized routine to physically coat all types

of antibodies on the surface of NPs [78], which are further applied for targeting different leukocytes. A specific lipoprotein (anchored secondary scFv enabling targeting, ASSET) was biosynthesized and purified from *Escherichia coli* [215]. Composed by two critical segment: (1) N-terminal signal sequence followed by a peptide which will undertake lipidation in the membrane of *Escherichia coli*; and (2) single chain antibody fragment (ScFv) of a monoclonal antibody (clone RG7/1.30) to bind with crystallizable fragment (Fc) constant region of Rat IgG antibodies. This lipoprotein can effectively bind with a different types of antibodies with the dissociation constant K_d of ~22.7 nM, and the lipidized part can spontaneously inserted into LNPs which encapsulate siRNA. The ASSET-loaded LNPs can be coated with diverse antibodies to target different leukocytes including $CD25^+$ T regulatory cells, $CD3/4^+$ T cells, $CD9^+$ B cells and $CD11b^+$ monocytes *in vivo*.

Besides of the conventional "targeting ligands functionalization" approach, other efforts have also been made to achieve a targeting-ligands free manner for RNAs delivery towards specific leukocytes subsets. Among which, typical methods like tailoring the NPs' surface property to alter the organ or cellular accumulation has been extensively investigated. The fundamental mechanism for the cell tropism from different NPs is speculated to be influenced by changes in their surface potentials and/or internal charges [216]. Generally, NPs with neutral surface charges exhibited longest circulation behavior, whereas anionic NPs (surface zeta-potential < –20 mV) strongly interact with reticuloendothelial system (RES), such as scavenging endothelial cells or blood resident macrophages, and cationic NPs are preferably uptake by virtually all cell

types, and they can be rapidly interact with the anionic surface of the blood vessel walls, and sequentially cleared via RES [217, 218]. Therefore, based on specific haemodynamics and resident cell type in different organs, the control over the internal and external charge of the NPs may subsequently resulted in organ or cellular tropism [219]. For example, Cheng *et al.* generated a strategy named as Selective Organ Targeting (SORT) which enabled the LNPs targeting of lung, liver and spleen [220]. Despite the paper aimed to deliver mRNA, Cas9 mRNA/ single guide RNA (sgRNA) and Cas9 ribonucleoprotein (RNP) complexes but not for RNAi, yet the detailed targeting strategy may be also transferred for RNAi based NPs design. In this work, different cationic, anionic, and zwitterionic molecules were added in different molar ratios to LNPs of pre-determined composition. The results found that with the increasing ratio of permanent cationic lipid SORT molecules (*e.g.*, 1,2-dioleoyl-3-trimethylammonium-propane, DOTAP; dimethyldioctadecylammonium, DDAB; 1,2-dimyristoyl-sn-glycero-3-ethylphosphocholine, EPC) in the formulation, the major LNPs accumulation gradually transferred from the liver to the spleen and eventually to the lung. With the addition of 50% of DOTAP, 80% of the LNPs accumulated in lung and transfected ~40% of all epithelial cells, ~65% of all endothelial cells and ~20% of immune cells. Whereas the addition of anionic lipid SORT molecules (1,2-dioleoyl-sn-glycero-3-phosphate, 18PA) enhanced the LNPs' accumulation in spleen, which transfected ~12% of all B cells, ~10% of all T cells, and ~20% of all macrophages. Interestingly, addition of ionizable cationic lipid (1,2-dioleoyl-3-dimethylammonium-propane, DODAP) significantly avoid the interaction with phagocytes, as rather than

Kupffer, 93% hepatocytes were transfected by the injected LNPs. Similarly, other reports suggested by reducing the surface PEG density and enhancing the surface charge could promote the NPs interaction with circulating monocytes and neutrophils, as such enhancing the siRNA delivery efficiency (**Figure 14A,B**) [201, 204]. The results suggested the critical function in manipulating the external/internal charges for altering the NPs interaction with immune cells.

However, this phenomenological approach to understand the "structure-tropism" is usually achieved with 1-by-1 *in vivo* analysis, which needs extensive lab work and animal numbers. A high throughput approach method is recently developed for screening T cells targeting NPs [203]. In this work, the authors adapted a phage-library-like strategy, and formulated over 100 types of LNPs with different lipid composition. Each type of LNPs will co-encapsulate a unique type of DNA sequence, as the function of "barcode" to identify the LNPs, and siRNA to knockdown GFP as RNAi readout. Then different LNPs were mixed, and the "LNPs cocktail" was injected to GFP expressing mice. After 3 days, the GFP^{low} cells were isolated and the "barcode DNAs" were deep sequenced for determining the LNPs that are preferably colocalized in GFP^{low} cells (**Figure 14C**). In this manner, the authors screened out an ionizable lipids which endows the LNPs massive accumulation in splenic T cells, and concluded that helper lipid DSPC containing LNPs will facilitate the splenic T cells targeting whereas DOPE containing LNPs will conversely reduce the ability.

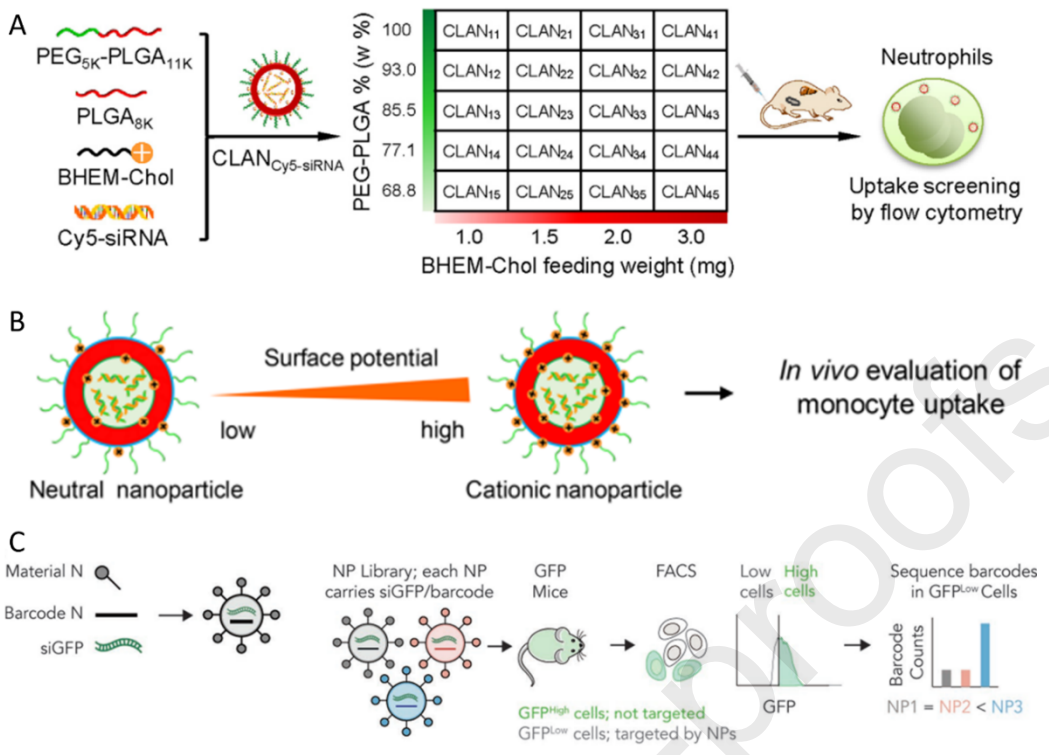

Figure 14. (A) Increasing the neutrophil targeting capability of NPs can be achieved by increasing the percentage of cationic lipid (N,N-bis(2-hydroxyethyl)eN-methyl-N-(2-cholesteryoxycarbonyl-aminoethyl) ammonium bromide, BHEM-Chol), or reducing the PEG density on NPs' surface. As a result, the formulation with the term $CLAN_{45}$ exhibits best neutrophils interaction capability. **(B)** Increasing the surface charge can also promote the targeting capability of siRNA loaded NPs towards monocytes. **(C)** Scheme for high throughput screen to select ionizable lipids which can potentially enhance the targeting capability of LNPs towards T cells. Modified and reproduced with permissions from (A) ref. [204]; Copyright © 2018, Elsevier B.V.; (B) ref. [201]; Copyright © 2018, American Chemical Society; and (C) ref. [155]; Copyright © 2019, Wiley-VCH.

6. Endosome escape

Endosome escape is the last, but a critical step, for successful NPs based RNAi [19, 20]. During the past decades, there has been significant progress in endocytosis mechanism and endosomal environment research. Such knowledge provides the basis of endosomal escape strategies, and the related endosomal escape mechanism studies. In the following sections, we first introduce the endosomal environment. Then we explain the current understanding of different endosomal escape mechanisms, and introduce the common reagents and materials used for siRNA endosomal escape. Specifically, we highlight prototypical examples of siRNA endosomal escape systems, and analyze the advantages/disadvantages of the material designs. Finally, we discuss the critical challenges and unresolved issues in the endosomal escape progress for future development.

6.1. Physiological environment for different endosome compartment

As we discussed in Section 2.2., endosome escape of siRNA will exclusively occur in specific endosome compartment. Therefore, understanding the physiological properties for each compartment is important for guiding the design and choose of endosome escape materials. Despite the different uptake mechanisms, most uptake vesicles fuse with early endosomes (EE). EE plays a very important role in the endocytosis process, because it acts as a “sorting center” of the endocytosed substances [39], similar to the sorting center of parcels in real life. The housekeeping membrane proteins, such as

transferrin receptors, are recycled to the plasma membrane surface, while those proteins to be downregulated go through the endosomal maturation process and degraded in lysosomes eventually. The different fate of endocytozed vesicles are regulated mainly by the Rab family of GTPases [221]. There are 70 Rab encoded in human's genome and more than 40 Rab are involved in the endocytic pathway regulations [222]. For example, Rab5 is enriched on EE membranes, and subsequently switch to Rab9 on late endosomes (LE, also named as multivescular body, MVB) membranes [221]. These Rab GTPases on the endosomal surface are similar to the barcode stick to the parcels, which direct the endosomal vesicles to different destinies. The directed transport relies on the binding of endosomal vesicles to actin filament- and microtubule-associated motors [221]. For example, Rab11 is a critical protein on the recycling endosomal surface [223]. By binding with actin filament-motor MYO5B, Rab11coated endosomes are exclusively transported back to plasma membranes [224]. Such delicate regulation of endosomal vesicles in the intracellular trafficking suggests the critical role of endocytosis for cell metabolism. Thus, the potential damage to the endocytosis machinery may lead to the metabolic disorder within the cell, or even cell death.

Regarding the endosomal environment, the membrane-bounded endocytic vesicles are very dynamic, with continuous ions and substances exchange with cytoplasm, Golgi apparatus and endoplasmic reticulum (ER) [39]. Specifically, endosomal environments have several characteristics distinguishable from cytoplasmic and extracellular environments. The most prominent character is the acidic lumens. The pH continuously decreases from early endosomes (pH 6.1–6.8) to late endosomes (pH 4.8–6.0), and

finally to lysosomes (pH around 4.5) [39]. The unique acidity is because of the continuous proton influx by vacuolar H(+)-ATPases (V-ATPases) [225]. The acidification of endosomal lumens is crucial for endosomal function, because it allows for the uncoupling of receptors and the binding ligands, and for maintaining the enzymatic activities within lysosomes. The acidic endosomal lumens also inactivates toxins and pathogens uptake by endocytosis, and protects cells from foreign invasions.

Other acidity, endosomal lumens also have identical ion concentrations compared with extracellular fluids. For example, Na^+ concentration decreases along the endosomal pathways from 120 mM (in extracellular fluids) to 20 mM (in lysosomes), while K^+ concentration gradually increases from approximately 5 mM to 60 mM [226]. Like Na^+, Ca^{2+} concentration has been found much lower in endosomal vesicles [227]. Regarding anions such as Cl^-, the concentration in EE is lower than extracellular environment, but during endosomes maturation, Cl^- concentration showed an increased trend probably due to the ion exchanges through intracellular chloride channels [228]. Similar to pH homeostasis, ion balance is important for endosomal function, including luminal osmolality maintenance, pH regulation, protein activation or even endosomal membrane curvature [226].

Besides the luminal contents, endosomal membranes have attracted significant attention because of their characteristic lipid compositions [229]. Although EE shares the similar membrane composition as plasma membranes, LE has a unique lipid, lysobisphosphatidic acid (LBPA) (or bis(monoacyl glycero)phosphate, BMP) [230]. Despite the continuous membrane flow and vesicle fissions/fusions, LBPA is

exclusively presented on EE membranes, and the membranes of intraluminal vesicles inside EE [229].

Based on the unique characters of endosomal lumens and membranes, there are several strategies developed for the endosomal escape, by entire endosomal rupture, or endosomal membrane destabilization or membrane fusion [231]. It is critical to ensure that all these strategies use endosomal environmental components, such as protons, enzymes and lipids, as triggers to ensure that the membrane disruption is limited to endosomes and lysosomes. Otherwise, the universal disruption on cellular membranes will lead to undesirable toxicity. In the following sessions, we will explain these endosomal escape strategies and discuss specific delivery systems applying these strategies.

6.2. Endosomal escape by rupture

Endosomal rupture is the first and most prominent endosomal escape strategy proposed [232]. Different types of endosomal rupture mechanisms are summarized in **Figure 15**. Endosomal rupture can originate from imbalanced osmotic pressure between the endosomal lumen and cytoplasm (**Figure 15A**). As V-ATPases import protons to endosomes, the counter ions Cl^- are also imported to balance the charge [233]. The chloride ion influx is accompanied by water influx, which increases the osmotic pressure inside endosomes [234]. In the presence of a buffering polymer, excessive protons are supposed to flow inside the endosomes, because the buffering polymer inhibit the endosomal acidification. The excessive protons, Cl^- and water intensify the

endosomal swelling and eventually lead to endosomal rupture [235].

This so-called "proton-sponge" hypothesis has been proposed to explain the endosomal escape mechanism of several cationic macromolecules, such as PEI, PDMAEMA, chitosan and PAMAM [232]. These polymers have ionizable primary, secondary, tertiary amine groups with buffering capacities within endo/lysosomal pH ranges [235]. However, evidence has shown that the buffering capacity alone does not make polymers escape from endosomes [236]. It was found that on model lipid membranes and plasma membranes, cationic PEI and PAMAM interact anionic membrane lipids via electrostatic interactions, and destabilize local membranes to create nanoscale pores [237]. This is supported by the real-time confocal microscopy images, confirming that PEI polyplexes induced transient membrane pores, where the payloads were burst released to the cytoplasm [238]. These results indicate that the "proton sponge" effects did not cause complete endosome lysis. Instead, after endosomal swelling, cargos escape from endosomes by the membrane defects caused by cationic polymer carriers (**Figure 15A**).

However, recent evidence argues the role of membrane defects during endosomal escape. Vermeulen *et al.* found that the membrane defects may prevent endosomal escape of macromolecular cargos [239]. In their study, similar burst release of oligonucleotides from endosomes enabled by PEI carriers was observed, but the release only happened to <10% polyplexes containing endosomes. Despite the unsuccessful escape, the majority of endosomes showed membrane leakiness, evidenced by the release of a small fluorescent molecule. The authors hypothesized that the membrane

leakiness prevented effective buildup of the osmotic pressure, thus preventing the cargos from burst release. The authors also found that endosomes with smaller sizes were more prone to the burst release than those larger ones, indicating both the size and membrane leakiness played a role in the final endosomal escape.

While the exact mechanism of "proton sponge" is still under debate, other approaches to induce endosomal rupture are being investigated. For example, vapor nanobubbles are proposed to break the endosomal vesicles, triggered by ultrasound or laser (**Figure 15B**). The bubble liposomes filled with perfluoropropane gas were applied to cells pre-treated with pDNA encapsulated liposomes [240, 241]. Then the cells were exposed to ultrasound, inducing transient pores for endosomal escape [242]. In terms of laser-triggered nanobubble generation, plasmonic nanoparticles (typically gold NPs) are applied to cells, exposed to high energy pulsed laser. The energy of the laser pulse (<10 ns) is transferred to heat by the gold NPs and vaporizes the surrounding water, generating nanobubbles, which quickly expand from the gold NP's surface and collapse [243]. The mechanical energy of the shock wave can generate transient pores on endosomal vesicles, allowing for endosomal escape of protein, siRNA and pDNA [244]. It was found that the endosomal escape enabled by laser-induced nanobubbles is efficient, and independent of cell type [245]. Moreover, with optimized laser energy and exposure time, this technique was non-cytotoxic, without any long-lasting effects on cell hemostasis [245].

Finally, some carriers can induce endosomal membrane rupture simply by physically piercing the membrane. For example, some NPs have sharp or prickly surfaces, which

enables much better cytoplasmic delivery than the round counterparts. This has been evidenced by prickly nanodiamonds, zinc-doped copper oxide nanoparticles, and star-shaped gold NPs [246, 247]. Another example reported a liquid metal NP, which has light-induced morphology transformation from nanospheres to nanorods [248]. The high aspect ratio nanorods led to physical disruption of endosomal membranes, visualized by confocal and electron microscopies [248]. Despite the endosomal escape capability, prickly nanocarriers should be used with caution, due to the potential damage to plasma membranes and the toxicity related to endosome impairment.

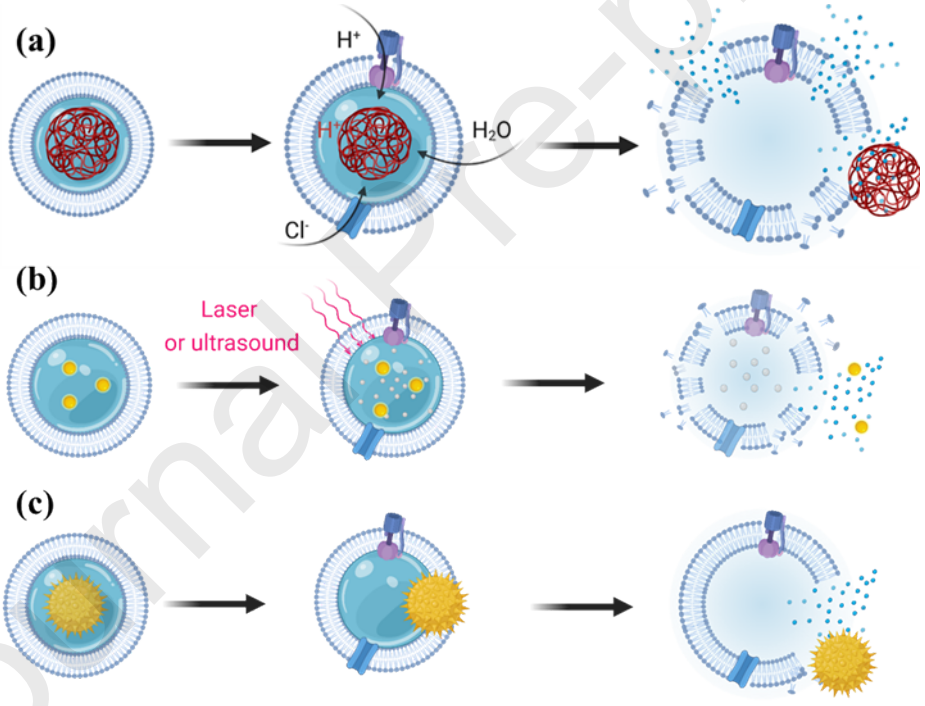

Figure 15. Schematic showing of different mechanisms of endosomal rupture. **(A)** "Proton sponge" hypothesis mediated by cationic buffering polymers. Endosomal rupture is induced by osmotic pressure between the endosomal lumen and the cytoplasm. **(B)** Nanobubble strategy induced by laser or ultrasound triggers. Endosomal

rupture is induced by the mechanical force when nanobubbles expand and collapse. **(C)** Physical disruption of endosomal membranes by prickly carriers. Endosomal rupture is induced by the mechanical force from the sharp surface piercing membranes. Created with BioRender.com.

6.3. Endosomal escape by membrane destabilization and membrane fusion

Endosomal escape by membrane destabilization and membrane fusion represents another strategy widely used, especially by virus and bacteria [249]. As indicated in the nomination, membrane destabilization carriers interact with endosomal membranes directly, and cause membrane defects or even pores to allow for the escape (**Figure 16A**). Membrane fusion inducer may penetrate inside the endosomal membrane and induce fusion to release the cargo (**Figure 16B**). Therefore, the tendency of carriers to associate with endosomal membranes and the capability to disrupt the lipid bilayers are crucial factors for successful endosomal escape. In the following paragraphs, we introduce three typical carriers for membrane destabilization and fusion, including cell penetrating peptides, amphiphilic endosomolytic polymers and fusogenic lipids, and discuss how the structure, charge and amphiphilicity affect the membrane destabilization and the escape.

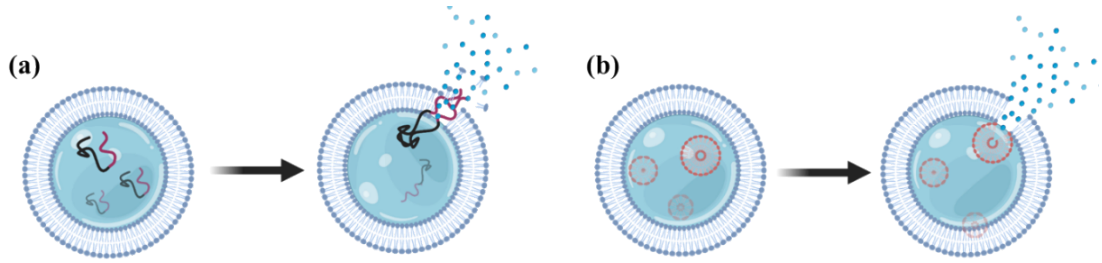

Figure 16. Schematic showing of different mechanisms of endosomal membrane destabilization by **(A)** endosomolytic molecules (CPPs, small molecules or polymers) and **(B)** fusion with lipid-based delivery systems. Created with BioRender.com.

6.3.1. Cell penetrating peptides (CPPs)

Although some CPPs translocate through cell membranes to deliver cargos directly to cytoplasm, the endocytic uptake and the following endosomal escape is still the major internalization route for CPP-cargo complexes [250]. Considering the great diversity in CPP structure, physiochemical properties of CPP-cargo complexes, and endocytosis pathways, the membrane destabilization mechanisms vary [250]. For example, amphiphilic CPPs, such as hemagglutinin-2 (HA2), INF7 (the N-terminal domain of HA2) and GALA (a synthetic peptide with a glutamic acid-alanine-leucine-alanine repeat), have pH-responsive conformational changes [251, 252]. At acidic endosomal pH, the protonation of glutamic acid (Glu) transformed the CPPs into α-helix structure, which enables the CPPs to penetrate into the endosomal membranes, and induce pore formation (**Figure 16A**) [253]. Arginine-rich CPPs (such as TAT, penetratin, oligoarginine), however, induce membrane-destabilization by electrostatic interaction

and hydrogen bonding with negatively charged membrane lipids and polysaccharides from membrane proteoglycans [254]. Recent studies found that the guanidinium groups from arginine residues have strong affinity towards negatively charged lipids in the LE, especially BMP [255]. The association with BMP led to membrane fusion between the intraluminal vesicles in the LE, and with LE outer membranes to allow the cargo escape **(Figure 17)** [256].

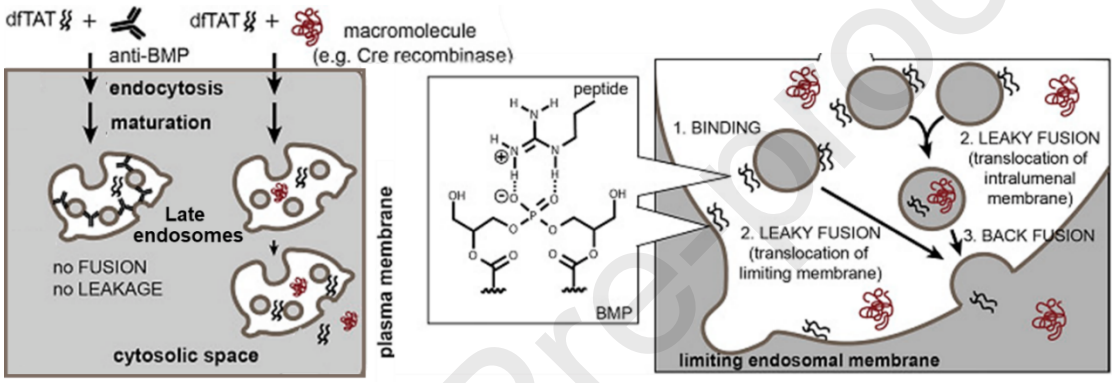

Figure 17. Schematic showing of BMP-dependent endosomal escape from LE. The guanidinium groups from arginine residues interact with BMP head groups. The interaction results in membrane fusion and leakage. Inside late endosomes, the arginine-rich CPP (a dimerized TAT, denoted as dfTAT) and the macromolecular cargos translocate into the cytosol by leaky fusion events (two non-mutually exclusive scenarios involving intraluminal vesicles and the limiting membrane of the organelle are represented). The introduction of anti-BMP monoclonal antibody blocks the fusion and subsequent leakage, confirming the endosomal escape mechanism. Modified and reproduced with the permission from ref. [256]; Copyright © 2016, Elsevier B.V.

Along with increased understanding of CPP endosomal escape mechanisms, significant efforts have been made to balance the endosomal escape capability and cytotoxicity, by modification of the natural CPP structure [257]. Although arginine-rich CPPs like TAT and oligoarginine are the prototypical examples for intracellular delivery applications, the naïve form of these CPPs are mostly trapped in endosomes [258]. Therefore, many studies dedicated to find out how to increase the endosomal escape property by changing characteristic parameters of a peptide, such as amino acid sequence, length and the topological structure [257, 258]. To this end, Pellois' lab has systemically investigated TAT variants with different guanidinium density, branching structure and chirality. They found a typical threshold of at least 10 arginine is essential for endosomal escape [259]. This is consistent with other reports with oligoarginine peptides with different lengths [260]. Dimerization or trimerization of TAT significantly improved the endosomal escape efficiency, despite the increased cytotoxicity of TAT multimers [261]. The multivalent effects derived from branching structure increase the membrane interaction, thus facilitating the escape but also increased the toxicity unfortunately [260]. Furthermore, the endosomal escape efficiency is affected by the chirality of the CPPs. Although cells have preferable uptake of natural L-amino acid peptides, peptides synthesized by artificial D-amino acids have longer half-lives because of the slower degradation by proteolytic enzymes [262]. The longer half-life is however, multifaceted. On one hand, it is beneficial for endosomal escape because of the long-lasting endosomolytic activity [263]. One the other hand, it is also associated with pronounced cytotoxicity because of the prevalent membrane-

lytic effects to organelles in the cytoplasm [263]. Other than changing the parameters from peptide synthesis, chemical ligation on natural CPP structure is another approach to enhance the endosomolytic activity. The conjugation of hydrophobic moieties (*e.g.*, stearyl, phenyl, and aromatic indole rings) promotes the endosomal escape [252, 264]. Both experimental data on model lipid membranes and computational simulations prove that hydrophobic groups facilitate the insertion inside the lipid bilayers, which contributes to the membrane association and the potential to create membrane leakiness [265].

Another approach to find optimal CPPs for endosomal escape, is to convert highly membrane-lytic cationic amphiphilic peptides into pH-dependent variants [266]. Instead of enhancing the membrane destabilization activity from those weak endosomal escape peptides, this approach selects the strong membrane-lytic candidates derived from venoms or antimicrobial peptides, and attenuates the their membrane-lytic activity at physiological pH by introducing anionic Glu residues or aspartic acid (Asp) residues [267]. The negative charge from both Glu and Asp decreases the interaction of these peptides with cell membranes, and thus, decreases the cytotoxicity. At endosomal pH, the protonation of Glu and Asp helps to recover the membrane-lytic activity to realize the endosomal escape. This strategy mimics the amphiphilic viral peptides HA2, which only initiates the endosomolytic activity upon acidification [253]. With Glu or Asp substitution, toxic and hemolytic peptides, such as M-lycotoxin, melittin, δ - hemolysin, chrysophsin and ponericin-W3, could be converted to attenuated variants with endosomolytic activity [267, 268]. The replacement position of Glu is critical to

manipulate the variant's cytotoxicity and endosomolytic activity [268]. It is optimal to substitute Glu on the boarder of the hydrophobic and hydrophilic face within the α-helical structure, because the substitution on the hydrophobic face diminished the membrane interaction capability completely, while the substitution on the hydrophilic face had little effects on the cytotoxicity [268].

Alternatively, the toxic CPPs could be masked by acid-cleavable protective groups and pH-responsive micelles [269]. By reacting with dimethylmaleic anhydride, the amine groups on cationic lysine and arginine residues could be converted into carboxylic acid groups with negative charges at physiological pH [269]. The charge conversion significantly reduced the cytotoxicity and hemolytic activity of melittin, and the membrane-lytic activity was restored after acid-induced cleavage of masking groups [270].

6.3.2. Endosomolytic polymers

Endosomolytic polymers have been developed mimicking the structure of CPPs. Inspired by arginine-rich CPPs, guanidinium-containing polymers with different backbones, molecular weights and topological structures have been synthesized for intracellular delivery [271-274]. Noticeably, the polymer backbone played an important role in membrane destabilization. For example, guanidinium-containing poly(disulfide)s have unique disulfide exchange with proteins on the plasma membrane, thus facilitating the association and translocation capacity of the polymers [275].

Regarding the topological structure, branching and dendritic structures generally have higher potency in endosomal escape [272], despite sometimes associated with higher cytotoxicity [271]. Regarding molecular weights, guanidinium-containing homopolymers and their analogues with longer chains (degree of polymerization, DP = 89) displayed higher siRNA transfection efficiency than shorter analogues (DP = 8, 22 and 43) at the same mass concentration (**Figure 18**) [276]. This was attributed to the charge distribution within the molecule by the authors [276]. Polymers with higher molecular weights displayed a densely charged coil, focusing on the membrane to induce destabilization. Although the higher transfection efficiency was also observed on other long chain polymers with different compositions [277], this charge-density membrane-destabilization hypothesis needs further investigation and validation. Similarly, higher molecular weight polymers are associated with higher cytotoxicity (**Figure 18**), possibly due to the non-biodegradability and accumulation in cells [278]. Thus, biodegradable monomers or linkers could be applied to achieve high molecular weight with lower cytotoxicity [279].

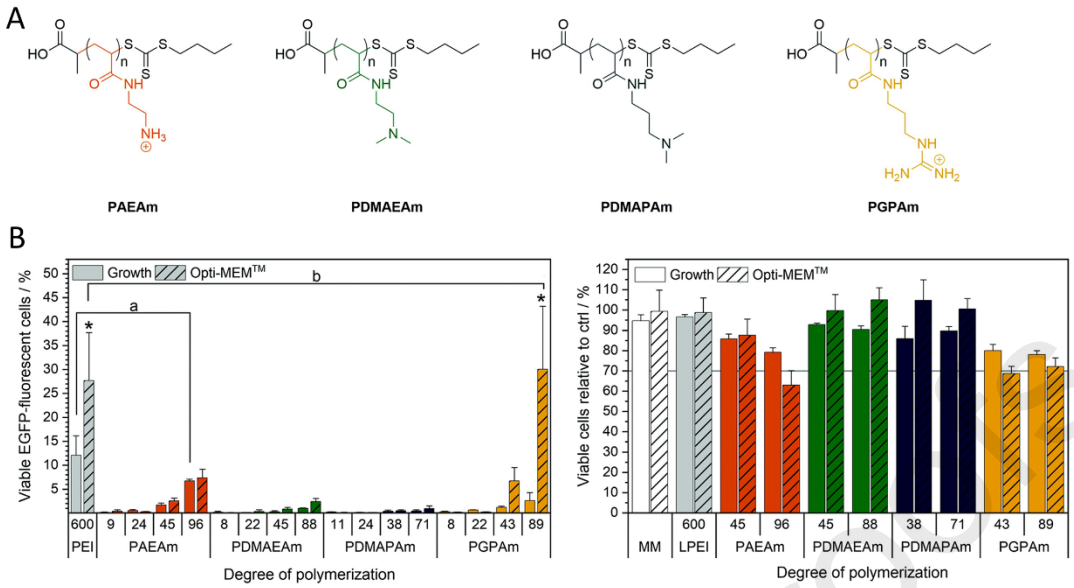

Figure 18. The molecular effects on guanidinium-containing homopolymers and their analogues. **(A)** The structures of polymers and **(B)** their transfection efficiency and cytotoxicity in HEK293T cells. Reproduced with the permission from ref. [276]; Copyright © 2020, Royal Society of Chemistry.

In addition to guanidinium-containing polymers, pH-responsive fusogenic amphiphilic polymers are intensively explored, for endosomal escape purposes. The pH-induced protonation of Glu and Asp on fusogenic CPPs, is mimicked by various carboxylic acid containing amphiphilic polymers [280, 281]. It is noticed that the balance of hydrophobic and hydrophilic monomers is important for their function. For example, adding a small portion of hydrophobic units (*i.e.*, 2% cholesteryl methacrylate or 10% lauryl methacrylate) on poly(methacrylic acid) significantly increased its membrane association capability [280]. However, excessive hydrophobic units (*i.e.*, 8% cholesteryl methacrylate or 40% lauryl methacrylate) compromised the polymer

solubility and decreased the membrane interaction, because of the enhanced association between polymer chains [280].

The mechanisms of most endosomolytic polymers remain inconclusive, partially due to the abundant structural diversity and the general focus in the field. Most studies focus more on the delivery efficiency and the overall therapeutic efficacy rather than the detailed mechanism inside the cells. Another difficulty may come from the polymer synthesis. Despite the huge achievements in polymerization techniques, it is still difficult to achieve complete control over the polymer sequence, at least not on monomer level. Therefore, it is not possible to study the subtle change on a single polymer chain (*e.g.*, the addition or substitution of one or two residues). Unlike the small molecules or peptides synthesized with identical structure, synthetic polymers may have monomers distributed statistically along the chain. Thus, their membrane destabilization behavior should be interpreted as the average potency from the whole polymer population with the same monomer composition.

6.4. Lipids

In Section 4.1, we discuss the general methodology and mechanism of efficient RNAs encapsulation by LNPs, whereas in this section, we will mainly focus on the other critical aspect of LNPs design: commonly used method and the potential mechanism for enhancing endosome escape capability of LNPs. Of course, lipid NPs may directly fuse with plasma membrane and translocate payloads into cytoplasm without endocytosis. However, endosomal escape remains to be the main internalization route

for lipid-based gene delivery systems [238]. The functional lipids for endosomal escape could be categorized according to their physiochemical properties: cationic lipids (*e.g.*, DOTAP), neutral phase transition inducer lipids (so-called "helper lipids", *e.g.*, DOPE) and pH-dependent conformation switchable lipids [104]. Because LNPs and liposomes are usually formulated as a mixture of different lipids, the lipids for endosomal escape purposes usually only constitute a small portion, with the majority composed of PC, cholesterol, PEGylated lipids, *etc.*, to stabilize the final NPs [102]. Therefore, the final endosomal escape properties resulted from combinational effects of the whole lipid formulation, instead of single membrane-destabilization moieties.

The endosomal escape mechanism of LNP and liposome are generally attributed to the fusion with endosomal membranes (**Figure 16B**). As endosomal membranes are rich in anionic lipids, the cationic lipids enhance the membrane interaction by electrostatic interactions [97, 282]. Once located on the endosomal membrane, the fusogenic lipids (DOPE) transformed the lipid phase from lamellar to inverted hexagonal, thus promoting the membrane fusion [283]. This theoretical explanation is as popular as the "proton-sponge effect", and has long been accepted in the field [282]. However, recent evidence suggest the translocation could happen by a transient pore model rather than fusion [238]. The authors found the endosome release of oligonucleotides by LNPs was in a gradual manner, which fits better to the "pore forming" mechanism, where a more subtle endosomal membrane destabilization, rather than a burst membrane fusion, can achieve (**Figure 19A-C**) [238]. In this new hypothesis, after interaction with endosomal membranes, the lipids from endosomal membranes could be taken away by LNPs, thus

creating transient pores for payload to escape, which is similar to membrane destabilization created by CPPs and endosomolytic polymers discussed in the previous sections (**Figure 19D**) [284]. This is evidenced by the endosomal damage markers and small cytosolic Ca^{2+} transients [20]. Despite the emerging evidence, more studies are needed to elucidate this new hypothesis.

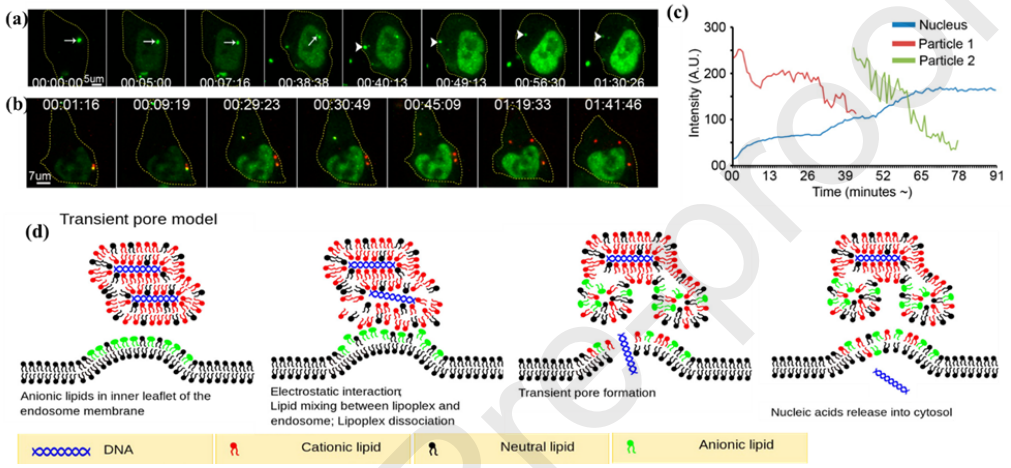

Figure 19. (A) HeLa cells incubated with Lipofectamine2000 carrying FITC-ODNs and monitored by confocal microscopy. White arrows indicated two NPs successively released parts of the ODN content, revealing a stepwise decrease in ODN fluorescence within the endosome, and a concomitant increase in ODN fluorescence within the nucleus. **(B)** Rhodamine-labeled Lipofectamine2000 (red) was complexed with FITC-ODNs (green) and added to HeLa cells. Three lipoplex-containing endosomes that initially appear yellow (due to colocalization of carrier (red) and contents (green)) gradually turn red while releasing ODNs into the cytoplasm. **(C)** The fluorescence of the particles (labelled with white arrows) and the nucleus showing in (A). **(D)** The schematic showing of the transient "pore-forming" mechanism induced by lipid-based delivery system. Modified and reproduced with the permission from (A-C) ref. [238];

Despite the successful delivery mediated by cationic lipids, the associated toxicity and immunogenicity was still a concern [285]. To solve this problem, pH-sensitive lipids have been developed. Typically, these lipids have ionizable head groups, which are protonated only in acidic endosomes [53]. Through high-throughput screening, several ionizable lipid candidates have been identified [99, 286], and the related formulations showed pK_a, phase transition temperature, number of hydrophobic tails and the tail saturation state are key factors in the design [287, 288]. A pK_a within EE pH range, lower transition temperature and unsaturated branched tails are beneficial to enhance endosomal escape properties [287, 288]. Furthermore, the conformational change of the ionizable lipid at molecular level with head-tail orientation switch could also facilitate the escape [289].

6.5. Small molecules facilitate endosome escape

A group of small molecules, termed as cationic amphiphilic drugs (CADs), have been shown to obtain the membrane-destabilizing properties [290, 291]. These drugs all had protonable secondary or tertiary amine groups. At physiological pH, these groups are not protonated, and the drugs can diffuse into the lysosomal lumen, where they are protonated upon acidification. The positive charge and the increased hydrophilicity prevents them from diffusing out of phagocytic compartments. Therefore, the drugs

retain in endosome/lysosomes, and inhibit lipid hydrolyzing enzymes especially acid sphingomyelinase [291]. Therefore, a hypothesis has been proposed to facilitate the RNA endosome escape due to the membrane disruption [290, 292]. Recent studies tried to develop endosomolytic molecules with better efficacy by repurposing FDA-approved cationic amphiphilic drugs, such as carvedilol, desloratadine, nortriptyline and salmeterol, and when co-administrated with siRNA carriers, the drugs, acting as "endosomal escape adjuvants", may enhance siRNA delivery efficiency both *in vitro* and *in vivo* [290, 292]. However, as we discussed in Section 2.2., release of the RNA payload may only has a particular "window of opportunity" during the endosomal maturation process, yet CADs are diverse and target multiple intracellular compartments. Therefore, it is important to understand whether the mismatch between NPs containing and CADs-targeted compartments will hinder the further knockdown efficiency improvement.

A recent study selected three different CADs (chloroquine, siramesine and amitriptyline), and separately investigated their corresponding effects on the gene knockdown efficiency from cholesterol-conjugated siRNA targeting d1-eGFP [293]. All these drugs can induce obvious endosome/lysosome rupture as reflected by galectin-3 and galectins-9 recruitment in the endosomal membrane, which is a typical signal for endosome damage (**Figure 20A**) [19, 20]. This membrane destabilization capability further improved siRNA-mediated knockdown in HeLa cells expressing a destabilized enhanced GFP (HeLa-d1-eGFP), yet the enhancement efficiency varied from drug to drug. Chloroquine lowered half-maximal inhibitory concentration (IC_{50})

for over 17-fold, whereas the number for amitriptyline and siramesine was only ~2- and 4-fold, respectively (**Figure 20B**). The authors purposed the following explanations for this phenomenon. First, the authors compared to other drugs, chloroquine exhibited better capability in triggering cytosolic release of macromolecules. This was confirmed by applying 10 kDa fluorescent dextran as cytosolic release indicator (**Figure 20C**). Internalized dextran was solely located in intracellular vesicles, whereas after incubating HeLa-d1-eGFP cells for 16 h with different CADs, chloroquine treatment group triggered the most significant cytosolic dextran release, which was 8-fold higher than siramesine treatment group, and amitriptyline treatment only provoked low-to-no cytosolic redistribution of dextran. The observed results were in consistence with the as-mentioned knockdown enhancement efficiency, indicated the enhanced siRNA endosome escape is correlated with the membrane destabilization degree.

Secondly, different drug targeted different phagocytic compartments. Authors identified the detailed compartments damage by different drugs, and divided the phagocytic compartments via the endosome maturation stages. For chloroquine treated HeLa-d1-eGFP cells, 43% of the damaged endosomes were featured as $Rab5^+$ (immature early endosome), while Rab5 was not recruited to vesicles damaged by siramesine. On the contrary, siramesine mainly showed damage towards $Rab9^+$ structures (late endosomes), as 42% of the $Rab9^+$ compartments were shown as galectins-9^+, whereas this number for chloroquine group was only 23%, suggesting chloroquine mainly interrupt the membrane integrity of endosome at early stages (**Figure 20D**). This is in good line with previous results, suggesting the siRNA

endosome escape majorly occurs in early endosome stages [19, 20]. Herein, the results further confirmed that, comparing to early endosomes, the disruption of late endosome or lysosome may show restrained effects on promoting the RNAi.

Besides of the CADs-specific effects on knockdown efficiency, the same CAD may exhibit altered effects on different delivery systems. For example, Wittrup *et al.* showed that treating HeLa-d1-eGFP (same cell line in Ref. [293] as discussed above) with chloroquine conversely reduced the knockdown efficiency of GFP targeting siRNA loaded in LNPs [20]. This difference can be attributed to the different endocytosis pathway from different delivery system. As phagocytosis of LNPs is mainly dominated through clathrin-dependent endocytosis [16], which can be effectively inhibited by chloroquine [294]. However, cellular uptake of cholesterol-conjugated siRNA is partly initiated with the cholesterol insertion into the cholesterol rich raft area of cell membranes, followed by internalization through caveolin-dependent endocytosis (also named as raft-dependent endocytosis) [295, 296]. Therefore chloroquine reduced siRNA knockdown efficiency from lipid NPs can be partly explained as the decreased intracellular NPs accumulation. Similar phenomenon was observed by Gilleron *et al.*, who screened a CADs compound library for evaluating effects of different CADs on RNAi from siRNA loaded lipid NPs and cholesterol conjugated-siRNAs. Despite in total 51 CADs exhibited RNAi enhancing efficiency, most enhancers displayed specificity for one delivery system only [297], confirming the delivery system specific effects from CADs.

CADs induced endosome escape is also cell type dependent. For example, pretreating

HeLa-d1-eGFP cells with 20 μM loperamide could induce a 47-fold siRNA IC_{50} reduction (Cholesterol-conjugated siRNA), whereas this RNAi enhancing efficiency was slightly observed in MCF-7-d1-eGFP breast cancer cells [293].

Overall, despite CADs induced RNAi enhancing has been observed, its further clinical application may be hindered by the multiple varieties and further investigations should be conducted to provide systematic guidance for proper CADs choose.

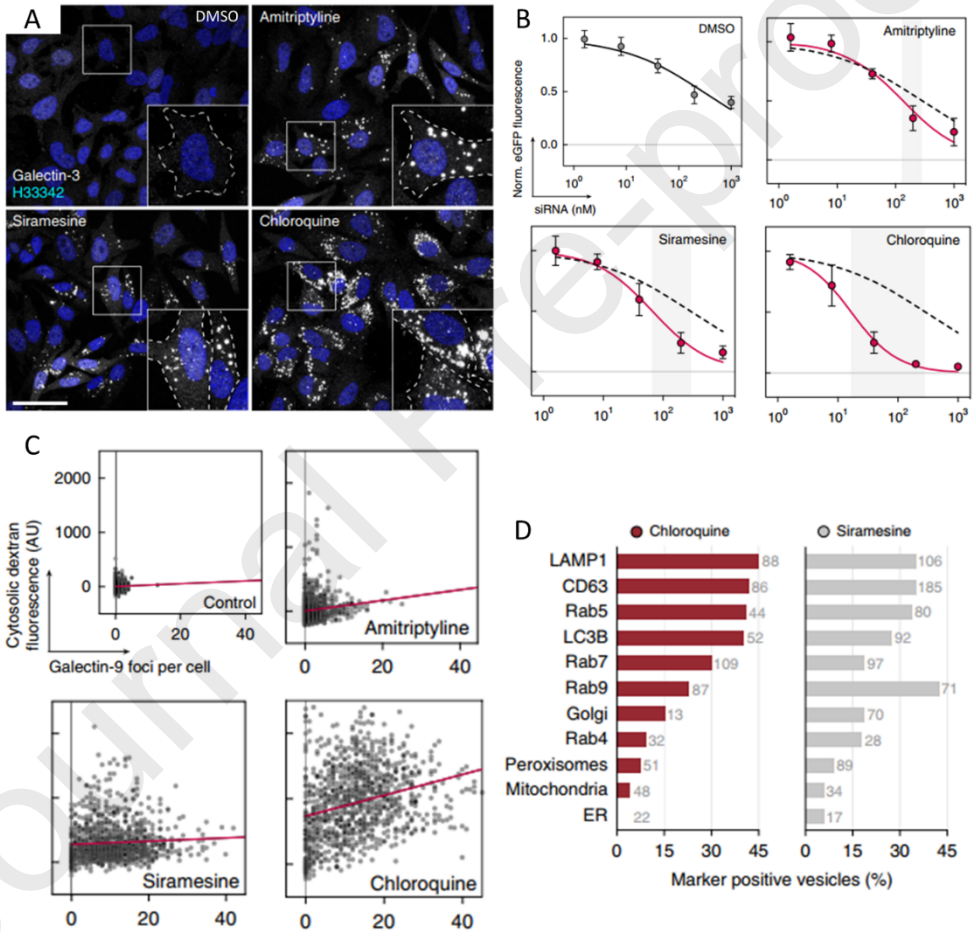

Figure 20. Enhanced RNAi efficiency from CADs. **(A)** HeLa cells incubated with 10 μM siramesine, 50 μM of amitriptyline or 50 μM of chloroquine for 24 h, and the galetin-3 were stained for as endosome damage indicator. Scale bar indicates 50 μm. **(B)** HeLa-d1-eGFP cells were first incubated with cholesterol-conjugated siRNA for 6

h, sequentially treated with 10 μM of siramesine, 60 μM of amitriptyline or 60 μM of chloroquine for 18 h. Then evaluate the GFP knockdown by flow cytometry. The knockdown enhancement efficiency is qualitatively correlated with the galetin-3 foci number in (A). **(C)** Correlation between number of galectin-9 foci and median cytosolic dextran fluorescence intensity per cell after 16 h CADs treatment. Cell number for control, amitriptyline, siramesine and chloroquine are separately 953, 1204, 1177, and 1139. Linear regression is outlined by red line. **(D)** Evaluated damaged vesicles numbers and their corresponding fraction within the total vesicles with endosomal markers. Modified and reproduced with permission from ref. [293]; Copyright © 2020, Springer Nature.

7. Future perspective of non-viral NPs based RNAi

7.1. Clinical translation of non-viral NPs based RNAi

Last, but not the least, we discuss about the clinical translation of non-viral NPs based RNAi. By summarizing the clinical translation of RNAi-based NPs, one can better understand the practical obstacles and challenges during NPs design and fabrication. By considering the general advances and failures in the field of nucleic acid delivery and the different formulation strategies used in clinically approved products, we hope to provide insights, from a market point of view, for future designing and optimization of NPs' formulations.

7.1.1 Approved nucleic acid therapies

The first nucleic acid therapy approved by FDA in 1998 was Vitravene (fomivirsen) by

Ionis Pharma and Novartis, a phosphorothioate antisense oligonucleotide for the treatment of cytomegalovirus renitis [298]. It was followed by Macugen (pegaptanib), a PEGylated aptamer for the treatment of neovascular age-related macular degeneration in 2004 [299], and nine years later by Kynamro (mipomersen) a gapmer oligonucleotide for treating homozygous familial hypercholesterolaemia [300]. These pioneering products faced commercial difficulties; Vitravene was withdrawn as a result of reduced clinical need [301] and the sales of both Macugen and Kynamro were limited due to competition [302, 303]. Furthermore, Kynamro's safety concerns led to its rejection by the European Medicines Agency (EMA) [304].

The latter half of 2010s saw a renaissance of oligonucleotide based therapies as new wave of products reached the clinics. Among these was the first FDA-approved RNAi drug and the first approved nanomedicine for nucleic acid delivery, Onpattro, in August 2018 [107]. Onpattro, developed by Alnylam Therapeutics, is a lipid complex injection of patisiran (siRNA) for the treatment of hereditary transthyretin-mediated amyloidosis. Of the recently approved oligonucleotide products, Onpattro (patisiran) is the only one that is based on nucleic acid encapsulated inside NPs. Spinraza (nusinersen), Tegsedi (inotersen), Exondys 51 (eteplirsen) and Vyondys 53 (golodirsen) are naked chemically modified ONs [305-307], Givlaari (givosiran) and Oxlumo (lumasiran) are N-acetylgalactosamine (GalNac) conjugated siRNAs [308], Luxturna (voretigene neparvovec) and Zolgensma (onasemnogene abeparvovec) are DNAs delivered by adeno-associated viral vectors (AVVs) [309, 310] and Defibrotide (defitelio) is a combination of naked single- and double-stranded DNA isolated from porcine intestinal

mucosa [311]. In 2018, the market approval of eteplirsen was withdrawn by EMA due to lack of efficacy [312].

In the clinically approved products, four main formulation strategies have been employed: (1) chemical modification of the oligonucleotide; (2) covalent conjugation to carrier polymers; (3) encapsulation in lipid nanoparticles; and (4) delivery using AVVs. As naked RNA is rapidly degraded in the bloodstream by nucleases, chemical modifications are necessary to improve the pharmacokinetics, pharmacodynamics and biodistribution of oligonucleotides. These include modifications to the backbone of the molecule, to the nucleobases or to the ribose moiety. For a detailed discussion on chemical modification strategies, the reader is referred to recent reviews [37, 313].

Drawbacks of chemical modification may include loss of binding affinity or potency or unexpected toxicity. For example, replacing phosphodiester bonds in the backbone with phosphorothioate greatly retards degradation by nucleases, but also reduces target binding affinity [37, 313]. Fluoro-modifications of the ribose sugar at the 2'-end are commonly used to improve pharmacokinetic profile and reduce immunogenicity, but may also result in non-specific loss of cellular proteins and hepatotoxicity [37, 313-315]. This formulation approach alone does not allow targeting to specific organs, and thus, the amount of dose reaching the target tissue is inherently limited. Regardless, this strategy has clearly been successful as the majority of the products currently on the market are naked, chemically modified oligonucleotides in solution.

For viral vectors, the main challenge remains to be the body's immune response against

the viral components, which can render up to 50% of patients unable to receive AAV-based therapies due to pre-existing immunity against the viral capsid [316, 317]. While additional measures, such as modification of the vector or immunosuppressive medication can be used to mitigate this issue, immune reactions remain a major limiting factor for these vectors, especially when repeated dosing is required. Still, the excellent transfection efficiency of viruses, evolved through natural selection, still makes them an attractive nucleic acid delivery agent. Nevertheless, the challenges encountered with AVVs and with the administration of free chemically modified nucleic acid encourage further development of polymer-oligonucleotide conjugates and nanoparticle-based delivery systems.

Conjugation of nucleic acids with polymers and biomolecules can and improve stability and pharmacokinetics. In currently marketed products, two classes of polymers have been applied for this purpose: poly(ethylene glygol) (PEG) and N-acetylgalactosamine (GalNac). Notably, conjugation with GalNac polymer allow efficient liver-targeted delivery as GalNac binds to asialoglycoprotein receptors expressed almost exclusively on hepatocytes [318, 319]. Compared to encapsulation in lipid NPs, using GalNac conjugation requires more extensive chemical modifications to the RNA to protect it from degradation by nucleases. Alnylam Therapeutics has developed and patented a set of chemical modification strategies, termed Enhanced Stabilization Chemistry (ESC), which they apply with GalNac conjugation to achieve high stability and knockout efficiency [308, 318-320]. The recently approved givosiran and lumasiran utilize this platform for siRNA delivery. While this method is expected to revolutionize the

treatment of many severe diseases, the platform is only suitable for liver delivery.

LNPs have been used in several commercial products to delivery small molecules since the approval of Doxil/Caelyx and Ambisome liposomal products in the 1990s and the approval of Onpattro proved that the lipid nanoparticle technology is clinically relevant also for nucleic acid delivery. The Onpattro formulation is based on the use of a unique combination of lipids, including PEGylated lipids to prevent immune clearance and cationic ionizable lipids to allow encapsulation of negatively charged RNA, efficient transfection and endosomal escape [94, 321]. Essential in the success of this lipid formulation was the development of novel synthetic ionizable lipids of high potency [321]. Despite of the success, Alnylam is no longer pursuing the NPs formulation and focuses on PMO (phosphorodiamidate Morpholino oligomer) and GalNAc-conjugate technologies instead [37, 320]. A major limitation of Onpatto is its immunogenicity, necessitating concurrent corticosteroid treatment [320].

The perpetual efforts in developing LNPs based RNAi vector may also accelerate the developments of other commercialized products. The most recent achievement for LNPs technology for RNA delivery are the COVID-19 mRNA vaccines developed by BioNTech/Pfizer (Comirnaty) and Moderna (mRNA-1273). These formulations are largely similar to that of Onpattro, using a combination of cholesterol, structural lipids, PEGylated lipids and proprietary cationic ionizable lipids [322-324]. This platform is now being applied by BioNTech in several clinical trials for vaccinations against both viral infections and cancers. However, detailed discussion of mRNA vaccines is beyond the scope of this review.

7.1.2 RNAi delivery systems under clinical investigation

Selected RNAi products currently in clinical studies are listed in **Table 3**. Excluded from this list are naked chemically modified RNAs, mRNA-vaccines, viral vector-based formulations and cell therapies (in which RNA is transfected *in vitro*). The formulations under study cover a wide range of drug delivery techniques and are discussed in more detail below.

Several subcutaneously administered siRNA products based on the GalNac-platform are currently under clinical trials. Cemdisiran is intended to reduce the production of complement protein 5 (C5), which plays an important role in several lethal rare diseases [325] and two phase II trials are underway for the treatment of atypical hemolytic uremic syndrome and immunoglobulin A nephropathy. Additionally, a phase I safety trial (NCT04601844) is ongoing for combination therapy of cemdisiran and pozelimab. Several phase II/III trials are ongoing (and several have been completed) for inclisiran on different patient populations with familial hypercholesterolemia or increased cardiovascular risk and elevated low-density lipoprotein (LDL) cholesterol. Inclisiran interferes with the synthesis of proprotein convertase subtilisin-kexin type 9 (PCSK9), an enzyme synthesized primarily in the liver [326]. PCSK9 binds to LDL receptors on hepatocytes and promotes their lysosomal degradation, which ultimately increases the production of LDL cholesterol. Additionally, one trial in ongoing for the product DCR-HBVS, now called RG6346, by Dicerna against chronic hepatitis B virus (HBV)

infection.

At least two relevant LNPs products are currently under study. A saRNA product called MTL-CEBPA by MiNA Therapeutics is evaluated for the treatment of advanced hepatocellular carcinoma by in a phase I trial. The activating RNA, encapsulated in "SMARTICLES" liposomal nanoparticles, is intended to increase production of CCAAT/enhancer-binding protein alpha (CEBPA) with the ultimate goal of reduction of fibrosis and reversal of liver dysfunction [327]. A liposomal formulation of EphA2 siRNA is currently under study at MD Anderson Cancer Center. According to a preclinical safety report, the liposome consists of 18:1 PC/DOPC lipids and is loaded with siRNA against EphA2, a receptor tyrosine kinase associated with cancer proliferation, migration, invasion, survival and angiogenesis [328].

Another interesting planned to start at MD Anderson Cancer Center is looking into mesenchymal stromal cells-derived exosomes (extracellular vesicles) for delivering KrasG12D siRNA in patients with the KrasG12D mutation. This mutation has been shown to be associated with the development of invasive and metastatic pancreatic ductal adenocarcinoma [329]. Several phase I/II studies are active for the polypeptide-siRNA complex platform STP705 of Sirnaomics where the platform is used to deliver siRNA by localized injection to treat several different liver and skin cancers as well as hypertrophic scar reduction and keloid scarless healing. In addition to these colloidal systems, also a macroscopic siRNA delivery system is under clinical study. This LODER technology by Silenseed Ltd. is based on poly(lactic-co-glycolic acid) (PLGA) biodegradable polymer implant for local, sustained delivery of siRNA.

Overall, several technologies have successfully been used for RNA delivery and many new approaches are under clinical investigation. These advances have already helped many patients and vastly expanded the range of treatable diseases. However, major challenges still remain in delivering RNA to tissues other than the liver through systemic circulation. The development of advanced, targetable colloidal drug delivery systems is required to enable efficient delivery to different organs and to expand the applications of RNAi therapy.

Table 3. Selected siRNA and saRNA therapeutics in clinical trials.[a]

Carrier class	Product / RNA type	Delivery system	Sponsor of study	Indications	Delivery target, RoA *	Phase	Clinicaltrials.gov identifier
Lipid	MTL-CEBPA / saRNA	Liposomal nanoparticle	Mina Alpha Limited	Hepatocellular carcinoma	Liver, intravenous	I	NCT02716012
	EphA2 siRNA	Liposome (DOPC)	National Cancer Institute (NCI)	Advanced solid tumors	Several organs, intravenous	I	NCT01591356
Exosomes	iExosomes with KRAS G12D siRNA	mesenchymal stromal cell-derived exosomes	M.D. Anderson Cancer Center, National Cancer Institute (NCI)	Metastatic pancreas cancer	metastatic cancer, intravenous	I	NCT03608631
Polypeptide	STP705	Histidine-Lysine-siRNA complex	Sirnaomics	Several liver cancers	Liver, intratumoral	I	NCT04676633
				Hypertrophic scar reduction, Keloid scarless healing	Skin, intradermal	I/II	NCT02956317
				Basal cell carcinoma	Skin, localized injection	II	NCT04669808
				Cutaneous Squamous Cell Carcinoma in Situ	Skin, intratumoral injection	I/II	NCT04293679
Polymer	LODER technology (local RNA delivery platform)	PLGA implant	Silenseed Ltd	Pancreatic cancer	Pancreas, intratumoral application	II	NCT01676259
Biomolecule conjugates	Cemdisiran / siRNA	GalNac conjugate	Alnylam	Atypical hemolytic uremic syndrome Immunoglobulin A nephropathy	Liver, subcutaneous	II	NCT03999840 NCT03841448
	Inclisiran / siRNA	GalNac conjugate	Novartis Pharmaceuticals, University of Oxford / The Medicines Company	Cardiovascular disease, High cholesterol, Homozygous familial hypercholesterolemia	Liver, subcutaneous	II - III	NCT03814187 NCT03060577 NCT04659863 NCT04652726 NCT03851705 NCT04666298 NCT04765657 NCT03705234
	DCR-HBVS / siRNA	GalNac conjugate	Dicerna	Chronic hepatitis B	Liver, subcutaneous	I	NCT03772249

[a] RoA = route of administration, saRNA = small activating RNA, DOPC = 1,2-dioleoyl-sn-glycero-3-phosphocholine, siRNA = small interfering RNA, , PLGA = poly(lactic-co-glycolic acid)

7.2. Adverse effects of RNAi

The discussion from previous section suggests the adverse effects and toxicity is the prerequisite yet the major obstacle for clinical applications of RNAi. Among the most pronounced side effects of RNAi are the off-target effects and immune stimulation [330]. Off-target effect is the undesired silencing of non-target genes expression [331]. It can occur due to the non-complete homology of RNAi to target mRNA that can result in partial binding [332]. In addition, coincident sufficient homology of RNAi (11 base pair) to other non-target mRNA can result in translational suppression or degradation of this mRNA [333]. Off-target effect can result as well from the loading of sense strand of dsRNA or miRNA (equivalent to target mRNA neuclotide sequence) into RISC instead of anti-sense strand (complementary to target mRNA) [332]. The improper RISC loading orientation results in neglecting the target mRNA and instead silencing of unintended transcripts complementary to the loaded strand [334]. Consequently, regardless the depleted effects on target genes, the off-target effects can result in knock-down of different gene expressions and toxicities with major consequences that can level-up to cell death [332].

The other commonly observed side-effect from RNAi is the immune stimulation. Non-specific administration of exogenous RNAi can result in the activation of innate immunity through the induction of interferon responses. This can be induced through binding to the cytosolic receptors; protein kinase R (PKR) and 2′ -5′ -oligoadenylate synthetase, which recognize long dsRNA. This is in addition to binding to toll-like receptor (TLRs) family (specifically TLR3, TLR7 and TLR8), which are responsible

for recognizing nucleic acid on the cell surface or in endosomes [335, 336]. This induces a molecular cascade, which leads to immune cells activation and release of type I interferons and inflammatory cytokines [337]. Although sometimes the immune stimulation can be a serious adverse effect, it can also be beneficial, for effective therapy against cancer or viruses [330].

The design of RNAi should be carefully considered to either avoid or induce immune stimulation, according to the specified application. Although dsRNA longer than 30 bp are known to activate the innate immunity [334], some shorter (>23-bp) dsRNA has also shown to induce interferon responses in some cell lines. The threshold length of RNAi may vary with different cell lines [338]. Specific sequence motifs, such as 5′ GUCCUUCAA3′ or 5′ UGUGU3′, can induce the production of interferon and interleukin by plasmacytoid dendritic cells [335]. These motifs are usually U-rich, which are difficult to be eliminated from RNAi drug candidates [334]. In addition to the immune stimulation, systemic administration of RNAi can result as well in non-specific distribution to non-target organs [339]. This would lead to gene silencing and toxicity in these organs, in addition to increasing the required dose of RNAi [340, 341]. Further unintended side effects may appear due to the saturation of cellular RNAi machinery by the synthetic siRNA. This will interfere with the gene silencing effect by endogenous miRNA, and finally results in overexpression of certain proteins and induction of toxicity [342].

The undesired side effects are the major obstacles for the successful clinical translation of RNAi. The first clinical trial with siRNA was on bevasiranib for targeting vascular

endothelial growth factor in age-related macular degeneration patients in order to suppress ocular neovascularization. The clinical studies were terminated off after reaching the phase III trial, because the medicinal effect is not due to gene silencing, but the non-specific immune stimulation via TLR3 activation [343]. ARC-520, which is a targeted anti hepatitis B virus (HBV) siRNA with promising therapeutic effects, was among the first antiviral siRNA to enter the clinical trials [344]. Its clinical trial was terminated due to death in non-human primates induced by administration of the highest siRNA dose [345]. MRX34 is a liposomal miR-34a mimic for advanced solid tumors, and was tested clinically on human as the first miRNA cancer therapy [346]. The trial was discontinued due to reported severe immune-related side effects, including severe cytokine release syndrome [345].

Different approaches can be considered through different stages of the development of RNAi candidates to eliminate the off target effects. Among these approaches are sequence design and optimization [334], chemical modifications [347] of RNAi candidates and development of effective delivery system and targeting [345]. The design of selective and hyperfunctional RNAi is a first step toward the reduction of off-target effects and short-list the potential candidates [348]. Bioinformatics tools can be useful to avoid the design RNAi of seed region that is complementary to off-target mRNA [334]. Additionally, an important factor that should be considered while designing RNAi is the sequence-potency relationship [334]. This highlight the importance of developing and advancing bioinformatics tools, as it is the first step toward the development of effective RNAi. Screening the RNAi drug candidates for

off-target effect is a helpful tool as well to early eliminate the non-potential candidates. Protein array technologies will help to provide a representative image about the effect of RNAi on cellular protein expression [349].

The design and sequence optimization of RNAi candidate is important to reduce the side effect; however, it is still not sufficient to totally eliminate all the possible immune reactions toward RNAi. In this regard, different chemical modifications have been developed to enhance the performance of RNAi and reduce the immune response and off-target effects and enhance the guide strand selection and delivery. It is also important that chemical modifications are not adversely affecting the potency of the RNAi or impair its pathway. These chemical modifications can be classified as modifications phosphate backbone, the ribose moiety or the base [347]. Among the commonly used modifications is ribose 2′ -OH group substitution with other groups; 2′ -O-methyl (2′ -OMe), 2′ -methoxyethyl (2′ -MOE) or 2′ -fluoro (2′ -F) [337]. This would protect siRNA from ribonucleases, which require the 2′ -OH group to hydrolyze RNA [347]. In addition to increasing the resistance to degradation, this modification can reduce the risk of immune stimulation and decrease cytokine production [350]. Modifications can be performed at the termini of RNAi, which are recognized by immune cells. For example, siRNA with added 3′ - UU can reduce immune stimulation and enhance the gene silencing efficiency [337] .However, modifications at 5' phosphate of the antisense strand cannot be easily applied, as it is essential for recognition and binding to RISC [351].

RNAi delivery systems should be non-immunogenic to reduce the side effects and avoid excipient-induced immune activation [345]. Additionally, designing the delivery systems to provide time-controlled RNAi delivery would be beneficial to control the intracellular concentration of RNAi. In turn, this can reduce the concentration-dependent side effects such as off-target effects, immune stimulation and saturation of the endogenous RNAi pathway [348]. Tissue or cell-specific targeting is important, especially with systemic administration of RNAi to avoid gene silencing in non-target tissues inducing unwanted toxicities [352]. Additionally, targeted delivery can increase the therapeutic window of RNAi drug and increase bioavailability in targeted site, while reducing the off-target effects [345]. Targeting ligands can decorate the NPs surface or be conjugated to the RNAi itself. Among the targeting ligands as mentioned before are aptamers [353], antibodies [354], folates [355] and N-Acetylgalactosamine (GalNAc) [319].

Ultimately, different strategies should be combined to reduce the side effects of RNAi, starting from the careful designing of RNAi sequence to designing an optimum delivery system. For example, Dicerna Pharmaceuticals developed Dicer-substrate siRNA (DsiRNA), functionalized with GalNAc moieties. GalNAc is a ligand to the endocytic asialoglycoprotein receptor (ASGPR), which is an endocytic receptor overexpressed on surface of hepatocytes, and barely on other cell types [356]. The ligand moieties are linked to the tetraloop hairpin of DsiRNA, which is connected to sense strand, constant sequence, and antisense strand composed of a 21–23 nucleotides complementing the target mRNA. The design would make it difficult for the sense strand to be loaded to

RISC due to the constant complementary structure in the siRNA sense strand. This in turn can diminish the off-target effect mediated by the sense strand loading to RISC [347]. Finally, different adverse effects of RNAi and the potential approaches to avoid such side effects are summarized in **Figure 20**.

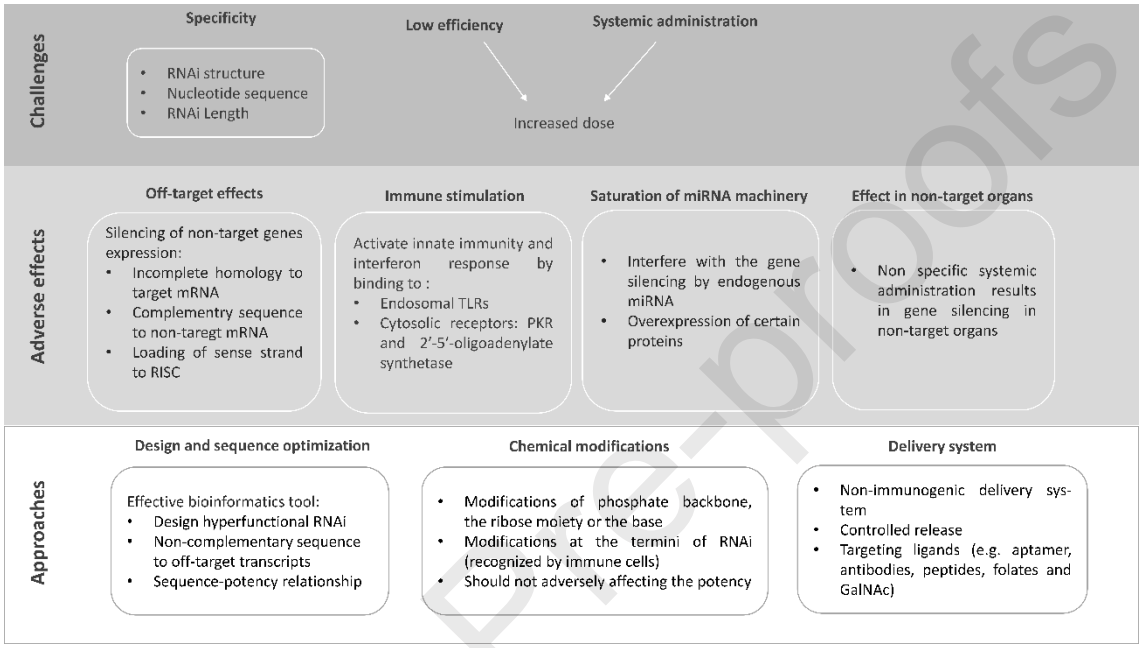

Figure 20. Schematic representation of the challenges that RNAi faces and the sequential adverse effect, which can hinder the clinical applications of RNAi, in addition to the potential approaches to reduce these side effects.

8. Conclusion

RNAi based genetic therapy provides hope for intractable and incurable diseases. Non-viral RNAi delivery systems have drawn increasing attention in the research community due to their advantages in safety, controllable physiochemical properties and economic feasibility. Challenges, ranging from NPs synthesizing conditions, successful RNAs

encapsulation, protection and efficient yet precise targeting capability and efficient endosome escape behavior, are potentially laid ahead to achieve efficient therapeutic outcomes. Understanding the potential mechanism of each step is the prerequisite to properly resolving these obstacles and, as a result, the recent advances in utilizing optimized NPs formulation has enhanced the RNAi efficiency, and expand the application scenario to a more broad area. Furthermore, the continuous efforts may also provide fundamental knowledge for facilitating the development of other nucleotide-based new cargos, such as self-amplifying mRNA, which holds promise for efficient next-generation vaccines.

However, further knowledge is still in demand to better promote their clinical translation perspectives of RNAs. From a pharmaceutical engineering point of view, the major challenges come from the issue of variability and reproducibility under laboratory setting [357]. Diversity in materials choices and detailed handling protocols from different laboratories may lead to inconsistencies between different studies. Further exploration of the underlying mechanisms of nanoparticle formation and RNA encapsulation remain paramount to achieve consistent results and enable rational formulation optimization. Meanwhile, the development of modular NP production methods, such as microfluidic-based production or continuous extrusion, may also reduce the batch-to-batch variation [93].

From a biological point of view, previous studies demonstrated the potential genome alteration as results of off-target RNAi delivery, also suggesting RNAi may not be in a traditional “dose-effect” relationship, where a conversely upregulated target gene

expression may be induced under high siRNA or miRNA concentrations [22-24]. However, despite the advances highlighting the increased RNAi efficiency by using NPs for intracellular delivery, a systematic investigation on the concentration thresholds for NP-based RNAi, and the potentially induced genome alteration with high RNAs dosages is still needed. Corresponding investigation may bring fundamental knowledge to the whole scientific community and facilitate the understanding to the physiological barriers of RNAi, thus holding enormous value for achieving precise gene therapy.

Acknowledgements

Z. Liu acknowledge the financial support from Orion Research Foundation (Finland). S. Wang acknowledge the financial support from Finnish Culture Foundation (grant no. 00201144) and from Academy of Finland (decision no. 331106). V. Känkänen and H.A. Santos acknowledge the financial support from Bayer Oy (Finland). H.A. Santos acknowledges financial support from Academy of Finland (grant no. 317042 and 331151) and the Sigrid Jusélius Foundation.

References

[1] M.P. Lokugamage, C.D. Sago, Z. Gan, B.R. Krupczak, J.E. Dahlman, Constrained Nanoparticles Deliver siRNA and sgRNA to T Cells In Vivo without Targeting Ligands, Adv Mater, 31 (2019) e1902251-e1902251.

[2] S.M. Elbashir, J. Harborth, W. Lendeckel, A. Yalcin, K. Weber, T. Tuschl, Duplexes of 21-nucleotide RNAs mediate RNA interference in cultured mammalian cells, Nature, 411 (2001) 494-498.

[3] P. Arbuthnot, Chapter 4 - Viral Vectors for Delivery of Antiviral Sequences, in: P. Arbuthnot (Ed.) Gene Therapy for Viral Infections, Academic Press, Amsterdam, 2015, pp. 95-126.

[4] H. Gao, R. Cheng, H. A. Santos, Nanoparticle-mediated siRNA delivery systems for cancer therapy, View, n/a (2021) 20200111.

[5] A. Fire, S. Xu, M.K. Montgomery, S.A. Kostas, S.E. Driver, C.C. Mello, Potent and specific genetic

interference by double-stranded RNA in Caenorhabditis elegans, Nature, 391 (1998) 806-811.
[6] G. Meister, T. Tuschl, Mechanisms of gene silencing by double-stranded RNA, Nature, 431 (2004) 343-349.
[7] M. Kalai, G. Van Loo, T. Vanden Berghe, A. Meeus, W. Burm, X. Saelens, P. Vandenabeele, Tipping the balance between necrosis and apoptosis in human and murine cells treated with interferon and dsRNA, Cell Death & Differentiation, 9 (2002) 981-994.
[8] S.M. Hammond, A.A. Caudy, G.J. Hannon, Post-transcriptional gene silencing by double-stranded RNA, Nature Reviews Genetics, 2 (2001) 110-119.
[9] S.M. Elbashir, W. Lendeckel, T. Tuschl, RNA interference is mediated by 21- and 22-nucleotide RNAs, Genes Dev, 15 (2001) 188-200.
[10] S.M. Hammond, E. Bernstein, D. Beach, G.J. Hannon, An RNA-directed nuclease mediates post-transcriptional gene silencing in Drosophila cells, Nature, 404 (2000) 293-296.
[11] J. Martinez, A. Patkaniowska, H. Urlaub, R. Lührmann, T. Tuschl, Single-Stranded Antisense siRNAs Guide Target RNA Cleavage in RNAi, Cell, 110 (2002) 563-574.
[12] J. Martinez, T. Tuschl, RISC is a 5' phosphomonoester-producing RNA endonuclease, Genes Dev, 18 (2004) 975-980.
[13] D.D. Rao, J.S. Vorhies, N. Senzer, J. Nemunaitis, siRNA vs. shRNA: Similarities and differences, Advanced Drug Delivery Reviews, 61 (2009) 746-759.
[14] R.E. Farrell, Chapter 23 - RNAi: Take a RISC – Role the Dicer, in: R.E. Farrell (Ed.) RNA Methodologies (Fourth Edition), Academic Press, San Diego, 2010, pp. 539-560.
[15] K. Chang, S.J. Elledge, G.J. Hannon, Lessons from Nature: microRNA-based shRNA libraries, Nature Methods, 3 (2006) 707-714.
[16] A. El-Sayed, H. Harashima, Endocytosis of Gene Delivery Vectors: From Clathrin-dependent to Lipid Raft-mediated Endocytosis, Molecular Therapy, 21 (2013) 1118-1130.
[17] J.J. Rennick, A.P.R. Johnston, R.G. Parton, Key principles and methods for studying the endocytosis of biological and nanoparticle therapeutics, Nature Nanotechnology, 16 (2021) 266-276.
[18] J. Gruenberg, F.R. Maxfield, Membrane transport in the endocytic pathway, Current Opinion in Cell Biology, 7 (1995) 552-563.
[19] J. Gilleron, W. Querbes, A. Zeigerer, A. Borodovsky, G. Marsico, U. Schubert, K. Manygoats, S. Seifert, C. Andree, M. Stöter, H. Epstein-Barash, L. Zhang, V. Koteliansky, K. Fitzgerald, E. Fava, M. Bickle, Y. Kalaidzidis, A. Akinc, M. Maier, M. Zerial, Image-based analysis of lipid nanoparticle–mediated siRNA delivery, intracellular trafficking and endosomal escape, Nature Biotechnology, 31 (2013) 638-646.
[20] A. Wittrup, A. Ai, X. Liu, P. Hamar, R. Trifonova, K. Charisse, M. Manoharan, T. Kirchhausen, J. Lieberman, Visualizing lipid-formulated siRNA release from endosomes and target gene knockdown, Nature Biotechnology, 33 (2015) 870-876.
[21] T.L.M. Thurston, M.P. Wandel, N. von Muhlinen, Á. Foeglein, F. Randow, Galectin 8 targets damaged vesicles for autophagy to defend cells against bacterial invasion, Nature, 482 (2012) 414-418.
[22] A.A. Khan, D. Betel, M.L. Miller, C. Sander, C.S. Leslie, D.S. Marks, Transfection of small RNAs globally perturbs gene regulation by endogenous microRNAs, Nature Biotechnology, 27 (2009) 549-555.
[23] A.L. Jackson, P.S. Linsley, Recognizing and avoiding siRNA off-target effects for target identification and therapeutic application, Nature Reviews Drug Discovery, 9 (2010) 57-67.
[24] S. Vankoningsloo, F. de Longueville, S. Evrard, P. Rahier, A. Houbion, A. Fattaccioli, M. Gastellier, J. Remacle, M. Raes, P. Renard, T. Arnould, Gene expression silencing with 'specific' small interfering RNA goes beyond specificity – a study of key parameters to take into account in the onset of small interfering

RNA off-target effects, The FEBS Journal, 275 (2008) 2738-2753.
[25] A. Lin, J.M. Sheltzer, Discovering and validating cancer genetic dependencies: approaches and pitfalls, Nature Reviews Genetics, 21 (2020) 671-682.
[26] A.D. Springer, S.F. Dowdy, GalNAc-siRNA Conjugates: Leading the Way for Delivery of RNAi Therapeutics, Nucleic Acid Therapeutics, 28 (2018) 109-118.
[27] J. Tushir-Singh, Antibody-siRNA conjugates: drugging the undruggable for anti-leukemic therapy, Expert Opinion on Biological Therapy, 17 (2017) 325-338.
[28] S.H. Lee, Y.Y. Kang, H.-E. Jang, H. Mok, Current preclinical small interfering RNA (siRNA)-based conjugate systems for RNA therapeutics, Advanced Drug Delivery Reviews, 104 (2016) 78-92.
[29] S.H. Lee, J.Y. Lee, J.S. Kim, T.G. Park, H. Mok, Amphiphilic siRNA Conjugates for Co-Delivery of Nucleic Acids and Hydrophobic Drugs, Bioconjugate Chemistry, 28 (2017) 2051-2061.
[30] H. Nemati, M.-H. Ghahramani, R. Faridi-Majidi, B. Izadi, G. Bahrami, S.-H. Madani, G. Tavoosidana, Using siRNA-based spherical nucleic acid nanoparticle conjugates for gene regulation in psoriasis, Journal of Controlled Release, 268 (2017) 259-268.
[31] C. Chen, Z. Wang, J. Zhang, X. Fan, L. Xu, X. Tang, Dextran-Conjugated Caged siRNA Nanoparticles for Photochemical Regulation of RNAi-Induced Gene Silencing in Cells and Mice, Bioconjugate Chemistry, 30 (2019) 1459-1465.
[32] C.H. Huang, H. Takemoto, T. Nomoto, K. Tomoda, M. Matsui, N. Nishiyama, Utility of the 2-Nitrobenzenesulfonamide Group as a Chemical Linker for Enhanced Extracellular Stability and Cytosolic Cleavage in siRNA-Conjugated Polymer Systems, ChemMedChem, 12 (2017) 19-22.
[33] L. Zhang, W. Zheng, R. Tang, N. Wang, W. Zhang, X. Jiang, Gene regulation with carbon-based siRNA conjugates for cancer therapy, Biomaterials, 104 (2016) 269-278.
[34] C.R. Allerson, N. Sioufi, R. Jarres, T.P. Prakash, N. Naik, A. Berdeja, L. Wanders, R.H. Griffey, E.E. Swayze, B. Bhat, Fully 2′-Modified Oligonucleotide Duplexes with Improved in Vitro Potency and Stability Compared to Unmodified Small Interfering RNA, Journal of Medicinal Chemistry, 48 (2005) 901-904.
[35] T.P. Prakash, C.R. Allerson, P. Dande, T.A. Vickers, N. Sioufi, R. Jarres, B.F. Baker, E.E. Swayze, R.H. Griffey, B. Bhat, Positional Effect of Chemical Modifications on Short Interference RNA Activity in Mammalian Cells, Journal of Medicinal Chemistry, 48 (2005) 4247-4253.
[36] Y. Dong, D.J. Siegwart, D.G. Anderson, Strategies, design, and chemistry in siRNA delivery systems, Advanced Drug Delivery Reviews, 144 (2019) 133-147.
[37] T.C. Roberts, R. Langer, M.J.A. Wood, Advances in oligonucleotide drug delivery, Nature Reviews Drug Discovery, 19 (2020) 673-694.
[38] W.A. Velema, E.T. Kool, The chemistry and applications of RNA 2′-OH acylation, Nature Reviews Chemistry, 4 (2020) 22-37.
[39] J. Huotari, A. Helenius, Endosome maturation, The EMBO Journal, 30 (2011) 3481-3500.
[40] W.H. Crestfield Am Fau - Stein, S. Stein Wh Fau - Moore, S. Moore, On the preparation of bovine pancreatic ribonuclease A, Journal of Biological Chemistry, 238 618-621.
[41] M. Nowotny, W. Yang, Stepwise analyses of metal ions in RNase H catalysis from substrate destabilization to product release, The EMBO Journal, 25 (2006) 1924-1933.
[42] T.W. Nilsen, The Fundamentals of RNA Purification, Cold Spring Harbor Protocols, 2013 (2013) pdb.top075838.
[43] R.E. Farrell, Chapter 2 - Creating a Ribonuclease-Free Environment, in: R.E. Farrell (Ed.) RNA Methodologies (Fifth Edition), Academic Press2017, pp. 55-74.

[44] A. Nagy, M. Gertsenstein, K. Vintersten, R. Behringer, General Procedures for Avoiding Contamination with RNase, Cold Spring Harbor Protocols, 2007 (2007) pdb.ip43.
[45] R.E. Farrell, Chapter 7 - Resilient Ribonucleases, in: R.E. Farrell (Ed.) RNA Methodologies (Fourth Edition), Academic Press, San Diego, 2010, pp. 155-172.
[46] S.L. Lee, K.A. Sevarino, 3 - Molecular Assays for Rat Thyrotropin-Releasing Hormone Gene, in: P.M. Conn (Ed.) Methods in Neurosciences, Academic Press1991, pp. 34-52.
[47] L. Ehrenberg, I. Fedorcsak, F. Solymosy, Diethyl Pyrocarbonate in Nucleic Acid Research, in: W.E. Cohn (Ed.) Progress in Nucleic Acid Research and Molecular Biology, Academic Press1976, pp. 189-262.
[48] M.R. Green, J. Sambrook, How to Win the Battle with RNase, Cold Spring Harbor Protocols, 2019 (2019) pdb.top101857.
[49] Z. Wang, S. Zong, Z. Wang, L. Wu, P. Chen, B. Yun, Y. Cui, Microfluidic chip based micro RNA detection through the combination of fluorescence and surface enhanced Raman scattering techniques, Nanotechnology, 28 (2017) 105501.
[50] B.E. Slatko, Laboratory Investigations in Molecular Biology, Jones and Bartlett Publishers.
[51] Y.H. Huang, P. Leblanc, V. Apostolou, B. Stewart, R.B. Moreland, Comparison of Milli-Q PF Plus water to DEPC-treated water in the preparation and analysis of RNA, Biotechniques, 19 (1995) 656-661.
[52] D.B. Volkin, A. Staubli, R. Langer, A.M. Klibanov, Enzyme thermoinactivation in anhydrous organic solvents, Biotechnology and Bioengineering, 37 (1991) 843-853.
[53] S. Rietwyk, D. Peer, Next-Generation Lipids in RNA Interference Therapeutics, ACS Nano, 11 (2017) 7572-7586.
[54] D. Witzigmann, J.A. Kulkarni, J. Leung, S. Chen, P.R. Cullis, R. van der Meel, Lipid nanoparticle technology for therapeutic gene regulation in the liver, Advanced Drug Delivery Reviews, 159 (2020) 344-363.
[55] K. Raemdonck, T.F. Martens, K. Braeckmans, J. Demeester, S.C. De Smedt, Polysaccharide-based nucleic acid nanoformulations, Advanced Drug Delivery Reviews, 65 (2013) 1123-1147.
[56] Y. Li, R.R. Breaker, Kinetics of RNA Degradation by Specific Base Catalysis of Transesterification Involving the 2'-Hydroxyl Group, Journal of the American Chemical Society, 121 (1999) 5364-5372.
[57] R.G. Kuimelis, L.W. McLaughlin, Mechanisms of Ribozyme-Mediated RNA Cleavage, Chemical Reviews, 98 (1998) 1027-1044.
[58] D.-M. Zhou, K. Taira, The Hydrolysis of RNA: From Theoretical Calculations to the Hammerhead Ribozyme-Mediated Cleavage of RNA, Chemical Reviews, 98 (1998) 991-1026.
[59] M. Oivanen, S. Kuusela, H. Lönnberg, Kinetics and Mechanisms for the Cleavage and Isomerization of the Phosphodiester Bonds of RNA by Brønsted Acids and Bases, Chemical Reviews, 98 (1998) 961-990.
[60] G.A. Soukup, R.R. Breaker, Relationship between internucleotide linkage geometry and the stability of RNA, RNA, 5 (1999) 1308-1325.
[61] R. Breslow, S.D. Dong, Y. Webb, R. Xu, Further Studies on the Buffer-Catalyzed Cleavage and Isomerization of Uridyluridine. Medium and Ionic Strength Effects on Catalysis by Morpholine, Imidazole, and Acetate Buffers Help Clarify the Mechanisms Involved and Their Relationship to the Mechanism Used by the Enzyme Ribonuclease and by a Ribonuclease Mimic, Journal of the American Chemical Society, 118 (1996) 6588-6600.
[62] P. Jarvinen, M. Oivanen, H. Lonnberg, Interconversion and phosphoester hydrolysis of 2',5'- and 3',5'-dinucleoside monophosphates: kinetics and mechanisms, The Journal of Organic Chemistry, 56 (1991) 5396-5401.

[63] J.H. Strauss Jr, R.B. Kelly, R.L. Sinsheimer, Denaturation of RNA with dimethyl sulfoxide, Biopolymers, 6 (1968) 793-807.
[64] D.R. Hickey, D.H. Turner, Solvent effects on the stability of A7U7p, Biochemistry, 24 (1985) 2086-2094.
[65] D.S. Bachoon, F. Chen, R.E. Hodson, RNA recovery and detection of mRNA by RT-PCR from preserved prokaryotic samples, FEMS Microbiology Letters, 201 (2001) 127-132.
[66] A.E. Krafft, K.L. Russell, A.W. Hawksworth, S. McCall, M. Irvine, L.T. Daum, J.L. Connoly, A.H. Reid, J.C. Gaydos, J.K. Taubenberger, Evaluation of PCR Testing of Ethanol-Fixed Nasal Swab Specimens as an Augmented Surveillance Strategy for Influenza Virus and Adenovirus Identification, Journal of Clinical Microbiology, 43 (2005) 1768.
[67] R. Shiman, D.E. Draper, Stabilization of RNA tertiary structure by monovalent cations11Edited by I. Tinoco, Journal of Molecular Biology, 302 (2000) 79-91.
[68] T. Astrid, E. Margit, F. Leopold, Ethanol: A simple and effective RNA-preservation for freshwater insects living in remote habitats, Limnology and Oceanography: Methods, 14 (2016) 186-195.
[69] A.J. Rissanen, E. Kurhela, T. Aho, T. Oittinen, M. Tiirola, Storage of environmental samples for guaranteeing nucleic acid yields for molecular microbiological studies, Applied Microbiology and Biotechnology, 88 (2010) 977-984.
[70] D.L. Evers, R.D. Slemons, J.K. Taubenberger, Effect of preservative on recoverable RT-PCR amplicon length from influenza A virus in bird feces, Avian Dis, 51 (2007) 965-968.
[71] P. Chomczynski, Solubilzation in formamide protects RNA from degradation, Nucleic Acids Research, 20 (1992) 3791-3792.
[72] S.-I. Nakano, Y. Kitagawa, D. Miyoshi, N. Sugimoto, Hammerhead ribozyme activity and oligonucleotide duplex stability in mixed solutions of water and organic compounds, FEBS Open Bio, 4 (2014) 643-650.
[73] W. Tao, A. Yurdagul, N. Kong, W. Li, X. Wang, A.C. Doran, C. Feng, J. Wang, M.A. Islam, O.C. Farokhzad, I. Tabas, J. Shi, siRNA nanoparticles targeting CaMKIIγ in lesional macrophages improve atherosclerotic plaque stability in mice, Science Translational Medicine, 12 (2020) eaay1063.
[74] H. Yu, T. Lin, W. Chen, W. Cao, C. Zhang, T. Wang, M. Ding, S. Zhao, H. Wei, H. Guo, X. Zhao, Size and temporal-dependent efficacy of oltipraz-loaded PLGA nanoparticles for treatment of acute kidney injury and fibrosis, Biomaterials, 219 (2019) 119368.
[75] Y. Byeon, J.-W. Lee, W.S. Choi, J.E. Won, G.H. Kim, M.G. Kim, T.I. Wi, J.M. Lee, T.H. Kang, I.D. Jung, Y.-J. Cho, H.J. Ahn, B.C. Shin, Y.J. Lee, A.K. Sood, H.D. Han, Y.-M. Park, CD44-Targeting PLGA Nanoparticles Incorporating Paclitaxel and FAK siRNA Overcome Chemoresistance in Epithelial Ovarian Cancer, Cancer Research, 78 (2018) 6247.
[76] N. Kimura, M. Maeki, Y. Sato, A. Ishida, H. Tani, H. Harashima, M. Tokeshi, Development of a Microfluidic-Based Post-Treatment Process for Size-Controlled Lipid Nanoparticles and Application to siRNA Delivery, ACS Applied Materials & Interfaces, 12 (2020) 34011-34020.
[77] J. Zhang, H. Shen, J. Xu, L. Liu, J. Tan, M. Li, N. Xu, S. Luo, J. Wang, F. Yang, J. Tang, Q. Li, Y. Wang, L. Yu, Z. Yan, Liver-Targeted siRNA Lipid Nanoparticles Treat Hepatic Cirrhosis by Dual Antifibrotic and Anti-inflammatory Activities, ACS Nano, 14 (2020) 6305-6322.
[78] R. Kedmi, N. Veiga, S. Ramishetti, M. Goldsmith, D. Rosenblum, N. Dammes, I. Hazan-Halevy, L. Nahary, S. Leviatan-Ben-Arye, M. Harlev, M. Behlke, I. Benhar, J. Lieberman, D. Peer, A modular platform for targeted RNAi therapeutics, Nature Nanotechnology, 13 (2018) 214-219.
[79] N. Veiga, M. Goldsmith, Y. Granot, D. Rosenblum, N. Dammes, R. Kedmi, S. Ramishetti, D. Peer, Cell

specific delivery of modified mRNA expressing therapeutic proteins to leukocytes, Nature Communications, 9 (2018) 4493.
[80] L. Wang, Y. Hao, H. Li, Y. Zhao, D. Meng, D. Li, J. Shi, H. Zhang, Z. Zhang, Y. Zhang, Co-delivery of doxorubicin and siRNA for glioma therapy by a brain targeting system: angiopep-2-modified poly(lactic-co-glycolic acid) nanoparticles, Journal of Drug Targeting, 23 (2015) 832-846.
[81] X. Sun, S. Dong, X. Li, K. Yu, F. Sun, R.J. Lee, Y. Li, L. Teng, Delivery of siRNA using folate receptor-targeted pH-sensitive polymeric nanoparticles for rheumatoid arthritis therapy, Nanomedicine: Nanotechnology, Biology and Medicine, 20 (2019) 102017.
[82] J. Xu, Y. Liu, Y. Li, H. Wang, S. Stewart, K. Van der Jeught, P. Agarwal, Y. Zhang, S. Liu, G. Zhao, J. Wan, X. Lu, X. He, Precise targeting of POLR2A as a therapeutic strategy for human triple negative breast cancer, Nature Nanotechnology, 14 (2019) 388-397.
[83] J. Gu, S. Yang, E.A. Ho, Biodegradable Film for the Targeted Delivery of siRNA-Loaded Nanoparticles to Vaginal Immune Cells, Molecular Pharmaceutics, 12 (2015) 2889-2903.
[84] M.J. Gomes, C. Fernandes, S. Martins, F. Borges, B. Sarmento, Tailoring Lipid and Polymeric Nanoparticles as siRNA Carriers towards the Blood-Brain Barrier – from Targeting to Safe Administration, Journal of Neuroimmune Pharmacology, 12 (2017) 107-119.
[85] A.M. Aldayel, H.L. O'Mary, S.A. Valdes, X. Li, S.G. Thakkar, B.E. Mustafa, Z. Cui, Lipid nanoparticles with minimum burst release of TNF-α siRNA show strong activity against rheumatoid arthritis unresponsive to methotrexate, Journal of Controlled Release, 283 (2018) 280-289.
[86] X. Mu, H. Lu, L. Fan, S. Yan, K. Hu, Efficient Delivery of Therapeutic siRNA with Nanoparticles Induces Apoptosis in Prostate Cancer Cells, Journal of Nanomaterials, 2018 (2018) 4719790.
[87] J.J. Butzow, G.L. Eichhorn, Different susceptibility of DNA and RNA to cleavage by metal ions, Nature, 254 (1975) 358-359.
[88] R. Yamagami, J.L. Bingaman, E.A. Frankel, P.C. Bevilacqua, Cellular conditions of weakly chelated magnesium ions strongly promote RNA stability and catalysis, Nature Communications, 9 (2018) 2149.
[89] D.E. Draper, A guide to ions and RNA structure, RNA, 10 (2004) 335-343.
[90] M. Komiyama, N. Takeda, H. Shigekawa, Hydrolysis of DNA and RNA by lanthanide ions: mechanistic studies leading to new applications, Chemical Communications, (1999) 1443-1451.
[91] M. Forconi, D. Herschlag, Chapter 5 - Metal Ion-Based RNA Cleavage as a Structural Probe, Methods in Enzymology, Academic Press2009, pp. 91-106.
[92] A. Kuzuya, R. Mizoguchi, F. Morisawa, K. Machida, M. Komiyama, Metal Ion-Induced Site-Selective RNA Hydrolysis by Use of Acridine-Bearing Oligonucleotide as Cofactor, Journal of the American Chemical Society, 124 (2002) 6887-6894.
[93] Z. Liu, F. Fontana, A. Python, J.T. Hirvonen, H.A. Santos, Microfluidics for Production of Particles: Mechanism, Methodology, and Applications, Small, 16 (2020) 1904673.
[94] E. Samaridou, J. Heyes, P. Lutwyche, Lipid nanoparticles for nucleic acid delivery: Current perspectives, Advanced Drug Delivery Reviews, (2020).
[95] L.-L. Li, H.-W. An, B. Peng, R. Zheng, H. Wang, Self-assembled nanomaterials: design principles, the nanostructural effect, and their functional mechanisms as antimicrobial or detection agents, Materials Horizons, 6 (2019) 1794-1811.
[96] S. Patel, N. Ashwanikumar, E. Robinson, Y. Xia, C. Mihai, J.P. Griffith, 3rd, S. Hou, A.A. Esposito, T. Ketova, K. Welsher, J.L. Joyal, O. Almarsson, G. Sahay, Naturally-occurring cholesterol analogues in lipid nanoparticles induce polymorphic shape and enhance intracellular delivery of mRNA, Nat Commun, 11 (2020) 983.

[97] R.L. Ball, K.A. Hajj, J. Vizelman, P. Bajaj, K.A. Whitehead, Lipid Nanoparticle Formulations for Enhanced Co-delivery of siRNA and mRNA, Nano Letters, 18 (2018) 3814-3822.
[98] J.A. Kulkarni, D. Witzigmann, J. Leung, Y.Y.C. Tam, P.R. Cullis, On the role of helper lipids in lipid nanoparticle formulations of siRNA, Nanoscale, 11 (2019) 21733-21739.
[99] K.A. Whitehead, J.R. Dorkin, A.J. Vegas, P.H. Chang, O. Veiseh, J. Matthews, O.S. Fenton, Y. Zhang, K.T. Olejnik, V. Yesilyurt, D. Chen, S. Barros, B. Klebanov, T. Novobrantseva, R. Langer, D.G. Anderson, Degradable lipid nanoparticles with predictable in vivo siRNA delivery activity, Nature Communications, 5 (2014) 4277.
[100] W. Wei, J. Sun, X.-Y. Guo, X. Chen, R. Wang, C. Qiu, H.-T. Zhang, W.-H. Pang, J.-C. Wang, Q. Zhang, Microfluidic-Based Holonomic Constraints of siRNA in the Kernel of Lipid/Polymer Hybrid Nanoassemblies for Improving Stable and Safe In Vivo Delivery, ACS Applied Materials & Interfaces, 12 (2020) 14839-14854.
[101] M.A. Younis, I.A. Khalil, Y.H.A. Elewa, Y. Kon, H. Harashima, Ultra-small lipid nanoparticles encapsulating sorafenib and midkine-siRNA selectively-eradicate sorafenib-resistant hepatocellular carcinoma in vivo, Journal of Controlled Release, 331 (2021) 335-349.
[102] Y. Eygeris, S. Patel, A. Jozic, G. Sahay, Deconvoluting Lipid Nanoparticle Structure for Messenger RNA Delivery, Nano Letters, 20 (2020) 4543-4549.
[103] A.K.K. Leung, I.M. Hafez, S. Baoukina, N.M. Belliveau, I.V. Zhigaltsev, E. Afshinmanesh, D.P. Tieleman, C.L. Hansen, M.J. Hope, P.R. Cullis, Lipid Nanoparticles Containing siRNA Synthesized by Microfluidic Mixing Exhibit an Electron-Dense Nanostructured Core, The Journal of Physical Chemistry C, 116 (2012) 18440-18450.
[104] J.A. Kulkarni, M.M. Darjuan, J.E. Mercer, S. Chen, R. van der Meel, J.L. Thewalt, Y.Y.C. Tam, P.R. Cullis, On the Formation and Morphology of Lipid Nanoparticles Containing Ionizable Cationic Lipids and siRNA, ACS Nano, 12 (2018) 4787-4795.
[105] A.K.K. Leung, Y.Y.C. Tam, S. Chen, I.M. Hafez, P.R. Cullis, Microfluidic Mixing: A General Method for Encapsulating Macromolecules in Lipid Nanoparticle Systems, The Journal of Physical Chemistry B, 119 (2015) 8698-8706.
[106] K. Buyens, J. Demeester, S.S. De Smedt, N.N. Sanders, Elucidating the Encapsulation of Short Interfering RNA in PEGylated Cationic Liposomes, Langmuir, 25 (2009) 4886-4891.
[107] FDA, Drug Approval Package: Onpattro (patisiran), 2018.
[108] Pfizer-BioNTech COVID-19 Vaccine, 2020.
[109] A. Parker, K. Miles, K.H. Cheng, J. Huang, Lateral Distribution of Cholesterol in Dioleoylphosphatidylcholine Lipid Bilayers: Cholesterol-Phospholipid Interactions at High Cholesterol Limit, Biophysical Journal, 86 (2004) 1532-1544.
[110] M. Yanez Arteta, T. Kjellman, S. Bartesaghi, S. Wallin, X. Wu, A.J. Kvist, A. Dabkowska, N. Székely, A. Radulescu, J. Bergenholtz, L. Lindfors, Successful reprogramming of cellular protein production through mRNA delivered by functionalized lipid nanoparticles, Proceedings of the National Academy of Sciences, 115 (2018) E3351.
[111] D. Bach, E. Wachtel, Phospholipid/cholesterol model membranes: formation of cholesterol crystallites, Biochimica et Biophysica Acta (BBA) - Biomembranes, 1610 (2003) 187-197.
[112] S. Patel, N. Ashwanikumar, E. Robinson, Y. Xia, C. Mihai, J.P. Griffith, S. Hou, A.A. Esposito, T. Ketova, K. Welsher, J.L. Joyal, Ö. Almarsson, G. Sahay, Naturally-occurring cholesterol analogues in lipid nanoparticles induce polymorphic shape and enhance intracellular delivery of mRNA, Nature Communications, 11 (2020) 983.

[113] J. Prades, O. Vögler, R. Alemany, M. Gomez-Florit, S.S. Funari, V. Ruiz-Gutiérrez, F. Barceló, Plant pentacyclic triterpenic acids as modulators of lipid membrane physical properties, Biochimica et Biophysica Acta (BBA) - Biomembranes, 1808 (2011) 752-760.
[114] G. Lou, G. Anderluzzi, S.T. Schmidt, S. Woods, S. Gallorini, M. Brazzoli, F. Giusti, I. Ferlenghi, R.N. Johnson, C.W. Roberts, D.T. O'Hagan, B.C. Baudner, Y. Perrie, Delivery of self-amplifying mRNA vaccines by cationic lipid nanoparticles: The impact of cationic lipid selection, Journal of Controlled Release, 325 (2020) 370-379.
[115] R.D. Harvey, N. Ara, R.K. Heenan, D.J. Barlow, P.J. Quinn, M.J. Lawrence, Stabilization of Distearoylphosphatidylcholine Lamellar Phases in Propylene Glycol Using Cholesterol, Molecular Pharmaceutics, 10 (2013) 4408-4417.
[116] A.E. Regelin, S. Fankhaenel, G. Laura, C. Prinz, K. Günter von, U. Massing, Biophysical and lipofection studies of DOTAP analogs, Biochimica et Biophysica Acta, 1464 (2000) 151-164.
[117] W. Ho, X.-Q. Zhang, X. Xu, Biomaterials in siRNA Delivery: A Comprehensive Review, Advanced Healthcare Materials, 5 (2016) 2715-2731.
[118] Y. Liu, Y. Li, D. Keskin, L. Shi, Poly(β-Amino Esters): Synthesis, Formulations, and Their Biomedical Applications, Advanced Healthcare Materials, 8 (2019) 1801359.
[119] Z. Wang, W. Liu, J. Shi, N. Chen, C. Fan, Nanoscale delivery systems for cancer immunotherapy, Materials Horizons, 5 (2018) 344-362.
[120] Y.S. Kim, R. Tamate, A.M. Akimoto, R. Yoshida, Recent developments in self-oscillating polymeric systems as smart materials: from polymers to bulk hydrogels, Materials Horizons, 4 (2017) 38-54.
[121] H.W. Ooi, S. Hafeez, C.A. van Blitterswijk, L. Moroni, M.B. Baker, Hydrogels that listen to cells: a review of cell-responsive strategies in biomaterial design for tissue regeneration, Materials Horizons, 4 (2017) 1020-1040.
[122] X.J. Loh, Supramolecular host–guest polymeric materials for biomedical applications, Materials Horizons, 1 (2014) 185-195.
[123] D. Cun, D.K. Jensen, M.J. Maltesen, M. Bunker, P. Whiteside, D. Scurr, C. Foged, H.M. Nielsen, High loading efficiency and sustained release of siRNA encapsulated in PLGA nanoparticles: Quality by design optimization and characterization, European Journal of Pharmaceutics and Biopharmaceutics, 77 (2011) 26-35.
[124] T. Merdan, J. Callahan, H. Petersen, K. Kunath, U. Bakowsky, P. Kopečková, T. Kissel, J. Kopeček, Pegylated Polyethylenimine−Fab' Antibody Fragment Conjugates for Targeted Gene Delivery to Human Ovarian Carcinoma Cells, Bioconjugate Chemistry, 14 (2003) 989-996.
[125] D. Li, A.S. Sharili, J. Connelly, J.E. Gautrot, Highly Stable RNA Capture by Dense Cationic Polymer Brushes for the Design of Cytocompatible, Serum-Stable SiRNA Delivery Vectors, Biomacromolecules, 19 (2018) 606-615.
[126] D. Li, L. Wu, F. Qu, M.C. Ribadeneyra, G. Tu, J. Gautrot, Core-independent approach for polymer brush-functionalised nanomaterials with a fluorescent tag for RNA delivery, Chemical Communications, 55 (2019) 14166-14169.
[127] K. Zhou, P. Kos, Y. Yan, H. Xiong, Y.-L. Min, K.A. Kinghorn, J.T. Minnig, J.B. Miller, D.J. Siegwart, Intercalation-mediated nucleic acid nanoparticles for siRNA delivery, Chemical Communications, 52 (2016) 12155-12158.
[128] W. Tai, Current Aspects of siRNA Bioconjugate for In Vitro and In Vivo Delivery, Molecules, 24 (2019).
[129] S. Grijalvo, A. Alagia, A.F. Jorge, R. Eritja, Covalent Strategies for Targeting Messenger and Non-

Coding RNAs: An Updated Review on siRNA, miRNA and antimiR Conjugates, Genes, 9 (2018).
[130] R. Acharya, S. Saha, S. Ray, S. Hazra, M.K. Mitra, J. Chakraborty, siRNA-nanoparticle conjugate in gene silencing: A future cure to deadly diseases?, Materials Science and Engineering: C, 76 (2017) 1378-1400.
[131] J. Yu, J. Li, S. Zhai, L. Lin, K. Wang, B. Tang, H. Meng, L. Tian, Enzymatically Synthesized DNA Polymer as Co-carrier for Enhanced RNA Interference, ACS Applied Bio Materials, 2 (2019) 5204-5215.
[132] Z. Zhang, T. Wan, Y. Chen, Y. Chen, H. Sun, T. Cao, Z. Songyang, G. Tang, C. Wu, Y. Ping, F.J. Xu, J. Huang, Cationic Polymer-Mediated CRISPR/Cas9 Plasmid Delivery for Genome Editing, Macromol Rapid Commun, 40 (2019) e1800068.
[133] J. Blersch, V. Francisco, C. Rebelo, A. Jimenez-Balsa, H. Antunes, C. Gonzato, S. Pinto, S. Simoes, K. Liedl, K. Haupt, L. Ferreira, A Light-Triggerable Nanoparticle Library for the Controlled Release of Non-Coding RNAs, Angew Chem Int Ed Engl, 59 (2020) 1985-1991.
[134] L. Zhang, Q. Feng, J. Wang, J. Sun, X. Shi, X. Jiang, Microfluidic Synthesis of Rigid Nanovesicles for Hydrophilic Reagents Delivery, Angewandte Chemie International Edition, 54 (2015) 3952-3956.
[135] X. Zhang, J. Pan, M. Yao, L. Palmerston Mendes, C. Sarisozen, S. Mao, V.P. Torchilin, Charge reversible hyaluronic acid-modified dendrimer-based nanoparticles for siMDR-1 and doxorubicin co-delivery, Eur J Pharm Biopharm, 154 (2020) 43-49.
[136] C. Feng, X. Huang, Polymer Brushes: Efficient Synthesis and Applications, Acc Chem Res, 51 (2018) 2314-2323.
[137] L.I.F. Moura, A. Malfanti, C. Peres, A.I. Matos, E. Guegain, V. Sainz, M. Zloh, M.J. Vicent, H.F. Florindo, Functionalized branched polymers: promising immunomodulatory tools for the treatment of cancer and immune disorders, Materials Horizons, 6 (2019) 1956-1973.
[138] Z. Yang, L. Li, A.J. Jin, W. Huang, X. Chen, Rational design of semiconducting polymer brushes as cancer theranostics, Materials Horizons, 7 (2020) 1474-1494.
[139] Q. Wei, R. Haag, Universal polymer coatings and their representative biomedical applications, Materials Horizons, 2 (2015) 567-577.
[140] Z.-l. Shen, Y.-q. Xia, Q.-s. Yang, W.-d. Tian, K. Chen, Y.-q. Ma, Polymer–Nucleic Acid Interactions, Topics in Current Chemistry, 375 (2017) 44.
[141] R. Godawat, S.N. Jamadagni, S. Garde, Characterizing hydrophobicity of interfaces by using cavity formation, solute binding, and water correlations, Proceedings of the National Academy of Sciences, 106 (2009) 15119.
[142] W. Li, D. Wang, X. Shi, J. Li, Y. Ma, Y. Wang, T. Li, J. Zhang, R. Zhao, Z. Yu, F. Yin, Z. Li, A siRNA-induced peptide co-assembly system as a peptide-based siRNA nanocarrier for cancer therapy, Materials Horizons, 5 (2018) 745-752.
[143] L. Liu, J. Wu, J. Gao, X. Lu, Bacteria-Derived Nanoparticles: Multifunctional Containers for Diagnostic and Therapeutic Applications, Advanced Healthcare Materials, 9 (2020) 2000893.
[144] X. Wu, T. Wu, J. Liu, B. Ding, Gene Therapy Based on Nucleic Acid Nanostructure, Advanced Healthcare Materials, 9 (2020) 2001046.
[145] M. Urello, W.-H. Hsu, R.J. Christie, Peptides as a material platform for gene delivery: Emerging concepts and converging technologies, Acta Biomaterialia, 117 (2020) 40-59.
[146] I. Serrano-Sevilla, Á. Artiga, S.G. Mitchell, L. De Matteis, J.M. de la Fuente, Natural Polysaccharides for siRNA Delivery: Nanocarriers Based on Chitosan, Hyaluronic Acid, and Their Derivatives, Molecules, 24 (2019).
[147] S. Mao, W. Sun, T. Kissel, Chitosan-based formulations for delivery of DNA and siRNA, Advanced

Drug Delivery Reviews, 62 (2010) 12-27.
[148] P. Holzerny, B. Ajdini, W. Heusermann, K. Bruno, M. Schuleit, L. Meinel, M. Keller, Biophysical properties of chitosan/siRNA polyplexes: Profiling the polymer/siRNA interactions and bioactivity, Journal of Controlled Release, 157 (2012) 297-304.
[149] J. Desbrieres, Viscosity of Semiflexible Chitosan Solutions: Influence of Concentration, Temperature, and Role of Intermolecular Interactions, Biomacromolecules, 3 (2002) 342-349.
[150] M. Alameh, M. Lavertu, N. Tran-Khanh, C.-Y. Chang, F. Lesage, M. Bail, V. Darras, A. Chevrier, M.D. Buschmann, siRNA Delivery with Chitosan: Influence of Chitosan Molecular Weight, Degree of Deacetylation, and Amine to Phosphate Ratio on in Vitro Silencing Efficiency, Hemocompatibility, Biodistribution, and in Vivo Efficacy, Biomacromolecules, 19 (2018) 112-131.
[151] V. Dehousse, N. Garbacki, S. Jaspart, D. Castagne, G. Piel, A. Colige, B. Evrard, Comparison of chitosan/siRNA and trimethylchitosan/siRNA complexes behaviour in vitro, International Journal of Biological Macromolecules, 46 (2010) 342-349.
[152] T. Sato, T. Ishii, Y. Okahata, In vitro gene delivery mediated by chitosan. Effect of pH, serum, and molecular mass of chitosan on the transfection efficiency, Biomaterials, 22 (2001) 2075-2080.
[153] Y.-M. Zhang, Y. Yang, Y.-H. Zhang, Y. Liu, Polysaccharide Nanoparticles for Efficient siRNA Targeting in Cancer Cells by Supramolecular pKa Shift, Scientific Reports, 6 (2016) 28848.
[154] M. Zheng, Z. Yang, S. Chen, H. Wu, Y. Liu, A. Wright, J.-W. Lu, X. Xia, A. Lee, J. Zhang, H. Yin, Y. Wang, W. Ruan, X.-J. Liang, Bioreducible Zinc(II)–Dipicolylamine Functionalized Hyaluronic Acid Mediates Safe siRNA Delivery and Effective Glioblastoma RNAi Therapy, ACS Applied Bio Materials, 2 (2019) 362-369.
[155] G.H. Kim, J.E. Won, Y. Byeon, M.G. Kim, T.I. Wi, J.M. Lee, Y.-Y. Park, J.-W. Lee, T.H. Kang, I.D. Jung, B.C. Shin, H.J. Ahn, Y.J. Lee, A.K. Sood, H.D. Han, Y.-M. Park, Selective delivery of PLXDC1 small interfering RNA to endothelial cells for anti-angiogenesis tumor therapy using CD44-targeted chitosan nanoparticles for epithelial ovarian cancer, Drug Delivery, 25 (2018) 1394-1402.
[156] X. Qu, Y. Hu, H. Wang, H. Song, M. Young, F. Xu, Y. Liu, G. Cheng, Biomimetic Dextran–Peptide Vectors for Efficient and Safe siRNA Delivery, ACS Applied Bio Materials, 2 (2019) 1456-1463.
[157] C. Siewert, H. Haas, T. Nawroth, A. Ziller, S.S. Nogueira, M.A. Schroer, C.E. Blanchet, D.I. Svergun, A. Radulescu, F. Bates, Y. Huesemann, M.P. Radsak, U. Sahin, P. Langguth, Investigation of charge ratio variation in mRNA – DEAE-dextran polyplex delivery systems, Biomaterials, 192 (2019) 612-620.
[158] M.-A. Nguyen, H. Wyatt, L. Susser, M. Geoffrion, A. Rasheed, A.-C. Duchez, M.L. Cottee, E. Afolayan, E. Farah, Z. Kahiel, M. Côté, S. Gadde, K.J. Rayner, Delivery of MicroRNAs by Chitosan Nanoparticles to Functionally Alter Macrophage Cholesterol Efflux in Vitro and in Vivo, ACS Nano, 13 (2019) 6491-6505.
[159] F. Chaharband, N. Daftarian, M.R. Kanavi, R. Varshochian, M. Hajiramezanali, P. Norouzi, E. Arefian, F. Atyabi, R. Dinarvand, Trimethyl chitosan-hyaluronic acid nano-polyplexes for intravitreal VEGFR-2 siRNA delivery: Formulation and in vivo efficacy evaluation, Nanomedicine: Nanotechnology, Biology and Medicine, 26 (2020) 102181.
[160] X. Yao, J. Mu, L. Zeng, J. Lin, Z. Nie, X. Jiang, P. Huang, Stimuli-responsive cyclodextrin-based nanoplatforms for cancer treatment and theranostics, Materials Horizons, 6 (2019) 846-870.
[161] Y.Y. Khine, M.H. Stenzel, Surface modified cellulose nanomaterials: a source of non-spherical nanoparticles for drug delivery, Materials Horizons, 7 (2020) 1727-1758.
[162] Z. Chen, B. Krishnamachary, M.F. Penet, Z.M. Bhujwalla, Acid-degradable Dextran as an Image Guided siRNA Carrier for COX-2 Downregulation, Theranostics, 8 (2018) 1-12.

[163] L. Liu, Y. Li, R. Liu, Q. Shen, Y. Li, Z. Shi, J. Shen, W. Ji, X. Zhang, Switchable nanoparticle for programmed gene-chem delivery with enhanced neuronal recovery and CT imaging for neurodegenerative disease treatment, Materials Horizons, 6 (2019) 1923-1929.
[164] B.L. Li, R. Li, H.L. Zou, K. Ariga, N.B. Li, D.T. Leong, Engineered functionalized 2D nanoarchitectures for stimuli-responsive drug delivery, Materials Horizons, 7 (2020) 455-469.
[165] J. Shen, W. Zhang, R. Qi, Z.-W. Mao, H. Shen, Engineering functional inorganic–organic hybrid systems: advances in siRNA therapeutics, Chemical Society Reviews, 47 (2018) 1969-1995.
[166] C.A. Mirkin, R.L. Letsinger, R.C. Mucic, J.J. Storhoff, A DNA-based method for rationally assembling nanoparticles into macroscopic materials, Nature, 382 (1996) 607-609.
[167] Á. Artiga, I. Serrano-Sevilla, L. De Matteis, S.G. Mitchell, J.M. de la Fuente, Current status and future perspectives of gold nanoparticle vectors for siRNA delivery, Journal of Materials Chemistry B, 7 (2019) 876-896.
[168] A. Banerjee, T. Pons, N. Lequeux, B. Dubertret, Quantum dots–DNA bioconjugates: synthesis to applications, Interface Focus, 6 (2016) 20160064.
[169] A.M. Derfus, A.A. Chen, D.-H. Min, E. Ruoslahti, S.N. Bhatia, Targeted Quantum Dot Conjugates for siRNA Delivery, Bioconjugate Chemistry, 18 (2007) 1391-1396.
[170] Y. Lei, L. Tang, Y. Xie, Y. Xianyu, L. Zhang, P. Wang, Y. Hamada, K. Jiang, W. Zheng, X. Jiang, Gold nanoclusters-assisted delivery of NGF siRNA for effective treatment of pancreatic cancer, Nature Communications, 8 (2017) 15130.
[171] Y. Wang, F. Wang, Y. Shen, Q. He, S. Guo, Tumor-specific disintegratable nanohybrids containing ultrasmall inorganic nanoparticles: from design and improved properties to cancer applications, Materials Horizons, 5 (2018) 184-205.
[172] R.A. Perez, R.K. Singh, T.-H. Kim, H.-W. Kim, Silica-based multifunctional nanodelivery systems toward regenerative medicine, Materials Horizons, 4 (2017) 772-799.
[173] W. Li, Z. Liu, F. Fontana, Y. Ding, D. Liu, J.T. Hirvonen, H.A. Santos, Tailoring Porous Silicon for Biomedical Applications: From Drug Delivery to Cancer Immunotherapy, Adv Mater, 30 (2018) 1703740.
[174] K.D. Patel, R.K. Singh, H.-W. Kim, Carbon-based nanomaterials as an emerging platform for theranostics, Materials Horizons, 6 (2019) 434-469.
[175] K. Zheng, B. Sui, K. Ilyas, A.R. Boccaccini, Porous bioactive glass micro- and nanospheres with controlled morphology: developments, properties and emerging biomedical applications, Materials Horizons, 8 (2021) 300-335.
[176] Y. Wang, Y. Xie, K.V. Kilchrist, J. Li, C.L. Duvall, D. Oupický, Endosomolytic and Tumor-Penetrating Mesoporous Silica Nanoparticles for siRNA/miRNA Combination Cancer Therapy, ACS Applied Materials & Interfaces, 12 (2020) 4308-4322.
[177] J. Kang, J. Joo, E.J. Kwon, M. Skalak, S. Hussain, Z.-G. She, E. Ruoslahti, S.N. Bhatia, M.J. Sailor, Self-Sealing Porous Silicon-Calcium Silicate Core–Shell Nanoparticles for Targeted siRNA Delivery to the Injured Brain, Adv Mater, 28 (2016) 7962-7969.
[178] B. Kim, S. Sun, J.A. Varner, S.B. Howell, E. Ruoslahti, M.J. Sailor, Securing the Payload, Finding the Cell, and Avoiding the Endosome: Peptide-Targeted, Fusogenic Porous Silicon Nanoparticles for Delivery of siRNA, Adv Mater, 31 (2019) 1902952.
[179] L.-C. Sang, A. Vinu, M.-O. Coppens, General Description of the Adsorption of Proteins at Their Iso-electric Point in Nanoporous Materials, Langmuir, 27 (2011) 13828-13837.
[180] K. Ye, L. Malinina, D.J. Patel, Recognition of small interfering RNA by a viral suppressor of RNA silencing, Nature, 426 (2003) 874-878.

[181] D.V. Svintradze, G.M. Mrevlishvili, Fiber molecular model of atelocollagen–small interfering RNA (siRNA) complex, International Journal of Biological Macromolecules, 37 (2005) 283-286.
[182] J.L. Steinbacher, C.C. Landry, Adsorption and Release of siRNA from Porous Silica, Langmuir, 30 (2014) 4396-4405.
[183] W. Song, C. Yang, D.Q. Svend Le, Y. Zhang, J. Kjems, Calcium–MicroRNA Complex-Functionalized Nanotubular Implant Surface for Highly Efficient Transfection and Enhanced Osteogenesis of Mesenchymal Stem Cells, ACS Applied Materials & Interfaces, 10 (2018) 7756-7764.
[184] E. Ruvinov, O. Kryukov, E. Forti, E. Korin, M. Goldstein, S. Cohen, Calcium–siRNA nanocomplexes: What reversibility is all about, Journal of Controlled Release, 203 (2015) 150-160.
[185] Z. Zhou, H. Li, K. Wang, Q. Guo, C. Li, H. Jiang, Y. Hu, D. Oupicky, M. Sun, Bioreducible Cross-Linked Hyaluronic Acid/Calcium Phosphate Hybrid Nanoparticles for Specific Delivery of siRNA in Melanoma Tumor Therapy, ACS Applied Materials & Interfaces, 9 (2017) 14576-14589.
[186] J. Li, Y.-C. Chen, Y.-C. Tseng, S. Mozumdar, L. Huang, Biodegradable calcium phosphate nanoparticle with lipid coating for systemic siRNA delivery, Journal of Controlled Release, 142 (2010) 416-421.
[187] T. Tenkumo, L. Rojas-Sánchez, J.R. Vanegas Sáenz, T. Ogawa, M. Miyashita, N. Yoda, O. Prymak, V. Sokolova, K. Sasaki, M. Epple, Reduction of inflammation in a chronic periodontitis model in rats by TNF-α gene silencing with a topically applied siRNA-loaded calcium phosphate paste, Acta Biomaterialia, 105 (2020) 263-279.
[188] L. Woythe, N.B. Tito, L. Albertazzi, A quantitative view on multivalent nanomedicine targeting, Advanced Drug Delivery Reviews, 169 (2021) 1-21.
[189] A.C. Marques, P.J. Costa, S. Velho, M.H. Amaral, Functionalizing nanoparticles with cancer-targeting antibodies: A comparison of strategies, Journal of Controlled Release, 320 (2020) 180-200.
[190] Z. Liu, Y. Li, W. Li, W. Lian, M. Kemell, S. Hietala, P. Figueiredo, L. Li, E. Mäkilä, M. Ma, J. Salonen, J.T. Hirvonen, D. Liu, H. Zhang, X. Deng, H.A. Santos, Close-loop dynamic nanohybrids on collagen-ark with in situ gelling transformation capability for biomimetic stage-specific diabetic wound healing, Materials Horizons, 6 (2019) 385-393.
[191] Y. Li, Z. Liu, L. Li, W. Lian, Y. He, E. Khalil, E. Mäkilä, W. Zhang, G. Torrieri, X. Liu, J. Su, Y. Xiu, F. Fontana, J. Salonen, J. Hirvonen, W. Liu, H. Zhang, H.A. Santos, X. Deng, Tandem-Mass-Tag Based Proteomic Analysis Facilitates Analyzing Critical Factors of Porous Silicon Nanoparticles in Determining Their Biological Responses under Diseased Condition, Advanced Science, 7 (2020) 2001129.
[192] Z. Liu, Y. Li, W. Li, C. Xiao, D. Liu, C. Dong, M. Zhang, E. Mäkilä, M. Kemell, J. Salonen, J.T. Hirvonen, H. Zhang, D. Zhou, X. Deng, H.A. Santos, Multifunctional Nanohybrid Based on Porous Silicon Nanoparticles, Gold Nanoparticles, and Acetalated Dextran for Liver Regeneration and Acute Liver Failure Theranostics, Adv Mater, 30 (2018) 1703393.
[193] Kathryn J. Moore, I. Tabas, Macrophages in the Pathogenesis of Atherosclerosis, Cell, 145 (2011) 341-355.
[194] G. Erel-Akbaba, L.A. Carvalho, T. Tian, M. Zinter, H. Akbaba, P.J. Obeid, E.A. Chiocca, R. Weissleder, A.G. Kantarci, B.A. Tannous, Radiation-Induced Targeted Nanoparticle-Based Gene Delivery for Brain Tumor Therapy, ACS Nano, 13 (2019) 4028-4040.
[195] T. Ganbold, Q. Bao, J. Zandan, A. Hasi, H. Baigude, Modulation of Microglia Polarization through Silencing of NF-κB p65 by Functionalized Curdlan Nanoparticle-Mediated RNAi, ACS Applied Materials & Interfaces, 12 (2020) 11363-11374.
[196] T. Bejerano, S. Etzion, S. Elyagon, Y. Etzion, S. Cohen, Nanoparticle Delivery of miRNA-21 Mimic

to Cardiac Macrophages Improves Myocardial Remodeling after Myocardial Infarction, Nano Letters, 18 (2018) 5885-5891.

[197] H. He, J. Wang, P.J. Yannie, W.J. Korzun, H. Yang, S. Ghosh, Nanoparticle-based "Two-pronged" approach to regress atherosclerosis by simultaneous modulation of cholesterol influx and efflux, Biomaterials, 260 (2020) 120333.

[198] T. Wu, H. Xiao, L. Lu, Y. Chen, Y. Wang, W. Xia, M. Long, J. Tao, J. Shen, X. Shuai, Polymeric Vector-Mediated Targeted Delivery of Anti-PAK1 siRNA to Macrophages for Efficient Atherosclerosis Treatment, ACS Biomaterials Science & Engineering, 5 (2019) 4455-4462.

[199] N. Shobaki, Y. Sato, Y. Suzuki, N. Okabe, H. Harashima, Manipulating the function of tumor-associated macrophages by siRNA-loaded lipid nanoparticles for cancer immunotherapy, Journal of Controlled Release, 325 (2020) 235-248.

[200] Y. Song, C. Tang, C. Yin, Combination antitumor immunotherapy with VEGF and PIGF siRNA via systemic delivery of multi-functionalized nanoparticles to tumor-associated macrophages and breast cancer cells, Biomaterials, 185 (2018) 117-132.

[201] S. Shen, Y. Zhang, K.-G. Chen, Y.-L. Luo, J. Wang, Cationic Polymeric Nanoparticle Delivering CCR2 siRNA to Inflammatory Monocytes for Tumor Microenvironment Modification and Cancer Therapy, Molecular Pharmaceutics, 15 (2018) 3642-3653.

[202] S. Ramishetti, I. Hazan-Halevy, R. Palakuri, S. Chatterjee, S. Naidu Gonna, N. Dammes, I. Freilich, L. Kolik Shmuel, D. Danino, D. Peer, A Combinatorial Library of Lipid Nanoparticles for RNA Delivery to Leukocytes, Adv Mater, 32 (2020) e1906128.

[203] M.P. Lokugamage, C.D. Sago, Z. Gan, B.R. Krupczak, J.E. Dahlman, Constrained Nanoparticles Deliver siRNA and sgRNA to T Cells In Vivo without Targeting Ligands, Adv Mater, 31 (2019) 1902251.

[204] Y. Liu, Z.-T. Cao, C.-F. Xu, Z.-D. Lu, Y.-L. Luo, J. Wang, Optimization of lipid-assisted nanoparticle for disturbing neutrophils-related inflammation, Biomaterials, 172 (2018) 92-104.

[205] C. Ge, J. Yang, S. Duan, Y. Liu, F. Meng, L. Yin, Fluorinated α-Helical Polypeptides Synchronize Mucus Permeation and Cell Penetration toward Highly Efficient Pulmonary siRNA Delivery against Acute Lung Injury, Nano Letters, 20 (2020) 1738-1746.

[206] B. Kim, H.-B. Pang, J. Kang, J.-H. Park, E. Ruoslahti, M.J. Sailor, Immunogene therapy with fusogenic nanoparticles modulates macrophage response to Staphylococcus aureus, Nature Communications, 9 (2018) 1969.

[207] D.-H. Kim, H.-J. Park, S. Lim, J.-H. Koo, H.-G. Lee, J.O. Choi, J.H. Oh, S.-J. Ha, M.-J. Kang, C.-M. Lee, C.G. Lee, J.A. Elias, J.-M. Choi, Regulation of chitinase-3-like-1 in T cell elicits Th1 and cytotoxic responses to inhibit lung metastasis, Nature Communications, 9 (2018) 503.

[208] S. Liang, J. Zheng, W. Wu, Q. Li, P.E. Saw, J. Chen, X. Xu, H. Yao, Y. Yao, A Robust Nanoparticle Platform for RNA Interference in Macrophages to Suppress Tumor Cell Migration, Frontiers in Pharmacology, 9 (2018) 1465.

[209] N. Veiga, M. Goldsmith, Y. Diesendruck, S. Ramishetti, D. Rosenblum, E. Elinav, M.A. Behlke, I. Benhar, D. Peer, Leukocyte-specific siRNA delivery revealing IRF8 as a potential anti-inflammatory target, Journal of Controlled Release, 313 (2019) 33-41.

[210] M. Krohn-Grimberghe, M.J. Mitchell, M.J. Schloss, O.F. Khan, G. Courties, P.P.G. Guimaraes, D. Rohde, S. Cremer, P.S. Kowalski, Y. Sun, M. Tan, J. Webster, K. Wang, Y. Iwamoto, S.P. Schmidt, G.R. Wojtkiewicz, R. Nayar, V. Frodermann, M. Hulsmans, A. Chung, F.F. Hoyer, F.K. Swirski, R. Langer, D.G. Anderson, M. Nahrendorf, Nanoparticle-encapsulated siRNAs for gene silencing in the haematopoietic stem-cell niche, Nature Biomedical Engineering, 4 (2020) 1076-1089.

[211] G. Arias-Alpizar, L. Kong, R.C. Vlieg, A. Rabe, P. Papadopoulou, M.S. Meijer, S. Bonnet, S. Vogel, J. van Noort, A. Kros, F. Campbell, Light-triggered switching of liposome surface charge directs delivery of membrane impermeable payloads in vivo, Nature Communications, 11 (2020) 3638.

[212] D.J. Lundy, K.-H. Chen, E.K.W. Toh, P.C.H. Hsieh, Distribution of Systemically Administered Nanoparticles Reveals a Size-Dependent Effect Immediately following Cardiac Ischaemia-Reperfusion Injury, Scientific Reports, 6 (2016) 25613.

[213] R. Weissleder, M. Nahrendorf, M.J. Pittet, Imaging macrophages with nanoparticles, Nature Materials, 13 (2014) 125-138.

[214] E.C. Wayne, C. Long, M.J. Haney, E.V. Batrakova, T.M. Leisner, L.V. Parise, A.V. Kabanov, Targeted Delivery of siRNA Lipoplexes to Cancer Cells Using Macrophage Transient Horizontal Gene Transfer, Advanced Science, 6 (2019) 1900582.

[215] M.-L. Laukkanen, T.T. Teeri, K. Keinänen, Lipid-tagged antibodies: bacterial expression and characterization of a lipoprotein—single-chain antibody fusion protein, Protein Engineering, Design and Selection, 6 (1993) 449-454.

[216] L.M. Kranz, M. Diken, H. Haas, S. Kreiter, C. Loquai, K.C. Reuter, M. Meng, D. Fritz, F. Vascotto, H. Hefesha, C. Grunwitz, M. Vormehr, Y. Hüsemann, A. Selmi, A.N. Kuhn, J. Buck, E. Derhovanessian, R. Rae, S. Attig, J. Diekmann, R.A. Jabulowsky, S. Heesch, J. Hassel, P. Langguth, S. Grabbe, C. Huber, Ö. Türeci, U. Sahin, Systemic RNA delivery to dendritic cells exploits antiviral defence for cancer immunotherapy, Nature, 534 (2016) 396-401.

[217] F. Campbell, F.L. Bos, S. Sieber, G. Arias-Alpizar, B.E. Koch, J. Huwyler, A. Kros, J. Bussmann, Directing Nanoparticle Biodistribution through Evasion and Exploitation of Stab2-Dependent Nanoparticle Uptake, ACS Nano, 12 (2018) 2138-2150.

[218] Y. Hayashi, M. Takamiya, P.B. Jensen, I. Ojea-Jiménez, H. Claude, C. Antony, K. Kjaer-Sorensen, C. Grabher, T. Boesen, D. Gilliland, C. Oxvig, U. Strähle, C. Weiss, Differential Nanoparticle Sequestration by Macrophages and Scavenger Endothelial Cells Visualized in Vivo in Real-Time and at Ultrastructural Resolution, ACS Nano, 14 (2020) 1665-1681.

[219] K.M. Tsoi, S.A. MacParland, X.-Z. Ma, V.N. Spetzler, J. Echeverri, B. Ouyang, S.M. Fadel, E.A. Sykes, N. Goldaracena, J.M. Kaths, J.B. Conneely, B.A. Alman, M. Selzner, M.A. Ostrowski, O.A. Adeyi, A. Zilman, I.D. McGilvray, W.C.W. Chan, Mechanism of hard-nanomaterial clearance by the liver, Nature Materials, 15 (2016) 1212-1221.

[220] Q. Cheng, T. Wei, L. Farbiak, L.T. Johnson, S.A. Dilliard, D.J. Siegwart, Selective organ targeting (SORT) nanoparticles for tissue-specific mRNA delivery and CRISPR-Cas gene editing, Nature Nanotechnology, 15 (2020) 313-320.

[221] T. Bhuin, J.K. Roy, Rab proteins: The key regulators of intracellular vesicle transport, Experimental Cell Research, 328 (2014) 1-19.

[222] T. Galvez, J. Gilleron, M. Zerial, G.A. O'Sullivan, SnapShot: Mammalian Rab Proteins in Endocytic Trafficking, Cell, 151 (2012) 234-234.e232.

[223] C.C. Scott, F. Vacca, J. Gruenberg, Endosome maturation, transport and functions, Seminars in Cell & Developmental Biology, 31 (2014) 2-10.

[224] J.T. Roland, D.M. Bryant, A. Datta, A. Itzen, K.E. Mostov, J.R. Goldenring, Rab GTPase–Myo5B complexes control membrane recycling and epithelial polarization, Proceedings of the National Academy of Sciences, 108 (2011) 2789.

[225] M. Forgac, Vacuolar ATPases: rotary proton pumps in physiology and pathophysiology, Nature Reviews Molecular Cell Biology, 8 (2007) 917-929.

[226] C.C. Scott, J. Gruenberg, Ion flux and the function of endosomes and lysosomes: pH is just the start, BioEssays, 33 (2011) 103-110.
[227] A.J. Morgan, F.M. Platt, E. Lloyd-Evans, A. Galione, Molecular mechanisms of endolysosomal Ca2+ signalling in health and disease, Biochemical Journal, 439 (2011) 349-378.
[228] T. Stauber, T.J. Jentsch, Chloride in Vesicular Trafficking and Function, Annual Review of Physiology, 75 (2013) 453-477.
[229] F. Hullin-Matsuda, T. Taguchi, P. Greimel, T. Kobayashi, Lipid compartmentalization in the endosome system, Seminars in Cell & Developmental Biology, 31 (2014) 48-56.
[230] H. Matsuo, J. Chevallier, N. Mayran, I. Le Blanc, C. Ferguson, J. Fauré, N.S. Blanc, S. Matile, J. Dubochet, R. Sadoul, R.G. Parton, F. Vilbois, J. Gruenberg, Role of LBPA and Alix in Multivesicular Liposome Formation and Endosome Organization, Science, 303 (2004) 531.
[231] S. Patel, J. Kim, M. Herrera, A. Mukherjee, A.V. Kabanov, G. Sahay, Brief update on endocytosis of nanomedicines, Advanced Drug Delivery Reviews, 144 (2019) 90-111.
[232] L.M.P. Vermeulen, S.C. De Smedt, K. Remaut, K. Braeckmans, The proton sponge hypothesis: Fable or fact?, European Journal of Pharmaceutics and Biopharmaceutics, 129 (2018) 184-190.
[233] N.D. Sonawane, F.C. Szoka, Jr., A.S. Verkman, Chloride Accumulation and Swelling in Endosomes Enhances DNA Transfer by Polyamine-DNA Polyplexes *, Journal of Biological Chemistry, 278 (2003) 44826-44831.
[234] M. Wojnilowicz, A. Glab, A. Bertucci, F. Caruso, F. Cavalieri, Super-resolution Imaging of Proton Sponge-Triggered Rupture of Endosomes and Cytosolic Release of Small Interfering RNA, ACS Nano, 13 (2019) 187-202.
[235] T. Bus, A. Traeger, U.S. Schubert, The great escape: how cationic polyplexes overcome the endosomal barrier, Journal of Materials Chemistry B, 6 (2018) 6904-6918.
[236] A.M. Funhoff, C.F. van Nostrum, G.A. Koning, N.M.E. Schuurmans-Nieuwenbroek, D.J.A. Crommelin, W.E. Hennink, Endosomal Escape of Polymeric Gene Delivery Complexes Is Not Always Enhanced by Polymers Buffering at Low pH, Biomacromolecules, 5 (2004) 32-39.
[237] S. Vaidyanathan, B.G. Orr, M.M. Banaszak Holl, Role of Cell Membrane–Vector Interactions in Successful Gene Delivery, Accounts of Chemical Research, 49 (2016) 1486-1493.
[238] Z.u. Rehman, D. Hoekstra, I.S. Zuhorn, Mechanism of Polyplex- and Lipoplex-Mediated Delivery of Nucleic Acids: Real-Time Visualization of Transient Membrane Destabilization without Endosomal Lysis, ACS Nano, 7 (2013) 3767-3777.
[239] L.M.P. Vermeulen, T. Brans, S.K. Samal, P. Dubruel, J. Demeester, S.C. De Smedt, K. Remaut, K. Braeckmans, Endosomal Size and Membrane Leakiness Influence Proton Sponge-Based Rupture of Endosomal Vesicles, ACS Nano, 12 (2018) 2332-2345.
[240] D. Omata, Y. Negishi, S. Hagiwara, S. Yamamura, Y. Endo-Takahashi, R. Suzuki, K. Maruyama, M. Nomizu, Y. Aramaki, Bubble Liposomes and Ultrasound Promoted Endosomal Escape of TAT-PEG Liposomes as Gene Delivery Carriers, Molecular Pharmaceutics, 8 (2011) 2416-2423.
[241] D. Omata, Y. Negishi, S. Yamamura, S. Hagiwara, Y. Endo-Takahashi, R. Suzuki, K. Maruyama, M. Nomizu, Y. Aramaki, Involvement of Ca2+ and ATP in Enhanced Gene Delivery by Bubble Liposomes and Ultrasound Exposure, Molecular Pharmaceutics, 9 (2012) 1017-1023.
[242] D. Omata, Y. Negishi, R. Suzuki, Y. Oda, Y. Endo-Takahashi, K. Maruyama, Chapter Two - Nonviral Gene Delivery Systems by the Combination of Bubble Liposomes and Ultrasound, in: L. Huang, D. Liu, E. Wagner (Eds.) Advances in Genetics, Academic Press2015, pp. 25-48.
[243] R. Xiong, F. Joris, S. Liang, R. De Rycke, S. Lippens, J. Demeester, A. Skirtach, K. Raemdonck, U.

Himmelreich, S.C. De Smedt, K. Braeckmans, Cytosolic Delivery of Nanolabels Prevents Their Asymmetric Inheritance and Enables Extended Quantitative in Vivo Cell Imaging, Nano Letters, 16 (2016) 5975-5986.

[244] X. Huang, A. Pallaoro, G.B. Braun, D.P. Morales, M.O. Ogunyankin, J. Zasadzinski, N.O. Reich, Modular Plasmonic Nanocarriers for Efficient and Targeted Delivery of Cancer-Therapeutic siRNA, Nano Letters, 14 (2014) 2046-2051.

[245] J.C. Fraire, G. Houthaeve, J. Liu, L. Raes, L. Vermeulen, S. Stremersch, T. Brans, G. García-Díaz Barriga, S. De Keulenaer, F. Van Nieuwerburgh, R. De Rycke, J. Vandesompele, P. Mestdagh, K. Raemdonck, W.H. De Vos, S. De Smedt, K. Braeckmans, Vapor nanobubble is the more reliable photothermal mechanism for inducing endosomal escape of siRNA without disturbing cell homeostasis, Journal of Controlled Release, 319 (2020) 262-275.

[246] Z. Chu, K. Miu, P. Lung, S. Zhang, S. Zhao, H.-C. Chang, G. Lin, Q. Li, Rapid endosomal escape of prickly nanodiamonds: implications for gene delivery, Scientific Reports, 5 (2015) 11661.

[247] H. Zhang, D. Liu, L. Wang, Z. Liu, R. Wu, A. Janoniene, M. Ma, G. Pan, L. Baranauskiene, L. Zhang, W. Cui, V. Petrikaite, D. Matulis, H. Zhao, J. Pan, H.A. Santos, Microfluidic Encapsulation of Prickly Zinc-Doped Copper Oxide Nanoparticles with VD1142 Modified Spermine Acetalated Dextran for Efficient Cancer Therapy, Advanced Healthcare Materials, 6 (2017) 1601406.

[248] Y. Lu, Y. Lin, Z. Chen, Q. Hu, Y. Liu, S. Yu, W. Gao, M.D. Dickey, Z. Gu, Enhanced Endosomal Escape by Light-Fueled Liquid-Metal Transformer, Nano Letters, 17 (2017) 2138-2145.

[249] M. Marsh, A. Helenius, Virus Entry: Open Sesame, Cell, 124 (2006) 729-740.

[250] W.B. Kauffman, T. Fuselier, J. He, W.C. Wimley, Mechanism Matters: A Taxonomy of Cell Penetrating Peptides, Trends in Biochemical Sciences, 40 (2015) 749-764.

[251] W. Li, F. Nicol, F.C. Szoka, GALA: a designed synthetic pH-responsive amphipathic peptide with applications in drug and gene delivery, Advanced Drug Delivery Reviews, 56 (2004) 967-985.

[252] D.K. Schach, W. Rock, J. Franz, M. Bonn, S.H. Parekh, T. Weidner, Reversible Activation of a Cell-Penetrating Peptide in a Membrane Environment, Journal of the American Chemical Society, 137 (2015) 12199-12202.

[253] E.K. Esbjörner, K. Oglęcka, P. Lincoln, A. Gräslund, B. Nordén, Membrane Binding of pH-Sensitive Influenza Fusion Peptides. Positioning, Configuration, and Induced Leakage in a Lipid Vesicle Model, Biochemistry, 46 (2007) 13490-13504.

[254] S. Futaki, I. Nakase, Cell-Surface Interactions on Arginine-Rich Cell-Penetrating Peptides Allow for Multiplex Modes of Internalization, Accounts of Chemical Research, 50 (2017) 2449-2456.

[255] D.J. Brock, H. Kondow-McConaghy, J. Allen, Z. Brkljača, L. Kustigian, M. Jiang, J. Zhang, H. Rye, M. Vazdar, J.-P. Pellois, Mechanism of Cell Penetration by Permeabilization of Late Endosomes: Interplay between a Multivalent TAT Peptide and Bis(monoacylglycero)phosphate, Cell Chemical Biology, 27 (2020) 1296-1307.e1295.

[256] A. Erazo-Oliveras, K. Najjar, D. Truong, T.-Y. Wang, Dakota J. Brock, Austin R. Prater, J.-P. Pellois, The Late Endosome and Its Lipid BMP Act as Gateways for Efficient Cytosolic Access of the Delivery Agent dfTAT and Its Macromolecular Cargos, Cell Chemical Biology, 23 (2016) 598-607.

[257] D.M. Copolovici, K. Langel, E. Eriste, Ü. Langel, Cell-Penetrating Peptides: Design, Synthesis, and Applications, ACS Nano, 8 (2014) 1972-1994.

[258] F. Milletti, Cell-penetrating peptides: classes, origin, and current landscape, Drug Discovery Today, 17 (2012) 850-860.

[259] K. Najjar, A. Erazo-Oliveras, J.W. Mosior, M.J. Whitlock, I. Rostane, J.M. Cinclair, J.-P. Pellois,

Unlocking Endosomal Entrapment with Supercharged Arginine-Rich Peptides, Bioconjugate Chemistry, 28 (2017) 2932-2941.

[260] M. Kosuge, T. Takeuchi, I. Nakase, A.T. Jones, S. Futaki, Cellular Internalization and Distribution of Arginine-Rich Peptides as a Function of Extracellular Peptide Concentration, Serum, and Plasma Membrane Associated Proteoglycans, Bioconjugate Chemistry, 19 (2008) 656-664.

[261] D.J. Brock, L. Kustigian, M. Jiang, K. Graham, T.-Y. Wang, A. Erazo-Oliveras, K. Najjar, J. Zhang, H. Rye, J.-P. Pellois, Efficient cell delivery mediated by lipid-specific endosomal escape of supercharged branched peptides, Traffic, 19 (2018) 421-435.

[262] D. Birch, M.V. Christensen, D. Staerk, H. Franzyk, H.M. Nielsen, Stereochemistry as a determining factor for the effect of a cell-penetrating peptide on cellular viability and epithelial integrity, Biochemical Journal, 475 (2018) 1773-1788.

[263] K. Najjar, A. Erazo-Oliveras, D.J. Brock, T.-Y. Wang, J.-P. Pellois, An l- to d-Amino Acid Conversion in an Endosomolytic Analog of the Cell-penetrating Peptide TAT Influences Proteolytic Stability, Endocytic Uptake, and Endosomal Escape*, Journal of Biological Chemistry, 292 (2017) 847-861.

[264] X. Jing, C. Foged, B. Martin-Bertelsen, A. Yaghmur, K.M. Knapp, M. Malmsten, H. Franzyk, H.M. Nielsen, Delivery of siRNA Complexed with Palmitoylated α-Peptide/β-Peptoid Cell-Penetrating Peptidomimetics: Membrane Interaction and Structural Characterization of a Lipid-Based Nanocarrier System, Molecular Pharmaceutics, 13 (2016) 1739-1749.

[265] H. Xing, M. Lu, T. Yang, H. Liu, Y. Sun, X. Zhao, H. Xu, L. Yang, P. Ding, Structure-function relationships of nonviral gene vectors: Lessons from antimicrobial polymers, Acta Biomaterialia, 86 (2019) 15-40.

[266] G. Wiedman, S.Y. Kim, E. Zapata-Mercado, W.C. Wimley, K. Hristova, pH-Triggered, Macromolecule-Sized Poration of Lipid Bilayers by Synthetically Evolved Peptides, Journal of the American Chemical Society, 139 (2017) 937-945.

[267] M. Akishiba, T. Takeuchi, Y. Kawaguchi, K. Sakamoto, H.-H. Yu, I. Nakase, T. Takatani-Nakase, F. Madani, A. Gräslund, S. Futaki, Cytosolic antibody delivery by lipid-sensitive endosomolytic peptide, Nature Chemistry, 9 (2017) 751-761.

[268] N. Tamemoto, M. Akishiba, K. Sakamoto, K. Kawano, H. Noguchi, S. Futaki, Rational Design Principles of Attenuated Cationic Lytic Peptides for Intracellular Delivery of Biomacromolecules, Molecular Pharmaceutics, 17 (2020) 2175-2185.

[269] M. Meyer, A. Philipp, R. Oskuee, C. Schmidt, E. Wagner, Breathing Life into Polycations: Functionalization with pH-Responsive Endosomolytic Peptides and Polyethylene Glycol Enables siRNA Delivery, Journal of the American Chemical Society, 130 (2008) 3272-3273.

[270] B.A. Paray, A. Ahmad, J.M. Khan, F. Taufiq, A. Pathan, A. Malik, M.Z. Ahmed, The role of the multifunctional antimicrobial peptide melittin in gene delivery, Drug Discovery Today, (2021).

[271] C.V. Bonduelle, E.R. Gillies, Dendritic Guanidines as Efficient Analogues of Cell Penetrating Peptides, Pharmaceuticals, 3 (2010).

[272] Y. Sun, L. Xian, J. Yu, T. Yang, J. Zhang, Z. Yang, J. Jiang, C. Cai, X. Zhao, L. Yang, P. Ding, Structure–Function Correlations of Poly(Amido Amine)s for Gene Delivery, Macromolecular Bioscience, 17 (2017) 1600297.

[273] E.-K. Bang, G. Gasparini, G. Molinard, A. Roux, N. Sakai, S. Matile, Substrate-Initiated Synthesis of Cell-Penetrating Poly(disulfide)s, Journal of the American Chemical Society, 135 (2013) 2088-2091.

[274] S. Wang, pH-Responsive Amphiphilic Carboxylate Polymers: Design and Potential for Endosomal Escape, Frontiers in Chemistry, 9 (2021) 145.

[275] G. Gasparini, E.-K. Bang, G. Molinard, D.V. Tulumello, S. Ward, S.O. Kelley, A. Roux, N. Sakai, S. Matile, Cellular Uptake of Substrate-Initiated Cell-Penetrating Poly(disulfide)s, Journal of the American Chemical Society, 136 (2014) 6069-6074.

[276] F. Richter, L. Martin, K. Leer, E. Moek, F. Hausig, J.C. Brendel, A. Traeger, Tuning of endosomal escape and gene expression by functional groups, molecular weight and transfection medium: a structure–activity relationship study, Journal of Materials Chemistry B, 8 (2020) 5026-5041.

[277] S.Y. Tzeng, J.J. Green, Subtle Changes to Polymer Structure and Degradation Mechanism Enable Highly Effective Nanoparticles for siRNA and DNA Delivery to Human Brain Cancer, Advanced Healthcare Materials, 2 (2013) 468-480.

[278] A.C. Rinkenauer, S. Schubert, A. Traeger, U.S. Schubert, The influence of polymer architecture on in vitro pDNA transfection, Journal of Materials Chemistry B, 3 (2015) 7477-7493.

[279] V. Delplace, J. Nicolas, Degradable vinyl polymers for biomedical applications, Nature Chemistry, 7 (2015) 771-784.

[280] S. Wannasarit, S. Wang, P. Figueiredo, C. Trujillo, F. Eburnea, L. Simón-Gracia, A. Correia, Y. Ding, T. Teesalu, D. Liu, R. Wiwattanapatapee, H.A. Santos, W. Li, A Virus-Mimicking pH-Responsive Acetalated Dextran-Based Membrane-Active Polymeric Nanoparticle for Intracellular Delivery of Antitumor Therapeutics, Advanced Functional Materials, 29 (2019) 1905352.

[281] B.C. Evans, R.B. Fletcher, K.V. Kilchrist, E.A. Dailing, A.J. Mukalel, J.M. Colazo, M. Oliver, J. Cheung-Flynn, C.M. Brophy, J.W. Tierney, J.S. Isenberg, K.D. Hankenson, K. Ghimire, C. Lander, C.A. Gersbach, C.L. Duvall, An anionic, endosome-escaping polymer to potentiate intracellular delivery of cationic peptides, biomacromolecules, and nanoparticles, Nature Communications, 10 (2019) 5012.

[282] L. Wasungu, D. Hoekstra, Cationic lipids, lipoplexes and intracellular delivery of genes, Journal of Controlled Release, 116 (2006) 255-264.

[283] L. Johannes, M. Lucchino, Current Challenges in Delivery and Cytosolic Translocation of Therapeutic RNAs, Nucleic Acid Therapeutics, 28 (2018) 178-193.

[284] I.M.S. Degors, C. Wang, Z.U. Rehman, I.S. Zuhorn, Carriers Break Barriers in Drug Delivery: Endocytosis and Endosomal Escape of Gene Delivery Vectors, Accounts of Chemical Research, 52 (2019) 1750-1760.

[285] R. Kanasty, J.R. Dorkin, A. Vegas, D. Anderson, Delivery materials for siRNA therapeutics, Nature Materials, 12 (2013) 967-977.

[286] S. Ramishetti, I. Hazan-Halevy, R. Palakuri, S. Chatterjee, S. Naidu Gonna, N. Dammes, I. Freilich, L. Kolik Shmuel, D. Danino, D. Peer, A Combinatorial Library of Lipid Nanoparticles for RNA Delivery to Leukocytes, Adv Mater, 32 (2020) 1906128.

[287] L. Miao, J. Lin, Y. Huang, L. Li, D. Delcassian, Y. Ge, Y. Shi, D.G. Anderson, Synergistic lipid compositions for albumin receptor mediated delivery of mRNA to the liver, Nature Communications, 11 (2020) 2424.

[288] C.A. Alabi, K.T. Love, G. Sahay, H. Yin, K.M. Luly, R. Langer, D.G. Anderson, Multiparametric approach for the evaluation of lipid nanoparticles for siRNA delivery, Proceedings of the National Academy of Sciences, 110 (2013) 12881.

[289] W. Viricel, S. Poirier, A. Mbarek, R.M. Derbali, G. Mayer, J. Leblond, Cationic switchable lipids: pH-triggered molecular switch for siRNA delivery, Nanoscale, 9 (2017) 31-36.

[290] T. Van de Vyver, B. Bogaert, L. De Backer, F. Joris, R. Guagliardo, J. Van Hoeck, P. Merckx, S. Van Calenbergh, S. Ramishetti, D. Peer, K. Remaut, S.C. De Smedt, K. Raemdonck, Cationic Amphiphilic Drugs Boost the Lysosomal Escape of Small Nucleic Acid Therapeutics in a Nanocarrier-Dependent Manner,

ACS Nano, 14 (2020) 4774-4791.
[291] C. Salata, A. Calistri, C. Parolin, A. Baritussio, G. Palù, Antiviral activity of cationic amphiphilic drugs, Expert Review of Anti-infective Therapy, 15 (2017) 483-492.
[292] F. Joris, L. De Backer, T. Van de Vyver, C. Bastiancich, S.C. De Smedt, K. Raemdonck, Repurposing cationic amphiphilic drugs as adjuvants to induce lysosomal siRNA escape in nanogel transfected cells, Journal of Controlled Release, 269 (2018) 266-276.
[293] H. Du Rietz, H. Hedlund, S. Wilhelmson, P. Nordenfelt, A. Wittrup, Imaging small molecule-induced endosomal escape of siRNA, Nature Communications, 11 (2020) 1809.
[294] T.Y. Hu, M. Frieman, J. Wolfram, Insights from nanomedicine into chloroquine efficacy against COVID-19, Nature Nanotechnology, 15 (2020) 247-249.
[295] S. Ly, D.M. Navaroli, M.-C. Didiot, J. Cardia, L. Pandarinathan, J.F. Alterman, K. Fogarty, C. Standley, L.M. Lifshitz, K.D. Bellve, M. Prot, D. Echeverria, S. Corvera, A. Khvorova, Visualization of self-delivering hydrophobically modified siRNA cellular internalization, Nucleic Acids Research, 45 (2017) 15-25.
[296] Y. Zheng, W. Tai, Insight into the siRNA transmembrane delivery—From cholesterol conjugating to tagging, WIREs Nanomedicine and Nanobiotechnology, 12 (2020) e1606.
[297] J. Gilleron, P. Paramasivam, A. Zeigerer, W. Querbes, G. Marsico, C. Andree, S. Seifert, P. Amaya, M. Stöter, V. Koteliansky, H. Waldmann, K. Fitzgerald, Y. Kalaidzidis, A. Akinc, M.A. Maier, M. Manoharan, M. Bickle, M. Zerial, Identification of siRNA delivery enhancers by a chemical library screen, Nucleic Acids Research, 43 (2015) 7984-8001.
[298] G. The Vitravene Study, A randomized controlled clinical trial of intravitreous fomivirsen for treatment of newly diagnosed peripheral cytomegalovirus retinitis in patients with AIDS, American Journal of Ophthalmology, 133 (2002) 467-474.
[299] E.S. Gragoudas, A.P. Adamis, E.T. Cunningham, M. Feinsod, D.R. Guyer, Pegaptanib for neovascular age-related macular degeneration, The New England Journal of Medicine, 351 (2004) 2805-2816.
[300] F. Fogacci, N. Ferri, P.P. Toth, M. Ruscica, A. Corsini, A.F.G. Cicero, Efficacy and Safety of Mipomersen: A Systematic Review and Meta-Analysis of Randomized Clinical Trials, Drugs, 79 (2019) 751-766.
[301] Emea, Public statement on Vitravene, London, 2002.
[302] M.S. Spitzer, E. Yoeruek, A. Sierra, B. Wallenfels-Thilo, U. Schraermeyer, B. Spitzer, K. Bartz-Schmidt, P. Szurman, Comparative antiproliferative and cytotoxic profile of bevacizumab (Avastin), pegaptanib (Macugen) and ranibizumab (Lucentis) on different ocular cells, Graefe's Archive for Clinical and Experimental Ophthalmology, 245 (2007) 1837-1842.
[303] J.S. Parham, A.C. Goldberg, Mipomersen and its use in familial hypercholesterolemia, null, 20 (2019) 127-131.
[304] Ema, Assessment report Kynamro, European Medicines Agency, London, 2013.
[305] I. Biogen, SPINRAZA (nusinersen) injection, for intrathecal use; US prescribing information, www.fda.gov, 2016.
[306] K. Dzierlega, T. Yokota, Optimization of antisense-mediated exon skipping for Duchenne muscular dystrophy, Gene therapy, 27 (2020) 407-416.
[307] S.J. Keam, Inotersen: First Global Approval, Drugs, 78 (2018) 1371-1376.
[308] L.J. Scott, Givosiran: First Approval, Drugs, 80 (2020) 335-339.
[309] T. Spark, LUXTURNA (voretigene neparvovec-rzyl) intraocular suspension for subretinal injection; US prescribing information, www.fda.gov, 2017.

[310] I. AveXis, ZOLGENSMA® (onasemnogene abeparvovec-xioi) Suspension for intravenous infusion; US prescribing information, www.fda.gov, 2019.
[311] C. Stein, D. Castanotto, A. Krishnan, L. Nikolaenko, Defibrotide (Defitelio): A New Addition to the Stockpile of Food and Drug Administration-approved Oligonucleotide Drugs, Molecular therapy.Nucleic acids, 5 (2016) e346.
[312] Ema, CHMP assessment report Exondys, European Medicines Agency, 2018.
[313] K. Dhuri, C. Bechtold, E. Quijano, H. Pham, A. Gupta, A. Vikram, R. Bahal, Antisense Oligonucleotides: An Emerging Area in Drug Discovery and Development, Journal of Clinical Medicine, 9 (2020) 2004.
[314] W. Shen, C.L. De Hoyos, H. Sun, T.A. Vickers, X.-h. Liang, S.T. Crooke, Acute hepatotoxicity of 2′ fluoro-modified 5 − 10 − 5 gapmer phosphorothioate oligonucleotides in mice correlates with intracellular protein binding and the loss of DBHS proteins, Nucleic acids research, 46 (2018) 2204-2217.
[315] W. Shen, X.-H. Liang, H. Sun, S.T. Crooke, 2'-Fluoro-modified phosphorothioate oligonucleotide can cause rapid degradation of P54nrb and PSF, Nucleic acids research, 43 (2015) 4569-4578.
[316] S. Boutin, V. Monteilhet, P. Veron, C. Leborgne, O. Benveniste, M.F. Montus, C. Masurier, Prevalence of Serum IgG and Neutralizing Factors Against Adeno-Associated Virus (AAV) Types 1, 2, 5, 6, 8, and 9 in the Healthy Population: Implications for Gene Therapy Using AAV Vectors, Human Gene Therapy, 21 (2010) 704-712.
[317] H.C. Verdera, K. Kuranda, F. Mingozzi, AAV Vector Immunogenicity in Humans: A Long Journey to Successful Gene Transfer, Molecular Therapy, 28 (2020) 723-746.
[318] Y. Huang, Preclinical and Clinical Advances of GalNAc-Decorated Nucleic Acid Therapeutics, Molecular Therapy - Nucleic Acids, 6 (2017) 116-132.
[319] J.K. Nair, J.L.S. Willoughby, A. Chan, K. Charisse, M.R. Alam, Q. Wang, M. Hoekstra, P. Kandasamy, A.V. Kel'in, S. Milstein, N. Taneja, J. O'Shea, S. Shaikh, L. Zhang, R.J. van der Sluis, M.E. Jung, A. Akinc, R. Hutabarat, S. Kuchimanchi, K. Fitzgerald, T. Zimmermann, T.J.C. van Berkel, M.A. Maier, K.G. Rajeev, M. Manoharan, Multivalent N-Acetylgalactosamine-Conjugated siRNA Localizes in Hepatocytes and Elicits Robust RNAi-Mediated Gene Silencing, Journal of the American Chemical Society, 136 (2014) 16958-16961.
[320] K. Garber, Alnylam launches era of RNAi drugs, Nature Biotechnology, 36 (2018) 777-778.
[321] A. Akinc, M.A. Maier, M. Manoharan, K. Fitzgerald, M. Jayaraman, S. Barros, S. Ansell, X. Du, M.J. Hope, T.D. Madden, B.L. Mui, S.C. Semple, Y.K. Tam, M. Ciufolini, D. Witzigmann, J.A. Kulkarni, R. van der Meel, P.R. Cullis, The Onpattro story and the clinical translation of nanomedicines containing nucleic acid-based drugs, Nature Nanotechnology, 14 (2019) 1084-1087.
[322] Ema, Marketing authorisation for Comirnaty; ANNEX I SUMMARY OF PRODUCT CHARACTERISTICS, European Medicines Agency, 2020.
[323] Moderna, CLINICAL STUDY PROTOCOL mRNA-1273-P301, ModernaTX, Inc, 2020.
[324] Ema, Marketing authorisation for COVID-19 vaccine Moderna; ANNEX I SUMMARY OF PRODUCT CHARACTERISTICS, ema.europa.eu, 2021.
[325] P. Badri, X. Jiang, A. Borodovsky, N. Najafian, J. Kim, V.A. Clausen, V. Goel, B. Habtemariam, G.J. Robbie, Pharmacokinetic and Pharmacodynamic Properties of Cemdisiran, an RNAi Therapeutic Targeting Complement Component 5, in Healthy Subjects and Patients with Paroxysmal Nocturnal Hemoglobinuria, Clinical pharmacokinetics, (2020).
[326] K. Fitzgerald, S. White, A. Borodovsky, B.R. Bettencourt, A. Strahs, V. Clausen, P. Wijngaard, J.D. Horton, J. Taubel, A. Brooks, C. Fernando, R.S. Kauffman, D. Kallend, A. Vaishnaw, A. Simon, A Highly

Durable RNAi Therapeutic Inhibitor of PCSK9, New England Journal of Medicine, 376 (2017) 41-51.
[327] V. Reebye, K.-W. Huang, V. Lin, S. Jarvis, P. Cutilas, S. Dorman, S. Ciriello, P. Andrikakou, J. Voutila, P. Saetrom, P.J. Mintz, I. Reccia, J.J. Rossi, H. Huber, R. Habib, N. Kostomitsopoulos, D.C. Blakey, N.A. Habib, Gene activation of CEBPA using saRNA: preclinical studies of the first in human saRNA drug candidate for liver cancer, Oncogene, 37 (2018) 3216-3228.
[328] M.J. Wagner, R. Mitra, M.J. McArthur, W. Baze, K. Barnhart, S.Y. Wu, C. Rodriguez-Aguayo, X. Zhang, R.L. Coleman, G. Lopez-Berestein, A.K. Sood, Preclinical Mammalian Safety Studies of EPHARNA (DOPC Nanoliposomal EphA2-Targeted siRNA), Mol Cancer Ther, 16 (2017) 1114.
[329] S.R. Hingorani, L. Wang, A.S. Multani, C. Combs, T.B. Deramaudt, R.H. Hruban, A.K. Rustgi, S. Chang, D.A. Tuveson, Trp53R172H and KrasG12D cooperate to promote chromosomal instability and widely metastatic pancreatic ductal adenocarcinoma in mice, Cancer Cell, 7 (2005) 469-483.
[330] Z. Meng, M. Lu, RNA Interference-Induced Innate Immunity, Off-Target Effect, or Immune Adjuvant?, Front Immunol, 8 (2017) 331-331.
[331] S. Qiu, C.M. Adema, T. Lane, A computational study of off-target effects of RNA interference, Nucleic Acids Res, 33 (2005) 1834-1847.
[332] M.A. Subhan, V.P. Torchilin, siRNA based drug design, quality, delivery and clinical translation, Nanomedicine: NBM, 29 (2020) 102239.
[333] B.R. Cullen, Enhancing and confirming the specificity of RNAi experiments, Nat Methods, 3 (2006) 677-681.
[334] R. Bartoszewski, A.F. Sikorski, Editorial focus: understanding off-target effects as the key to successful RNAi therapy, Cell Mol Biol Lett, 24 (2019) 69-69.
[335] V. Hornung, M. Guenthner-Biller, C. Bourquin, A. Ablasser, M. Schlee, S. Uematsu, A. Noronha, M. Manoharan, S. Akira, A. de Fougerolles, S. Endres, G. Hartmann, Sequence-specific potent induction of IFN-alpha by short interfering RNA in plasmacytoid dendritic cells through TLR7, Nature medicine, 11 (2005) 263-270.
[336] A.D. Judge, V. Sood, J.R. Shaw, D. Fang, K. McClintock, I. MacLachlan, Sequence-dependent stimulation of the mammalian innate immune response by synthetic siRNA, Nature Biotechnology, 23 (2005) 457-462.
[337] M.S. Draz, B.A. Fang, P. Zhang, Z. Hu, S. Gu, K.C. Weng, J.W. Gray, F.F. Chen, Nanoparticle-mediated systemic delivery of siRNA for treatment of cancers and viral infections, Theranostics, 4 (2014) 872-892.
[338] A. Reynolds, E.M. Anderson, A. Vermeulen, Y. Fedorov, K. Robinson, D. Leake, J. Karpilow, W.S. Marshall, A. Khvorova, Induction of the interferon response by siRNA is cell type- and duplex length-dependent, RNA, 12 (2006) 988-993.
[339] S.D. Larson, L.N. Jackson, L.A. Chen, P.G. Rychahou, B.M. Evers, Effectiveness of siRNA uptake in target tissues by various delivery methods, Surgery, 142 (2007) 262-269.
[340] S.-S. Kim, H. Garg, A. Joshi, N. Manjunath, Strategies for targeted nonviral delivery of siRNAs in vivo, Trends Mol Med, 15 (2009) 491-500.
[341] D.H. Kim, J.J. Rossi, Strategies for silencing human disease using RNA interference, Nature reviews. Genetics, 8 (2007) 173-184.
[342] D. Grimm, The dose can make the poison: lessons learned from adverse in vivo toxicities caused by RNAi overexpression, Silence, 2 (2011) 8-8.
[343] H. Akita, H. Hatakeyama, I.A. Khalil, Y. Yamada, H. Harashima, 4.425 - Delivery of Nucleic Acids and Gene Delivery, in: P. Ducheyne (Ed.) Comprehensive Biomaterials, Elsevier, Oxford, 2011, pp. 411-

444.
[344] T. Schluep, J. Lickliter, J. Hamilton, D.L. Lewis, C.-L. Lai, J.Y. Lau, S.A. Locarnini, R.G. Gish, B.D. Given, Safety, Tolerability, and Pharmacokinetics of ARC-520 Injection, an RNA Interference-Based Therapeutic for the Treatment of Chronic Hepatitis B Virus Infection, in Healthy Volunteers, Clin Pharmacol Drug Dev, 6 (2017) 350-362.
[345] X. Chen, L.S. Mangala, C. Rodriguez-Aguayo, X. Kong, G. Lopez-Berestein, A.K. Sood, RNA interference-based therapy and its delivery systems, Cancer metastasis reviews, 37 (2018) 107-124.
[346] M.S. Beg, A.J. Brenner, J. Sachdev, M. Borad, Y.-K. Kang, J. Stoudemire, S. Smith, A.G. Bader, S. Kim, D.S. Hong, Phase I study of MRX34, a liposomal miR-34a mimic, administered twice weekly in patients with advanced solid tumors, Invest New Drug, 35 (2017) 180-188.
[347] A.M. Flores, N. Hosseini-Nassab, K.-U. Jarr, J. Ye, X. Zhu, R. Wirka, A.L. Koh, P. Tsantilas, Y. Wang, V. Nanda, Y. Kojima, Y. Zeng, M. Lotfi, R. Sinclair, I.L. Weissman, E. Ingelsson, B.R. Smith, N.J. Leeper, Pro-efferocytic nanoparticles are specifically taken up by lesional macrophages and prevent atherosclerosis, Nature Nanotechnology, 15 (2020) 154-161.
[348] K. Gao, L. Huang, Achieving efficient RNAi therapy: progress and challenges, Acta Pharm Sin B, 3 (2013) 213-225.
[349] K. Gao, L. Huang, Nonviral methods for siRNA delivery, Molecular Pharmaceutics, 6 (2009) 651-658.
[350] J.T. Marques, B.R.G. Williams, Activation of the mammalian immune system by siRNAs, Nature Biotechnology, 23 (2005) 1399-1405.
[351] S. Shah, S.H. Friedman, Tolerance of RNA interference toward modifications of the 5' antisense phosphate of small interfering RNA, Oligonucleotides, 17 (2007) 35-43.
[352] K. Tiemann, J.J. Rossi, RNAi-based therapeutics-current status, challenges and prospects, EMBO Mol Med, 1 (2009) 142-151.
[353] X. Li, Q. Zhao, L. Qiu, Smart ligand: Aptamer-mediated targeted delivery of chemotherapeutic drugs and siRNA for cancer therapy, Journal of Controlled Release, 171 (2013) 152-162.
[354] T.L. Cuellar, D. Barnes, C. Nelson, J. Tanguay, S.F. Yu, X. Wen, S.J. Scales, J. Gesch, D. Davis, A. van Brabant Smith, D. Leake, R. Vandlen, C.W. Siebel, Systematic evaluation of antibody-mediated siRNA delivery using an industrial platform of THIOMAB-siRNA conjugates, Nucleic Acids Res, 43 (2015) 1189-1203.
[355] S.K. Jones, V. Lizzio, O.M. Merkel, Folate Receptor Targeted Delivery of siRNA and Paclitaxel to Ovarian Cancer Cells via Folate Conjugated Triblock Copolymer to Overcome TLR4 Driven Chemotherapy Resistance, Biomacromolecules, 17 (2016) 76-87.
[356] O. Khorev, D. Stokmaier, O. Schwardt, B. Cutting, B. Ernst, Trivalent, Gal/GalNAc-containing ligands designed for the asialoglycoprotein receptor, Bioorganic & medicinal chemistry, 16 (2008) 5216-5231.
[357] H.J. Vaughan, J.J. Green, S.Y. Tzeng, Cancer-Targeting Nanoparticles for Combinatorial Nucleic Acid Delivery, Adv Mater, 32 (2020) 1901081.

Graphical abstract